PARTICLE BREAKAGE AND MATERIAL TRANSPORT IN THE DESIGN OF HIGH-EFFICIENCY COMMINUTION DEVICE

by

Satya Deb Misra

B.E. (Mining Engineering), Calcutta University, 1964
M.S. (Mining Engineering), Columbia University, 1979

SUBMITTED TO THE DEPARTMENT OF MECHANICAL ENGINEERING IN PARTIAL FULFILLMENT OF THE REQUIREMENTS FOR THE DEGREE OF

MASTER OF SCIENCE IN MECHANICAL ENGINEERING

at the

MASSACHUSETTS INSTITUTE OF TECHNOLOGY

August 1991

Signature of Author _____
Department of Mechanical Engineering
August 9, 1991

Certified by _____
Professor Carl R. Peterson
Thesis Supervisor

Accepted by _____
Professor Ain A. Sonin
Chairman, Graduate Thesis Committee

PARTICLE BREAKAGE AND MATERIAL TRANSPORT IN THE DESIGN OF HIGH-EFFICIENCY COMMINUTION DEVICE

by

Satya Deb Misra

Submitted to the Department of Mechanical Engineering on August 9, 1991
in partial fulfillment of the requirements for the degree of Master of Science
in Mechanical Engineering.

Abstract

Today's comminution techniques are notoriously inefficient, energy intensive, and lack full understanding of the particle breakage and material transport processes occurring within the comminution device, which mainly govern the comminution efficiency.

Focussing on compressive comminution, study on single spherical (glass) particles, monolayer and multilayer particle beds, and granular (sand) particle beds was conducted. The results showed that the fracture efficiency within a particle bed: (1) reaches its maximum when the bed is compressed to an amount at which point the original inter-particle voids become filled with fine products from primary crushing, (2) drops sharply until the bed is about 3 particles deep and the rate of drop thereafter decreases slowly with increasing bed thickness, (3) is practically unaffected by compression rate and presence of shear loading but is adversely affected by the presence of excessive amounts of fines. This indicates that crushing energy can be better utilized with prompt removal of fines and segregation of coarse particles before crushing, which effectively reduces the number of inter-particle contacts and the resulting frictional loss and blunting effect on the load. A controlled fluidized transport system can effectively remove the fines by elutriation while segregating the coarse particles by size, smaller ones occupying the upper layers within the crushing zone. This prompted the study of the fluidization behavior of binary size mixtures of particles (representing the fines and coarse fractions in the crushing zone). The results demonstrated the superiority of water over air as a working fluid, columnar vertical beds over tapered and/or inclined beds for better segregation quality and shorter over taller beds for faster segregation.

Finally this research has led to the formulation of a simple mathematical model of the integrated particle breakage/material transport phenomenon and selection of preliminary design parameters for a high-efficiency comminution device.

Thesis Supervisor: Professor Carl R. Peterson
Title: Associate Professor of Mechanical Engineering

Dedication

Leaving my family far behind to pursue my mid-life dream of graduate study at MIT could not have materialized without the unfailing love, continuous support and encouragement from my wife, Rachel. With deepest love I dedicate this work to her.

Acknowledgement

My sincerest thanks and appreciation go to all who helped me in successfully carrying out this research and making my stay enjoyable at MIT.

I thank Professor Carl Peterson specially for all his academic, financial and personal support, as well as practical insights, constructive suggestions, patience and friendly attitude without which I could not have completed this thesis. He told me when to stop when I got too attached to my crushing device.

I express my gratitude to Professor Frank McClintock for his valuable suggestions, guidance and constructive criticisms at our weekly meetings and also at any other time I approached him. His ability to explain complicated scientific matters in a simple manner amazed me. Thanks also go to Professor Harri Kytomaa for the helpful discussions and Professor Ain Sonin for his advisement and other help.

I thank Bob Samuels for the help in fabricating parts of the research apparatus, Don Fitzgerald for setting up the Instron machine, my wife Rachel for doing all the word processing, my 12 year old son Ronnie for finding time to process my entire thesis using the *scribe* (in spite of his busy schedule with the Junction Program at MIT) and Carolyn Beckman-Stitson and Leslie Regan for handling many last minute things, with sincerety. I also thank Surya Kalidindi, S.R. Venkatesh, Andrzej Skoskiewicz, Chahid Ghaddar and Karen Annis for their help with the experiments and friendship.

To my children Ronnie and Sheila, I owe a heavy debt of time and emotion. They gave me abiding love and patient understanding in spite of my being away from them as I pursued my study. My gratitude also goes to my brothers, sisters and my late parents for their love, blessing, prayer and encouragement which provided me the needed strength over the years.

This work was funded by a grant from the U.S. Department of Energy.

Table of Contents

List of Figures

List of Tables

Chapter 1

Introduction

1.1 Comminution Process

Comminution, the process of reduction of coarse material to fine, is utilized in a wide range of applications. Major industries like power (from coal), construction, cement, ceramic, paper, paint, fertilizer, agricultural, pharamaceutical, etc. all use crushing and grinding either to pulverize the coarse material to smaller sizes or fines to make it suitable for downstream processing or end use, or to free valuable constituents from the gangue material (as in ore beneficiation). The process can be either single or multi-stage, as well as dry or wet.

1.2 Motivation for Research

The comminution process, consuming about 2% of the electricity used in the United States and 5% of that used worldwide, is a huge consumer of energy and is horrendously inefficient (less than 1% of the energy input reports as new surface area in the product) [1]. Efficiency of primary and secondary crushers is of the order of 5-10%, whereas, that of tumbling mills is around 0.1%. Metal wear of the crushing elements, which is more for inefficient machines, is an expensive item in the size reduction process. Reduction of energy consumption in comminution has continuously been addressed by the processing industry. These facts provide sufficient incentive to conduct research to improve the efficiency of the comminution process, because it has been estimated that even a modest 10% reduction in energy consumption in comminution would save more than 3 million megawatt hours of electricity annually in the US alone (tens of millions of megawatt hours of electricity globally), which is equivalent to about $200 million in imported oil.

1.3 Scope of This Research

Comminution is carried out using various kinds of equipment or processes and utilizing various methods of force application such as: explosive disintegration, crushing by compression (as in primary or secondary crushing using jaw, gyratory or roll crushers), impact (as in hammer machine, pin mill, stamp mill, and vibration mill), tumbling or projection (as in ball mill, rod mill and autogenous mill), cutting or shreading (as in cutting mill, shear machine, saws and harrows), attrition (as in colloid mill, petit pulverizer and fluid energy mill) and other methods (such as thermal decrepitation, chemical, ultrasonic, electrohydraulic crushing, etc.).

This research will focus on crushing process utilizing compressive loading, as this method performs the major comminution task in the industry in terms of tonnage handled. Also, since this research is based on the study of the behavior of particles [1] within particle beds subjected to compressive loading, the findings will moslty relate to comminution devices such as jaw and gyratory crushers.

In passing, it may be worthwhile to mention here that in tumbling or projection machines (such as ball or rod mills) the comminution action of the particles takes place between the balls or rods in jostling in the lift up, in the rolling action, and in the impact during falling down, whereas, the comminution action in the crushers under study is from compressive loading. It has been observed that compressive comminution is many times more efficient than impact comminution (as in tumbling mills), but about 85% of the total comminution energy needed in a typical industrial installation goes for fine grinding or milling operation using tumbling mills. Typically a conventional crushing circuit is generally set up with three stages of crushing and one to three stages of fine grinding or milling.

---

[1] meaning fragments of materials regardless of shape and size

Currently, equipment manufacturers are focussing their attention to upgrade and retrofit conventional crushing equipment for fine crushing or grinding so that the new generation crushers (such as water-flush high speed cone crusher) can be progressively substituted for the tumbling machines. By applying as much of the total energy used in the comminution circuit as possible to the crushing portion, overall energy savings can be realized. This also indicates why research on compressive comminution is important.

The particles used in this research were spherical in shape (the reason being explained in Chapter 2) and they were of brittle material (glass) as compressive loading in crushing machines is best suited for brittle materials to achieve high fracture efficiency. Since the previous researchers at MIT had been using glass spheres for their study, use of glass spheres in this research maintained continuity.

Following the earlier research work of Kurfess, experiments were done on single spherical glass and plastic spheres subject to multiple loads to determine a meaningful failure criteria [2]. In her research secondary loads in the equitorial plane of the sphere (i.e. normal to the primary axial load direction) were about 25% in magnitude of the primary load. However, in the current research the secondary loads approached the primary load in magnitude. These results are discussed in Chapter 4.

Experiments on particle beds (as are present in devices used in practical crushing operations which handle a large throughput) extended the scope of the recent work of Ghaddar, who established a qualitative measure of the "bed efficiency"[2] [3]. In the current research variation of bed efficiency with the following interesting parameters was studied in depth:

---

[2]defined as the ratio of the energy required to fracture an individual particle crushed between two rigid flat plates to that required to fracture a similar particle within a particle bed - the definition being at least a first order approximation of the efficiency of crushing process due to primary fracturing within a particle bed.

- bed thickness, expressed in particle diameters,
- rate and amount of compression,
- size distribution within the original bed before crushing,
- boundary motion causing a combined compression and shearing action,
- friction from the wall of the crushing chamber,
- hardness of the crushing elements, and
- local load concentration within bed due to the inclusion of large strong particles.

Limited experiments were also conducted with beds of granular sand, and similarities in behavior compared to those of beds of uniform-sized spheres were noticed.

The scope of this research also includes a thorough literature survey on fluidization of binary mixtures of particles and their segregation behavior since the comminution research at MIT is currently focussed on exploring the feasibility of fluidized transport of fines from the crushing chamber to enhance the comminution efficiency [4]. The primary objective of fluidization research outside MIT (fluidized bed combustion, catalytic coversion, etc.) is the attainment of a well-mixed mixture of particles which is quite opposite to the current goals. This study strengthened the understanding of the fluidization process so that certain conclusions could be made as to the way fluidization can be helpful to meet the current objectives. The conditions or situations which are detriminental to the objectives of other fluidized bed experiments turn out to be the pillars of success for the current experiments. This study, augmented by group discussions and experimental verifications by Annis who investigated the segregation control of binary size particles in a comminution device [5], promoted the further understanding of the process of crushing and fluidized transport of fines within a comminution machine.

Finally, this research culminates in the conceptualization of a new high-efficiency

crushing machine. The knowledge from the various useful findings of the comminution research at MIT leads to the design process of a new generation crushing machine and provides future research directions for further improvement and refinement of such a machine, as will be presented in chapters 5 and 6.

Chapter 2

Background

2.1 Preview

The physics of particle breakage is a vast and complicated subject. Bilby (1979) made a review of this with nearly three hundred references [6]. In this background survey previous research work on particle breakage and the behavior of particle beds under compressive loading (such as within a crusher) has been reviewed. Transport of material into, through, and out of the crusher governs the efficiency of a comminution device, and one efficient process of material transport is the fluidized transport of the fine materials from the crushing zone.

With the advent of a new generation crushing machine concept at MIT, which integrates both the crushing and fluidized transport, it was necessary to gain a thorough understanding of the fluidization science as well, particularly from the point of view of removing the fines from a mixture of fine and coarse particles and segregating the uncrushed or partly crushed particles. The importance of this will be explained later. Therefore, a review of literature related to fluidization is also presented, the findings of which will be utilized later for the guidance of further experimental research.

The background study has been divided into several sections under appropriate headings. This review has been made from a more or less qualitative stand point. Sources of empirical correlations have been cited but in most cases the correlations have not been presented in the text for the purpose of brevity.

2.2 Comminution Theories

Various laws and theories relating energy for breakage of single particles to simple parameters, such as characteristic dimensions of feed and product, were advanced by various researchers over the years.[3]. A review of such works has been given by Prasher, Larson and Laffey.[4] and therefore not repeated here. There is much disagreement between these theories and most of them cover only a limited range of size, particle characteristics, and other variables. These theories are thus inadequate to express the test-found relationship between applied energy and some chosen size-reduction parameters. Furthermore, the practical comminution process, which processes very large numbers of particles in particle beds, is far too complex for such elementary concepts describing single particle behavior to be applicable, according to Austin ([19], and [20]) and Austin and Luckie ([21]).

2.3 Past Research on Comminution

Past research on comminution, as summarized by Prasher in his *Crushing and Grinding Process Handbook* [16], focusses on the following major topics:

- fracture physics in the context of size reduction,
- controlled fracture tests involving the measurement of size distributions and the energy for breakage with (a) single particles or (b) particle beds,
- size reduction and classification in laboratory and pilot scale mills,
- scale-up from small to large mills,
- mathematical simulation of the comminution process and particle transport in moving beds and classification,
- mathematical modelling for comminution product size distribution, throughput capactiy and power consumption, and

---

[3] [7], [8], [9], [10], [11], [12], [13], [14], and [15]

[4] [16], [17] and [18]

- new methods of comminution.

However, single particle studies in fracture physics have received more attention than assemblages of fragments. A great deal of effort has also gone into the study of particle shape and size distribution of the comminuted products. But since the current research is focussed primarily on the enhancement of efficiency of primary breakage within a crushing machine regardless of product shape or size, a detailed review of such topics is omitted, but some of the more general research findings may be summarized as follows:

- particles get stronger as their size decreases due to depletion of the flaws within the particles during size reduction,
- when a brittle particle is stressed by an applied force, particle degradation is intense in the immediate area of force contact. Fines are derived chiefly from these cone shaped zones and a much coarser grade from the rest of the particles,
- the rate of application of force is more important for visco-elastic material than for brittle materials. Visco-elastic materials are better fractured by high-speed (impact) than by slow-speed compression,
- the size distribution from primary breakage is usually bimodal,
- there is a critical particle size below which transition from elastic to plastic behavior for brittle material takes place,
- the particle size distribution of the different products of comminution from homogeneous brittle material can be reduced to a single self-similar and self-preserving size spectra. This is done by nondimensionalizing the particle size of a given distribution with reference to the median size of the distribution,
- the characteristics of the self-preserving particle size distribution are specific to the combination of feed material and the type of the comminution device, but independent of the size or most of the operating conditions of the size reduction device,
- complete particle size distribution of the comminuted product for a given specific energy (kWh/kg) expenditure on the size reduction device can be predicted using Charles-type energy-size reduction relation,
- compression yields a higher energy utilization than impact, especially in particle bed comminution,
- a monomodal product density size distribution pattern gradually emerges with continued comminution beyond primary breakage, and

- repeated fracture produces more fines than that produced by single fracture for the same expenditure of applied energy.

Some industrial research work leading to comminution efficiency improvement and design of new generation comminution machines are noteworthy. Schonert[5] developed a roll-press as an alternative to tumbling mill. Karra[6] worked on the development of a new cone crusher which has the potential to replace tumbling mills (which are notoriously inefficient comminution devices).

2.3.1 Research on Particle Breakage at MIT

Researchers at MIT have looked at comminution through theoretical and empirical studies, as well as computer simulation. The ultimate intention of these inquiries has been to find out which loading and bed conditions maximize the failure of particles within a particle bed under compression (or crushing external load).

Though real comminution machines process granular materials, only spherical, brittle (glass) particles were tested, as a starting point, to keep things simple because these have a sharp and distinct failure. One can avoid complexity due to shape and orientation variables by using spheres. Glass is easily available in uniform spherical shapes and has been used previously by other researchers. Again, comminution by compression loading which is being studied at MIT as a start, is better suited to brittle than to plastic particles.

Cubic or cylindrical particles of glass are also easily available but were not considered since earlier studies have shown that these shapes cause load concentrations at any irregularity on the platen surface supplying the force or on the particle surface, causing longitudinal cleavage. Another difficulty noticed by Obert is that particle and platen

---

[5] [22], [23], [24]

[6] [25], [26]

expand laterally by different amounts under applied force, causing a friction force between platen and particle [27]. Another good reason for using spheres is what Hiramatsu and Oka have shown that spheres have similar internal stress distribution patterns under compression as irregularly shaped specimens, as long as the local curvature of the specimen is not very different from that of a sphere [28]. Finally, Snow and Paulding have found that density-size distributions from breakage of irregularly shaped particles are not dissimilar from those obtained from the breakage of spheres under similar conditions [29].

Larson, experimenting on small individual glass spheres, empirically related failure force and fracture energy to size of the particle [17]. Figure 2-1 shows these relations.

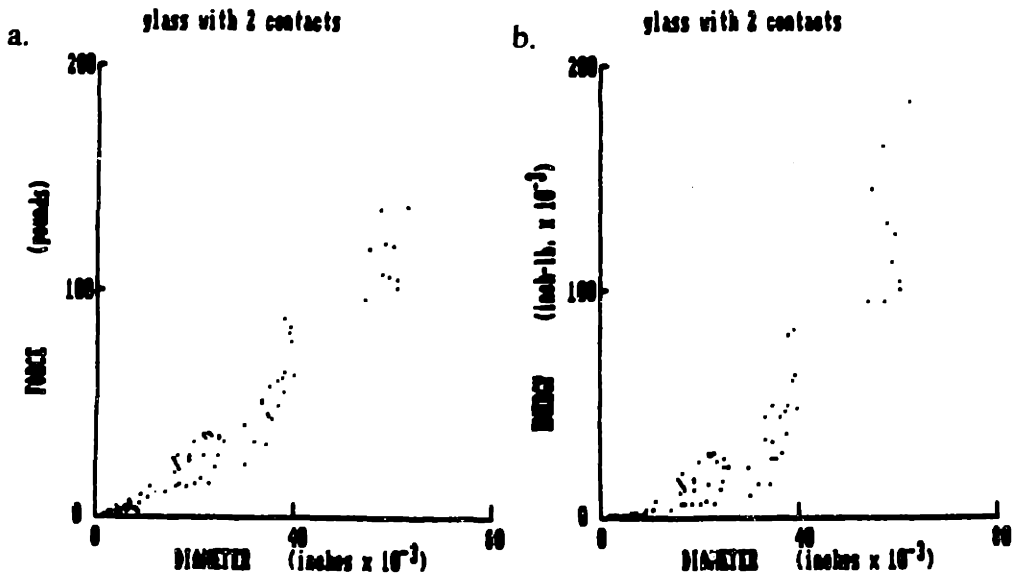

Figure 2-1: Typical glass spheres fracture data [from Larson 86]
(a) crushing force vs. diameter; (b) fracture energy vs. diameter.

Application of load on particles in a particle bed (as within a real crushing machine) is hardly ever through two diametrically opposite points, and therefore, the selection of an

appropriate failure criteria for brittle spheres under multiple-loading conditions is very important. Kurfess, subjecting one-inch glass spheres between flat platens to opposing primary or axial loads and then to such primary loads plus lateral loads in the equitorial plane of the sphere (i.e. normal to the axial load direction), found no inhibiting effect on fracture stress from lateral loading, even when the lateral loads were upto 25% of the axial failure load in magnitude [2].

Easter wrote a computer program to calculate the approximate stress distribution within elastic spheres under multiple loading conditions and found that catastrophic failure or primary fracture is a very local phenomenon under the primary load and is essentially independent of loads at other locations [30].

Laffey experimented with particle beds of 2 mm nominal diameter glass spheres, as well as with a binary mixture of 2 mm and 0.3 mm glass spheres [18]. The force displacement curve for beds of single-sized spheres (2 mm) shows a first region with the force on the bed rising as the bed is compressed and packed, a middle region with decreased slope of the curve but with several large peaks as the compression increases and a third region where the slope becomes relatively constant but steeper. In the first region the particles shift and form a more compact and ordered structure, while the force level builds up with continuing compression of the bed. A few particles fail as the local stress on individual sphere exceeds a size-dependent critical value. In the middle region the fluctuations of the load with continuing bed compression (which is repeatable in experiments) are explained by the development of load-bearing structures within the bed due to wall and particle-to-particle friction and subsequent collapse of this structure triggered by the failure of some key particles. Bed conditions, such as ordered or disordered packing, may also cause this bed behavior as the bed shifts from random to more ordered arrays which causes major peaks in load which in turn collapse again due to the failure of temporary load bearing structures in random portions of the

bed. In a deeper bed the packing is normally random on the top portion of the bed while the bottom is packed more orderly.

Laffey also noted that the particles at the top of the bed fail first and the failure progresses downward as the compression on the bed continues. This behavior is repeatable and may be due to the effect of friction from the wall causing a difference in bed packing between the top and bottom of the particle bed. Another most important observation was that the presence of fine materials around larger particles protects the large particles from failure by more evenly distributing the local force through an increased number of contact points, thus promoting a packing condition within the bed and causing a blunting effect on the force. The fines simply occupy the crusher cavity volume and do not undergo any significant size reduction. This indicates that fines should be removed from the crushing zone as soon as they are formed. Figure 2-2 shows the force-deflection curves with various bed conditions.

Laffey's experimental work was complimented by computer simulation of a two-dimensional bed of spheres (as a start) initially by Drlik [31] and then by Pflueger, who used a more flexible program [32]. The program simulates the behavior of a two dimensional bed containing about 100 to 150 spheres, each of which breaks into small fragments (spheres) when the loads on the sphere exceed a specified failure criterion. Four failure criteria were chosen from which the maximum force criterion gave the best simulation results, consistent with Laffey's experimental work on particle beds, as well as with work on individual brittle spheres. Figure 2-3 shows the build-up and collapse of frictional load structures, breakage of particles due to particle-to-particle and partricle-to-boundary forces (shown by vectors with the line thickness proportional to force magnitude) and simulated bed behavior showing particle damage for maximum force and maximum shear criteria.

Figure 2-4 shows the variation of energy storage and losses with bed compression as calculated by the simulation program.

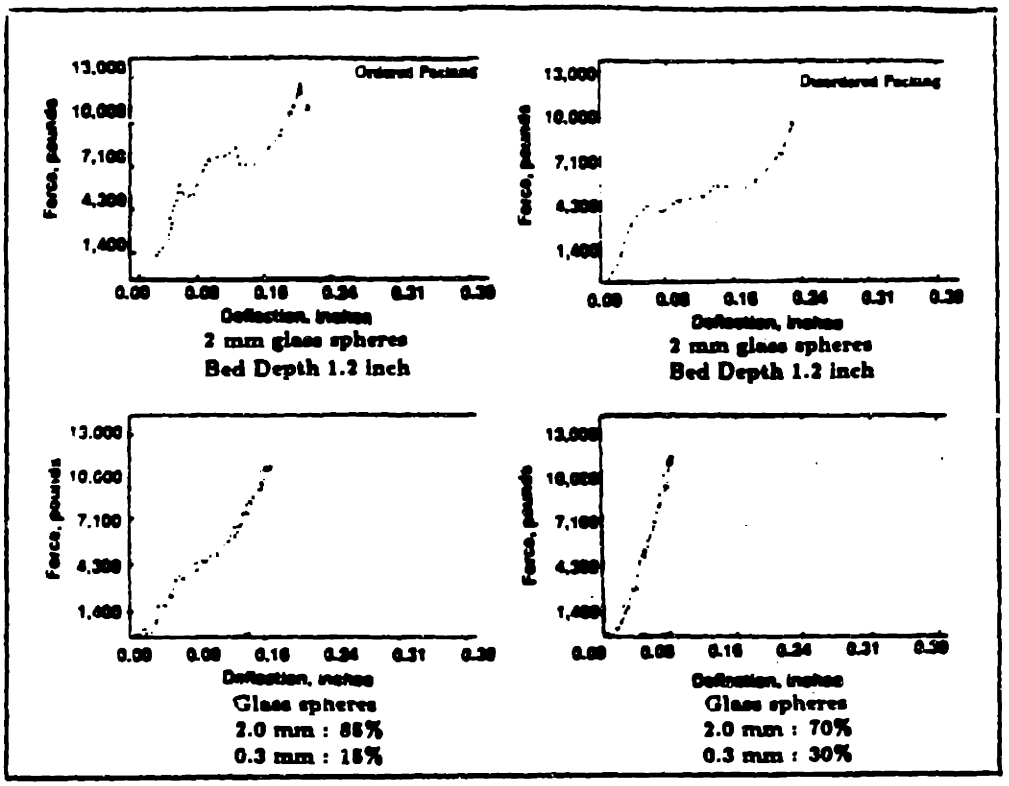

Figure 2-2: Force deflection curves for bed compression with various bed conditions [from Laffey 87]

In a recent work, Ghaddar used a simple first order definition of the fracture efficiency of a particle bed subjected to a crushing load between flat plates (see chapter 1). The energy required to crush a single particle[7] between two flat plates includes energy losses associated with the excessive elastic energy stored within the particles at the moment of frature. Taking the total energy necessary to fracture a single particle under these conditions as the realistc minimum for mechanical devices, this definition of bed

[7] so long it is greater than the critical particle size at which transition from brittle to plastic behavior takes place [33]

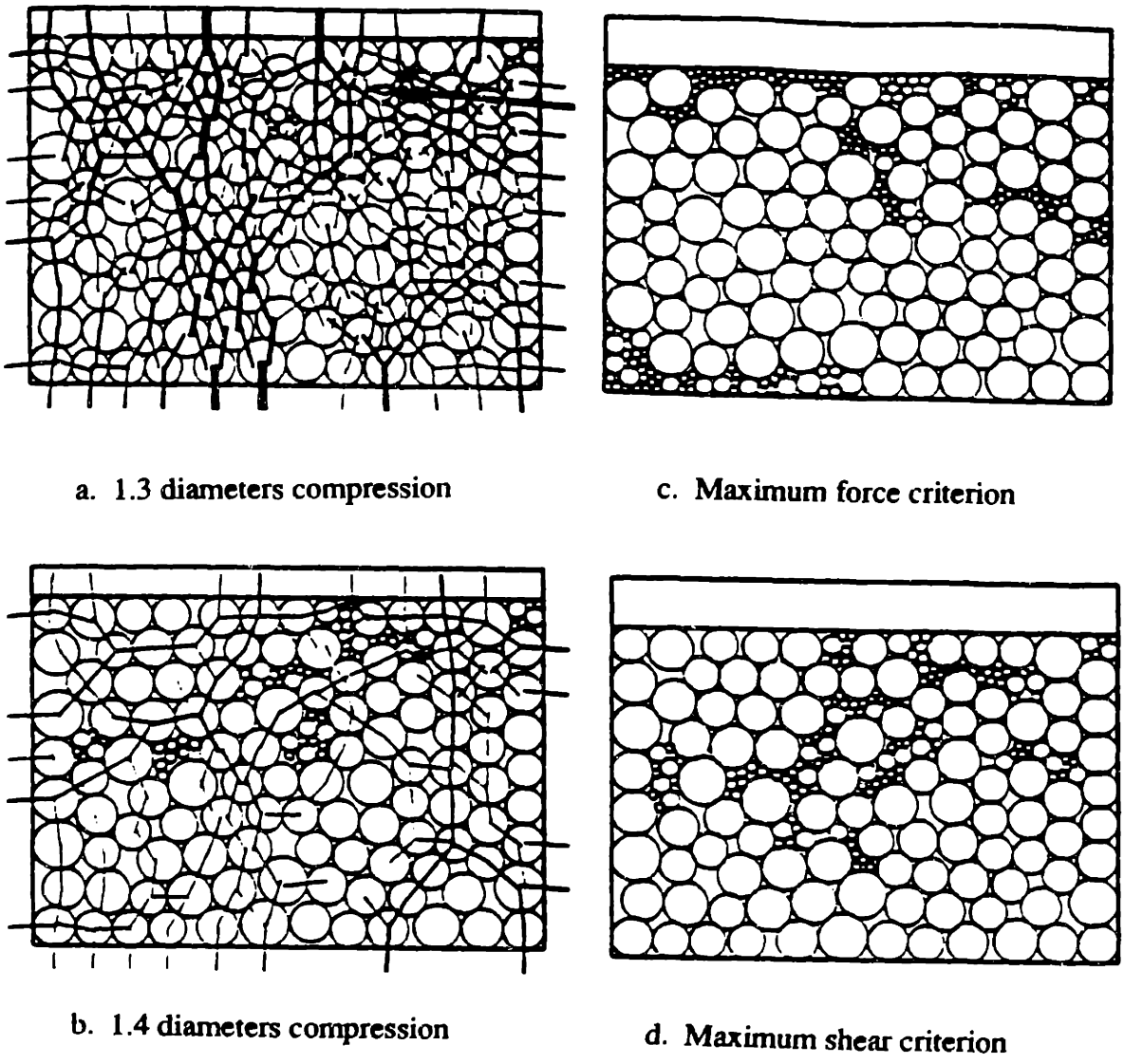

a. 1.3 diameters compression

c. Maximum force criterion

b. 1.4 diameters compression

d. Maximum shear criterion

Figure 2-3: Simulated behavior of particle bed showing particle damage [from Pflueger 88]

(a) & (b) build-up and collapse of frictional load structures; (c) bed behavior for maximum force criterion; (d) bed behavior for maximum shear criterion.

efficiency is then a measure of the additional energy losses which arise because of particle bed behavior. This efficiency is a function of bed conditions which might be controllable by design to improve the efficiency. This definition, however, considers only the crushing of full sized particles as primary fractures (catastrophic failure under excessive point loads).

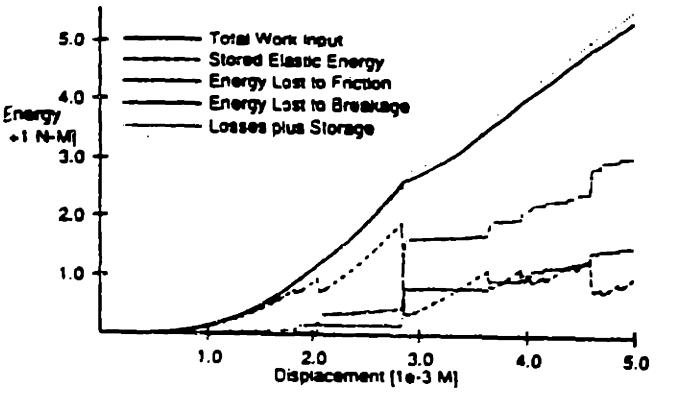

Figure 2-4: Bed energy storage and losses [from Pflueger 88]

Ghaddar's experiments suggest that primary fractures are the dominant fractures taking place within a bed, at least up to the optimum % compression, at which state the original inter-particle void volumes are filled or nearly so by the fines produced due to crushing. Further discussion on this bed efficiency and its usefullness, as well as applicability to crushing of beds of granular materials, will be provided later in this thesis.

Ghaddar also found that this efficiency displays a maximum value at an optimum compression of the bed (at about 18-22% compression for a bed of uniformly sized spherical brittle particles) while dropping off at higher or lower compression. This behavior is related to the force-deflection behavior of the bed as noted by both Laffey and Ghaddar.

2.4 Research on Material Transport

2.4.1 Introduction

As pointed out earlier, the process of material transport into, through, and out of the crushing zone of a comminution device significantly affects its performance efficiency. Also, the importance of prompt removal of fines in between crushing strokes and size-wise segregation of the uncrushed or partly crushed material within the crushing zone was discussed earlier. Fluidized transport offers promise of achieving all the desired goals of the material transport process.

In conventional jaw or gyratory crushers, as shown in Figures 2-5 and 2-6, the exit through-flow area is limited by the desired product size. This becomes a disadvantage and causes a choking problem if a very fine product size is desired. In fluidization processes the size of the fine product elutriating out of the fluidized bed can be be controlled by the superficial fluid velocity. Therefore, the product size is not controlled by the exit opening. This is an advantage of the fluidized transport process over the gravity transport process in conventional crushers since choking problems could be avoided and large throughputs can be achieved. Another advantage of the fluidized material transport system is that it can handle the entire material transport into, through, and out of the crusher. Also, saving in energy consumption due to increase in crushing efficiency (which is the most energy intensive item in the beneficiation process) should exceed the energy requirement of the fluidized transport process.

Maximizing fines removal and coarse particle segregation requires a basic understanding of the transport behavior of a mixture of particles within a fluidized bed. As a start, one can imagine the crushing zone as an intermittently fluidized bed during the time interval between two consecutive crushing strokes, i.e., when the crushing element or piston receeds from the crushing wall surface, say within a Jaw Crusher.

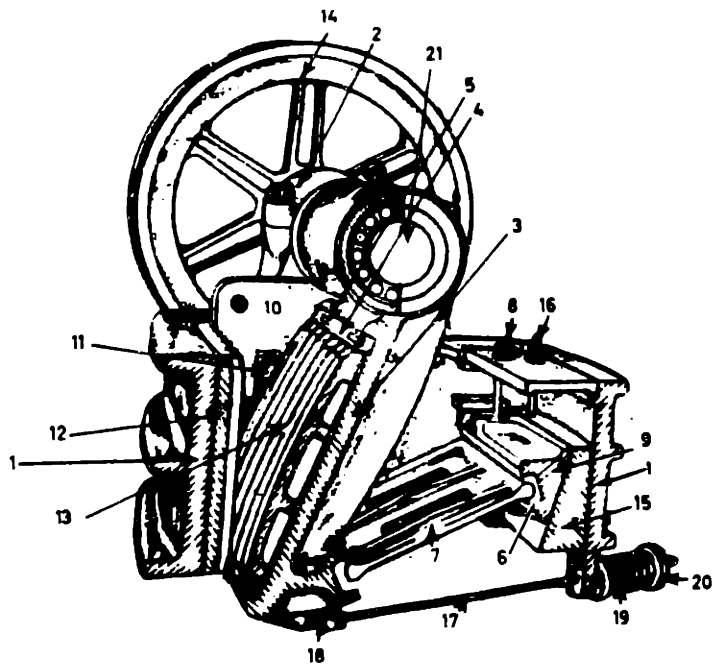

Figure 2-5: Jaw crusher

Single-toggle jaw crusher: 1. main frame; 2. main journal caps; 3., 4. & 5. swingstock, wedge & bolts; 6., 7., 8. & 9. toggle cushion, toggle, bolts & block; 10. & 11. cheek plates & bolts; 12. fixed jaw face; 13. swing jaw face; 14. flywheel; 15. & 16. adjusting wedge & bolts; 17., 18., 19. & 20. drawback rod, bolt, spring and coverplate; 21. eccentric shaft. (Courtsey Newell Dunford Ltd.)

The material within the crushing zone could be considered as a first approximation to be a binary mixture of particles, the coarse one representing the large-sized uncrushed or partly crushed feed material and the fines representing the desired fine-sized output produced during the compression stroke. In fact, it has been observed that the size distribution of products from primary fracture of single brittle spherical particles or particle beds is usually bimodal. Arbiter et al. produced Figures 2-7 (a) and (b) for the size distribution of products from primary fracture of 1 inch diameter glass spheres due

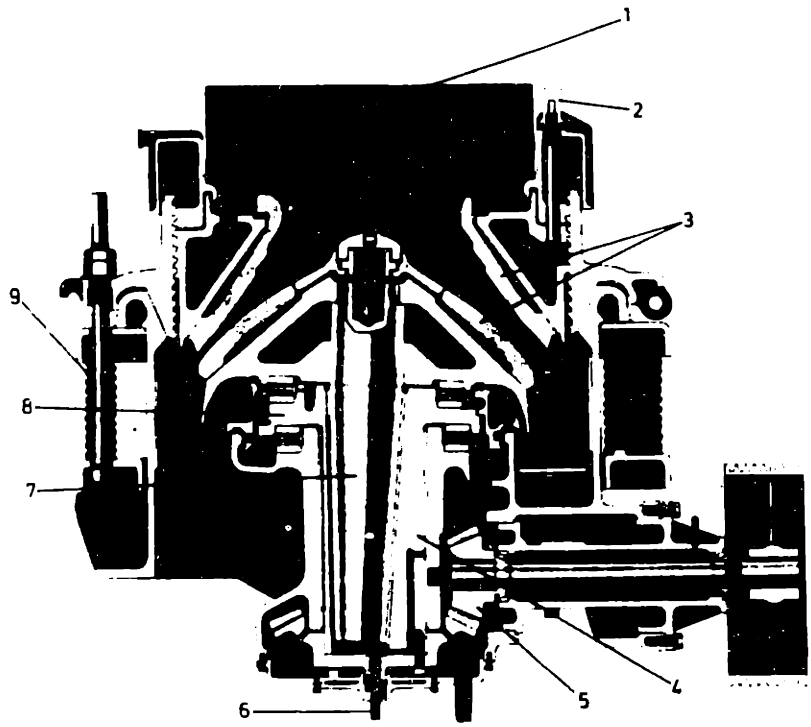

Figure 2-6: Gyratory crusher

Gyrosphere gyratory crusher: 1. hopper; 2. discharge size adjustment; 3. crushing members; 4. eccentric; 5. drive gear; 6. oil supply; 7. main shaft; 8. cam; 9. spring relief. (Courtsey Pegson Ltd.)

to slow compression where one can see that for all practical purposes the size distribution is almost bimodal (since in practical crushing machines product sizes about one sixth of the size of the original particle is considered fine) [34]. Therefore, as a first approximation it will be reasonable to model the particle bed within the crusher as a binary mixture. This topic will be dealt in more detail in chapter 4.

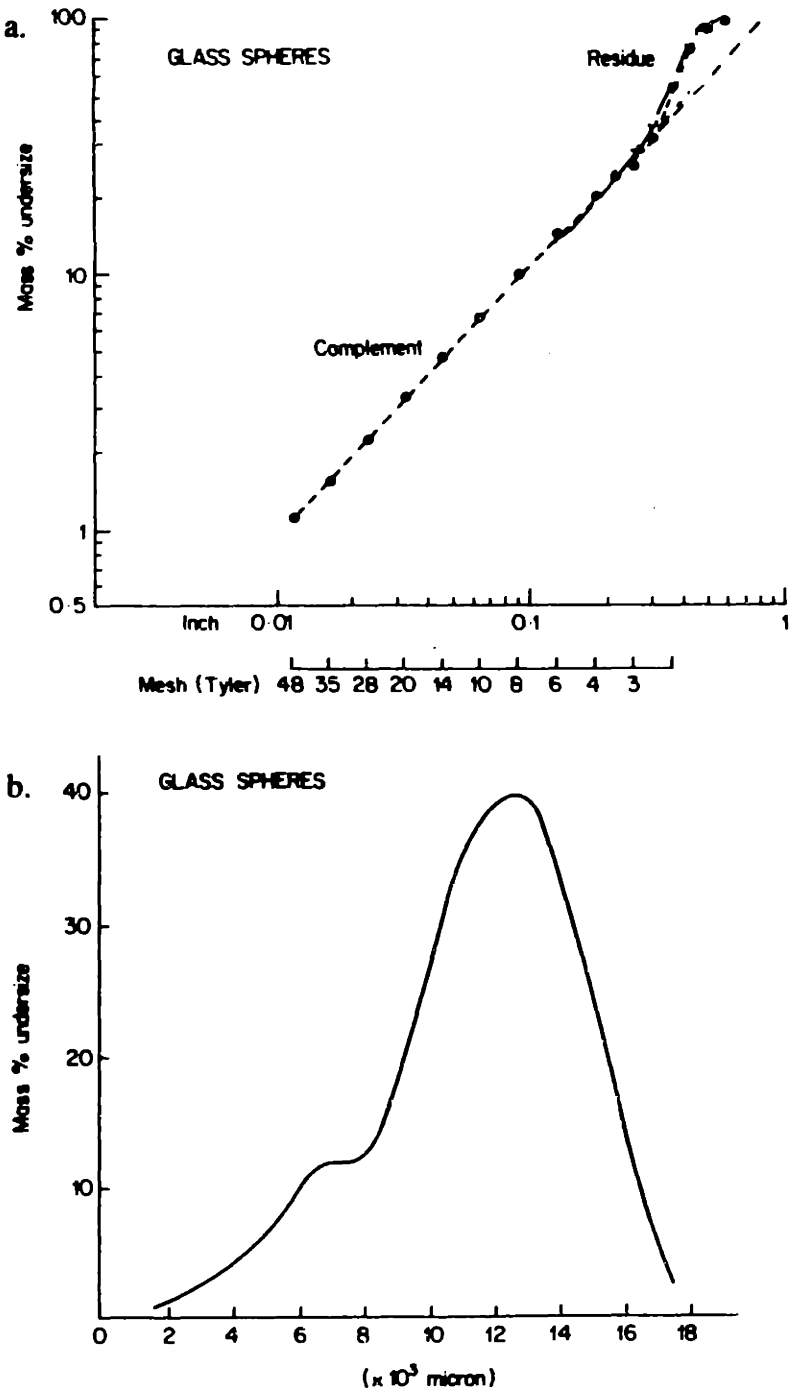

Figure 2-7: Size distribution of products from primary fracture of 1 inch diameter glass spheres [from Arbiter et al., 69]

(a) Cumulative-size distribution from breakage of 1 inch diameter glass spheres by slow compression; (b) Density-size distribution from breakage of 1 inch diameter glass spheres by slow compression.

2.4.2 General Background

Fluidization takes place when a bed of solid particles comes in contact with a vertical upward fluid flow, in a low to intermediate range of flow rates or fluid velocity, where each particle becomes individually suspended in the fluid flow, while on the whole the bed remains motionless relative to the fluidizing column walls. For better fluidization:

- the inlet or homogenizing section of a fluidized bed has to produce a uniform fluid velocity distribution throughout the entire cross section to avoid channeling or gulf-streaming, and
- the distributor, which constitutes the bottom of the fluidizing column, must support the solid particles when they are not fluidized while allowing the flow of fluid through it.

At low flow rates or velocities the particles lie on one another and on the porous bottom of the fluidizing column and are said to be in a fixed state. At high flow rates or velocities, the solid particles are conveyed out of the column, which is known as hydraulic or pneumatic transport. The minimum fluidization velocity is the superficial fluid velocity, u_{mf} , as calculated through a completely open section of the fluidizing column, at which the bed just lifts up and is suspended. This is accompanied by some bed expansion, but nothing is conveyed out. Terminal velocity, u_t, is the velocity of the free fall of a single particle through a fluid medium. u_{mf} and u_t for spherical and nonspherical paricles can be calculated using various formulae which are given in various fluidization engineering text books, e.g., Kunii and Levenspiel [35].

It should be noted here that for non-spherical partcles a term called *sphericity*, ϕ_s, is incorporated in such formulae, which is the ratio of the surface of a sphere to the surface of a particle, both of the same volume; another term, mean diameter $\overline{d}_p$ is used in such calculations for a mixture of particles of different sizes. (Reference: Fluidization Engineering by Kunii & Levenspiel, Chapter 3). The ratio u_t/u_{mf} is a measure for flexibility of fluidization and an indication of the maximum possible height

of the fluidized bed. This ratio is smaller for large-sized particles and bigger for small-sized particles, whereas u_{mf} increases with size for a bed containing uniform-sized particles. Thus for a mixture of particles the superficial fluid velocity should be more than the u_t of fine particles to carry the fines away but equal to or slightly more than the u_{mf} of the coarse-sized particles.

In fluidization two different behaviors have been noticed, i.e., particulate and aggregative fluidizations, corresponding approximately to the liquid-solid and gas-solid systems. In liquid-solid fluidization the operation is stable with a spatially uniformly distributed concentration of solid partricles. Bed expansion is regular, with a continuous increase of the inter-particle distance, from fixed bed to hydraulic transport. Particulate fluidized bed is also known as homogeneously fluidized bed, a smoothly fluidized bed or simply a liquid fluidized bed.

Sometimes channeling, characterized by locally organized solid movements with vertical upward motions in some regions and downward motions in others, is observed in liquid fluidized bed which can be linked to maldistribution of liquid at the bottom of the bed. However, channeling can be avoided with a homogenizing section and a better distributor at the inlet.

Parvoids or low density high-voidage horizontal bands, about one centimeter deep, are often observed in liquid fluidized bed. They originate near the distributor and propagate in succession upward where they evanesce. They may occupy the whole section of the column or a portion of it depending upon the flow rate. Propagation results from the raining of solids from its top to its bottom. This is due to the natural instability of the fluidized bed and is unavoidable. However, unlike bubbles in gas-fluidized beds, parvoids do not affect segregation much.

Gas-solid fluidization systems behave in a different way. With an increase in flow rate beyond minimum fluidization, large instabilities with bubbling and channeling of gas

are observed. At high flow rates there is more vigorous solid movement and the bed does not expand much beyond its volume at minimum fluidization. Gas-solid fluidized bed is called an aggregative fluidized bed, a heterogeneously fluidized bed or a bubbling fluidized bed.

At sufficiently high fluid flow rate, in either gas or liquid fluidized bed, the terminal velocity of the solids is exceeded. This is associated with the disappearance of the upper surface of the bed and transport of the solids with the fluid. This is known as lean phase fluidization with pneumatic transport. Figure 2-8 shows various modes of fluidization.

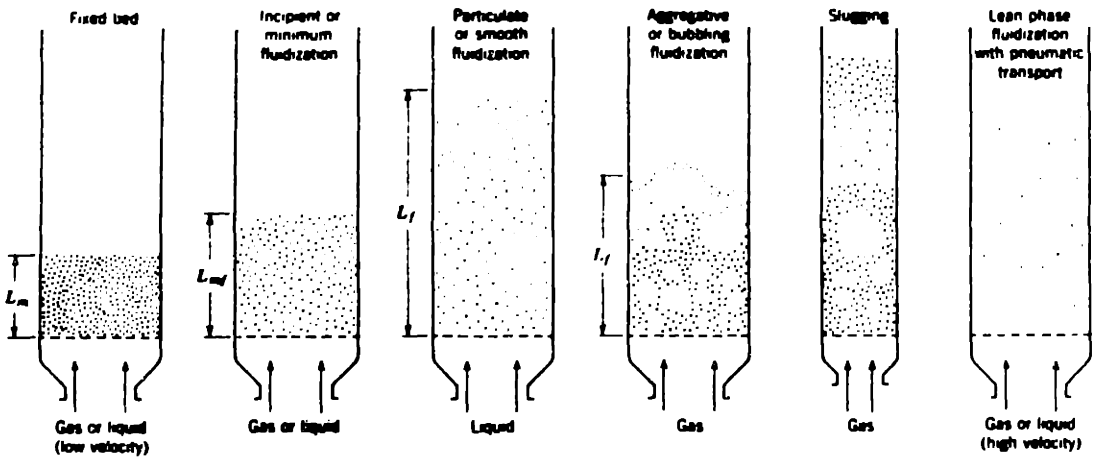

Figure 2-8: Various kinds of contacting of a batch of solids by fluid [From Kunii and Levenspiel : Fluidization Engineering]

As noted earlier, the range of operation of gas velocities to achieve elutriation of fines and segregation of coarse-sized particles is very limited because of the compressibility of the gas, since the pressure drop through the bed causes an increase in gas velocity near the top of the fluidizing column. Wilhelm and Kwauk suggested the use of

Froude group at minimum fluidization,[8] as a criterion for fluidization behavior [36]. For $Fr < 1$, the aggregative behavior is noticed, whereas for $Fr > 1$ the particulate behavior dominates. For Fr value of the order of 1, particulate behavior is noticed only with liquid-solid systems with very dense solids or with gas-solid systems with fines and light solid particles or dense gas under pressure. Other researchers have suggested the use of Archemedes number[9]. Gas-solid systems generally show an aggregative fluidization behavior commonly associated with bubbles which form at the bottom of the bed and rise through the system coalescing and increasing in size and thus causing considerable mixing. This is very detrimental, if the purpose of fluidization is to remove only the fines and segregate the coarser particles. With this background this research will only focus on particulate fluidization process.

2.4.3 Previous Research on Segregation in Fluidized Beds

Most of the past research work in fluidization has been focussed on how to eliminate segregation and elutriation of fines since the objective of many fluidized bed operations is to mix particles thoroughly for better combustion, catalytic conversions or other chemical processes without losing (or limiting the loss of) fines. The following paragraphs summarize some of the more important and relevant research work.

Katz established a criterion for particle segregation to occur in gas-solid fluidized bed with a mixture of particle sizes. The ratio of the minimum fluidizing velocities for two consecutive-sized solid particles should be at least two [37]. Rowe et al. observed that for a binary mixture of particles segregation is particularly sensitive to particle-to-

---

[8] u^2_{mf}/gd_p,
where, u_{mf} = the minium fluidization velocity, g = acceleration due to gravity, and d_p = particle diameter

[9] $d_p^3 g\rho_f(\rho_s - \rho_f)/\mu_f^2$
where, ρ_f and ρ_s = the densities of the solid particles and fluidizing fluid respectively, μ_f = the fluid viscosity, and g and d_p, as defined before.

particle density differences but less sensitive to particle size differences [38]. The degree of separation, expressed as the heavy or large particle concentration remaining in the upper portion of the bed, was found to be proportional to the size ratio (large to small) raised to the power of 0.5, and to the density ratio (heavy to light) raised to the power of 2.5. In comminution processes the ratio of product size to feed size is often the most important factor, though sometimes the density ratio between ore and gangue material is also important. The liberation of valuable minerals from gangue material is enhanced with progressive crushing. It is worthwhile to mention, in passing, that for a strongly segregated system (mixture fluidized at low velocity) the separation is sharp into uniform concentration layers. For a weakly segregated system (mixture fluidized at higher velocity) a slight concentration gradient in either phase of the segregated mixture is noted. Sometimes a transition zone sandwiched between two completely segregated top and bottom layers occurs. Bed porosity or void fraction varies from one end of the column to the other.

Kondukov and Sosna were the first to construct phase equilibrium diagrams for composition versus fluidizing velocity for a bed with a binary mixture of particles [39]. These phase diagrams show the equilibrium concentration of components in both phases of a segregated bed and can be used to select operating velocities for achieving the desired separation. Furthermore, they noticed that segregation occurs at a velocity in between u_{bf} (beginning fluidization velocity at which fine or light particles start to fluidize) and u_{ff} (total fluidization velocity at which large or heavy particles start to fluidize). Chen et al. conducted further research on particle segregation in gas-fluidized beds and found that segregation of particles usually reaches the steady state in less than 30 seconds [40].

Kennedy and Bretton [41] and Dutta et al. [42] attempted to give a theoretical interpretation of experimental data on solid concentration profiles and bed porosities in

a bidisperse liquid fluidized column by visualizing segregation process as diffusional in nature. According to them a diffusional flux is generated in the direction of decreasing concentration similar to that in the case of a nonuniform solution. At steady state this flux is counterbalanced by a convective flux resulting from relative motion between the particles and the liquid. They observed that the dispersion coefficient of a species increases with superficial liquid velocity and bed porosity. In a mixture the particles of larger size have a higher dispersion coefficient.

Fan et al. developed a mathematical model for expansion of a liquid-solid fluidized bed with uniformly sized particles [43] based on the Richardson and Zuki equation which relate bed porosity to fluidizing velocity for a steady state behavior [44]:

$$\frac{u_{ss}}{u_t} = \varepsilon_{ss}^n$$

where, u_{ss} = steady state superficial liquid velocity; u_t = terminal or free falling velocity of particles; ε_{ss} = steady state porosity, dimensionless; and n = an experimentally determined constant which depends on particle diameter, fluidizing column diameter and Reynolds number of flow.

Their model found a relation for the change in fluidizing bed height versus time for a step input in fluidizing velocity, and an expression for the time constant of the bed to attain steady state.

Couderc has tabulated numerous empirical correlations [45] already developed by various researchers relating to:

- expansions of beds of spheres of uniform diameter,
- expansion characteristics of beds of non-spherical particles,
- equations for minimum fluidization velocity, and
- equations for gas-solid fluidized beds.

Noda [46] and Huarui's [47] research on fluidization velocity and bed expansion characteristics of binary particle mixtures of different sizes and densities are

noteworthy. It has been demonstrated that the void fraction[10] - velocity relationship for a liquid fluidized bed is independent of the total mass of particles and fluidizing column diameter when *D* column/*d* particle > 10 to 20.

The expansion properties and minimum fluidization correlations developed for monosized beds are not valid for real beds with a size distribution. Some researchers have suggested that a bed of mixed solids can be considered as a bed of particles of uniform size only by defining a convenient mean diameter. But this averaging model is not suited to predict the behavior (especially, the expansion) of a segregating fluidized bed. It has been noted that for a binary mixture of particles in liquid-fluidized bed, the bed voidage must be below 0.6 and the size ratio d_R of the two particle diameters should be greater than 2.2 for segregation to occur. For a multi-component mixture d_R should refer to that between two consecutive sizes. Other researchers have suggested that for a segregating fluidized bed the bed can be divided into a finite number of parallel layers, each of which constitutes one class of particles which can be analyzed using existing correlations for single-sized fluidized particle bed. Lewis and Bowerman [48] and Richardson and Zaki [44], assuming the overall two or even multi-component fluidized bed expansion to be equal to the sum of each component bed expansion, expressed:

$$H = H_1 + H_2 \text{ and}$$

$$H(1-\varepsilon) = H_1(1-\varepsilon_1) + H_2(1-\varepsilon_2)$$

which can be solved for H, since H_1, ε_1 and H_2, ε_2 for individual components can be calculated using existing correlations.

Here, H is the overall bed height and ε, the hypothetical bed voidage fraction of the combined beds (if considered a single bed) when the two-component bed is just totally fluidized; H_1, H_2 and ε_1 and ε_2 are the bed heights and bed void fractions at minimum fluidization condition for the individual components when fluidized separately.

---

[10] $(V_{column} - V_{solid})/V_{column}$

Huarui et al. experimenting on binary particle mixtures has concluded that the serial model is capable of predicting the bed expansion for a segregating fluidized bed with much accuracy [47]. They also observed that for a mixture there is a velocity range from beginning fluidization to complete fluidization. The beginning fluidization velocity u_{bf} is larger than the fine particle minimum fluidization velocity u_{1f} due to the obstructing effect of the coarse particles on the fine particles. Based on experimental data they expressed:

$$u_{bf}=u_{1f}+(u_{2f}-u_{1f})X_2^a$$

where X_2 = coarse particle fraction in the mixture and a is an experimetally determined exponent value.

They further observed that the complete fluidization velocity u_{ff} was smaller than the coarse particle minimum fluidization velocity u_{2f} due to fluidizing effect of the fine particles on the coarse particles and thus:

$$u_{ff}=u_{2f}-(u_{2f}-u_{1f})X_1^b$$

where X_1 = fine particle fraction in the mixture and b an experimentally determined exponent.

Jean and Fan studied a phenomenon called *solids layer inversion* in a liquid-solid fluidized bed containing binary mixtures of particles that are heavy and small, and light and large [49]. The process occurs when a bed of a binary mixture of solid particles, containing light or small particles in the bottom layer and heavy or big particles in the top layer, is fluidized at a velocity sufficient to cause segregation but not high enough to cause mixing. Upon fluidization the bottom and top layers will reverse their positions and this is known as the solids layer inversion. They proposed a method for the prediction of solids layer inversion velocity in a liquid-solid fluidized bed containing a binary mixture of particles with solid layer inversion properties [49]. It was found from experiments that the segregation velocity for the particle which is at the bottom of the bed at low velocity peaks at the point where solid layer inversion occurs.

Gibilaro [50] and Poncelet et al. [51] threw further light on the unsteady state expansion of liquid-fluidized bed with uniformly sized particles and on the characteristic time to reach steady state following a step change (either step increase or step decrease) in the superficial velocity. They observed that during a suddden increase in fluid superficial velocity, the fluidized bed divides into two zones, first, a top zone with initial porosity (meaning bed voidage or liquid volume fraction), in an upward movement, the height of which decreases with time; secondly, a bottom zone with the final porosity, without ascensional movement, the height of which increases with time. The interface separating the two zones at the height H_a as shown in Figure 2-9 (a), where the porosity transition takes place, moves upwards. At the end of the transient state, the interface disappears: H_a becomes equal to H_f or the total expanded bed height. During a sudden decrease in fluid superficial velocity (which finally causes contraction of the solid-liquid fluidized bed) the bed divides into two zones as in the case of fluidized bed expansion, but in this contraction step the top zone moves downwards and has the lowest porosity. The interface moves upwards and disappears at the end. The total height decreases with time. They developed correlations for the velocity of the porosity transition interface and the characterisitcs time of the transient phase. They also observed that the upward velocity of the porosity transition interface, as well as the velocity at which the top of the bed expands or contracts (depending on whether the step change in superficial velocity is positive or negative) depends only upon the initial and final state of bed porosity and fluid superficial velocity. This results in a linear evolution with time of the total bed height and the height of the porosity transition interface. Figure 2-9 (a) and (b) show this behavior.

However, their treatment of this topic did not take into consideration the time for initial acceleration and final deceleration steps of the solid particles (which time interval according to Gibilaro et al. is very small and negligible) but was based on constant

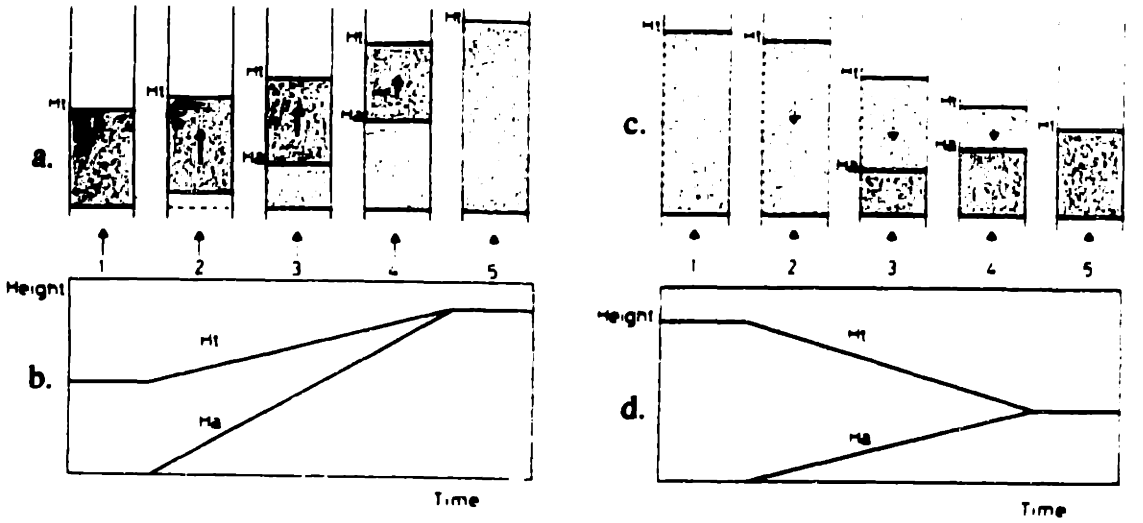

Figure 2-9: Fluidized bed behavior during a step change in fluid superficial velocity [from Poncelet et al., 90]

(a) Evolution of a fluidized bed during an expansion step following a step increase in fluid superficial velocity, u; (b), (d) Evolution of the total bed height, H_t, and the height of the porosity transition interface, H_a, as a function of time; (c) Evolution of a fluidized bed during a contraction step following a step decrease in fluid superficial velocity, u.

velocity of the particles after a step change in fluid superficial velocity). Also these observations are valid mainly in the laminar region of flow.

Patwardhan and Tien [52] proposed a method to predict the porosity transition interface velocity of an initially well mixed bed of binary size or density particles. Knowledge of the segregation time is very important for the conceptual fluid-flushed, upward flow crushing machine, from the production point of view, since segregation may have to take place in between consecutive crushing strokes.

Masliyah et al. experimented on continuous separation of bidisperse suspensions in inclined channels and observed that increasing the angle of inclination resulted in greater degree and faster separation since the vertical height for the segregation interface to travel will be less [53]. However, the separation is not in horizontal layers stacked up on one another which is the objective of the current research at MIT.

Shi et al. reported the findings of their research on tapered (i.e., expanding in the flow direction) fluidized bed [54]. The hydrodynamic features of the tapered fluidized bed are very different from those of the columnar fluidized bed. Much mixing has been observed in this type of bed due to recirculation in the tapered area around the central columnar zone.

2.4.4 Previous Research on Elutriation from Fluidized Beds

For design of a crushing device with fluidized transport of fines, the rate of elutriation of fines and the size distribution of these fine solids in relation to the distribution in the bed and the variation of both these quantities with the location of the exit fluid stream must be known.

Kunii and Levenspiel treated elutriation from gas-fluidized systems very well in "Fluidization Engineering" (chapter 10 and 11). But in this treatment the fluidized bed is of aggregative type and elutriation is not a desired objective. Therefore, the conclusions will not be quite applicable to the current research.

Ganguly researched on elutriation characteristics of solids from liquid fluidized bed systems and introduced the concept of minimum elutriation velocity u_{me}, as the lowest carrying velocity for the particles, which is similar to the terminal settling velocity u_t [55]. The advantage of using u_{me} is that it is based on the actual carrying velocity rather than the velocity assumed in ideal free fall condition. He noted that $u_{me}$is dependent on the free-board height[11]. For a particular fluidizing column, with an increase in the mass of the solids charged, the static bed height H_s increases, consequently decreasing the free-board height H and, hence, the ratio H/H_s is decreased. The velocity above the minimum fluidization velocity required to expand

[11]height of the column which is not occupied by the solids

the bed height up to the full length of the column to initiate elutriation decreases progressively with a decrease in H or H/H_s ratio. Effect of d_t/d_p (ratio of fluidizing tube diameter to particle diameter) has no significant effect on u_{md}, if this ratio is about 10 or more. He also studied the variations of the mass fraction of the elutriating component with various important parameters and obtained the plots shown in Figure 2-10.

2.4.5 Current Research at MIT on Fluidized Bed Segregation

Annis's recent work on segregation control of binary size mixtures of particles in a fluidized bed has shown that:

- overall segregation is fastest with short beds as the separation time varies linearly with bed height,
- pulsation of fluid flow causes more harm to the segregation of taller beds than of shorter beds,
- inclination of the bed from the vertical and the divergence in cross section beyond a few degrees are detrimental to segregation, and
- segregation in gas-fluidized bed occurs within a very narrow range of gas velocity and even then segregation control is very difficult [5].

Results of her research on segregation control of binary size mixture of particles in a fluidized bed are shown in Figures 2-11 to 2-13.

2.4.6 Research Direction

The past research work has been highly empirical and done on a piecemeal basis. However, this provides a solid foundation based on which the current research will:

- explore additional bed conditions and bed compression parameters that could enhance the crushing efficiency,
- identify the optimum parameters for improved material transport to provide quicker removal of generated fines by fluidized transport of the fines and segregation of the coarser particles within the crushing zone before a compression stroke,
- treat the combined crushing and solids transport phenomenon as an integrated process which can be expressed in a mathematical model, and

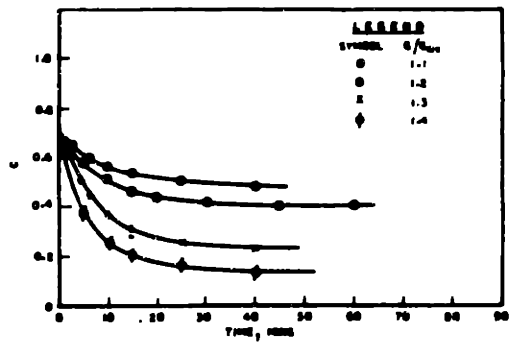

a. Variation of the mass fraction of the elutriating component in the bed with time at different values of: G/G_{me}

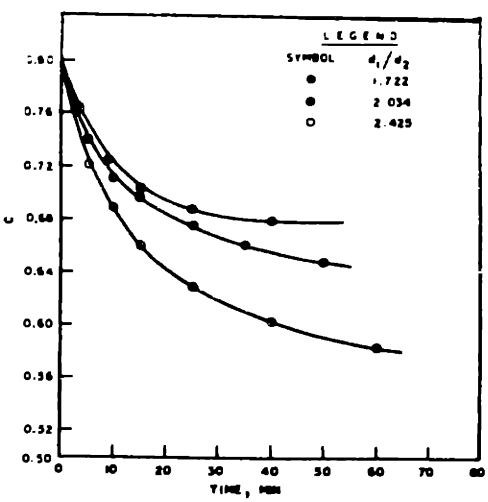

b. Variation of the mass fraction of the elutriating component in the bed with time at different values of: diameter ratio, d_1/d_2

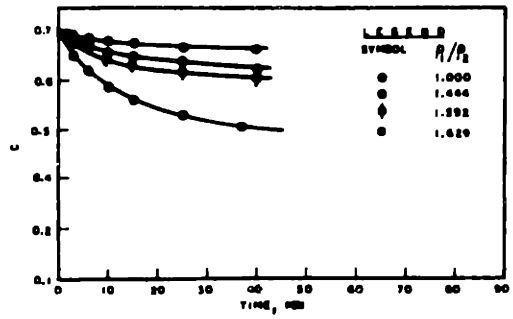

c. Variation of the mass fraction of the elutriating component in the bed with time at different values of: density ratio, ρ_1/ρ_2

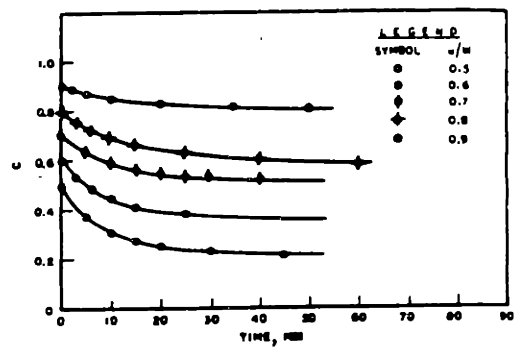

d. Variation of the mass fraction of the elutriating component in the bed with time at different values of: ratio of the free-board to static bed height.

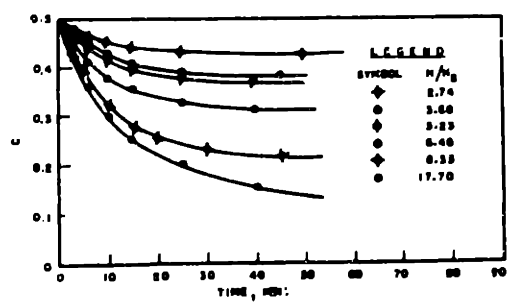

e. Variation of the mass fraction of the elutriating component in the bed with time at different values of: initial concentration of the elutriating component.

Figure 2-10: Variation of the mass fraction of the elutriating component with various important parameters: Figures (a) through (e) [from Ganguly 82]

Nomenclature: c = concentration or mass fraction of elutriating component; G = superficial mass velocity of liquid; G_{me} = minimum elutriation velocity; d_1, d_2 = diameters of binary size particles; ρ_1, ρ_2 = densities of binary size particles; w = mass of the finer/lighter particles in the bed, W = mass of the feed; H = free-board height, H_s = height of the static bed

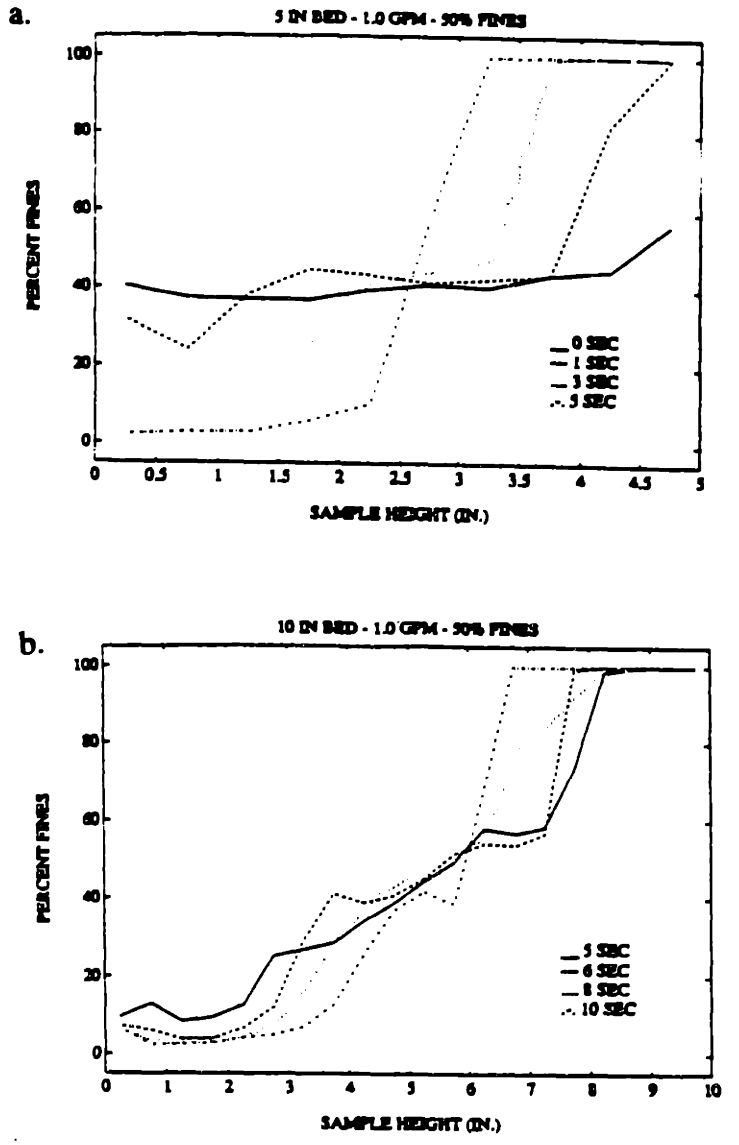

Figure 2-11: Segregation of: (a) 5-inch beds with steady flow at 1.0 GPM; (b) 10-inch beds with steady flow at 1.0 GPM. [Annis 91]

- finally, as a culmination of this research, look for preliminary design parameters for an innovative high-efficieny comminution device.

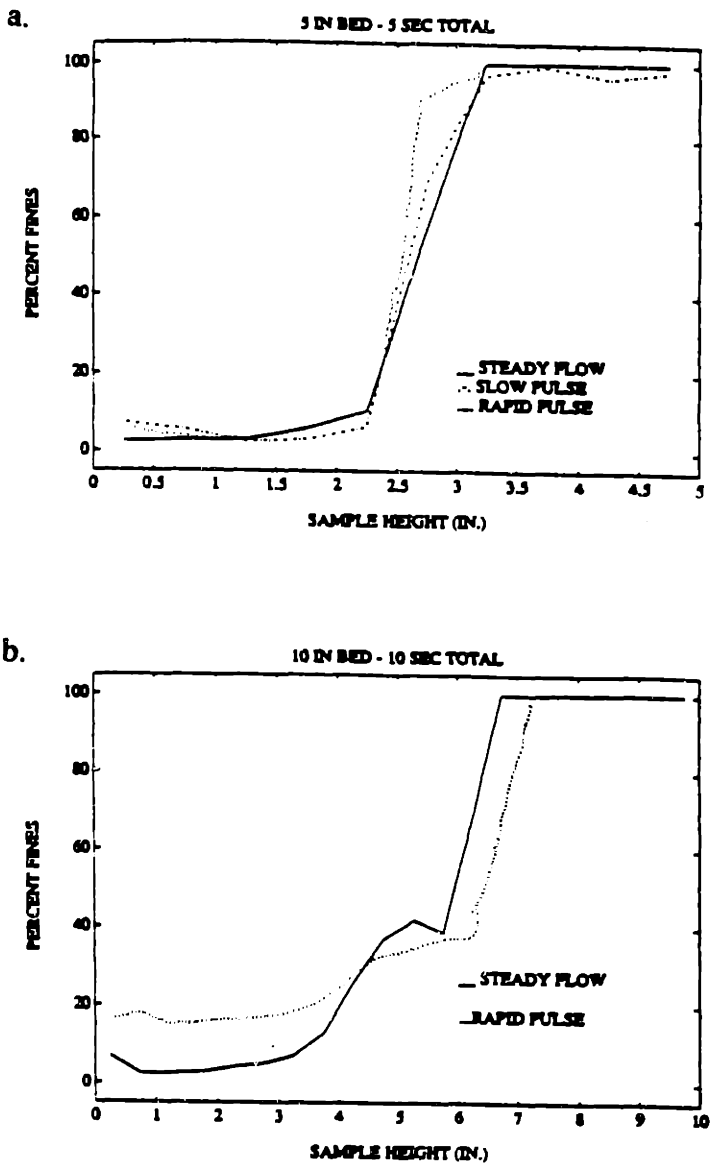

Figure 2-12: Comparison of pulsing to steady flow in: (a) 5 inch beds; (b) 10 inch beds

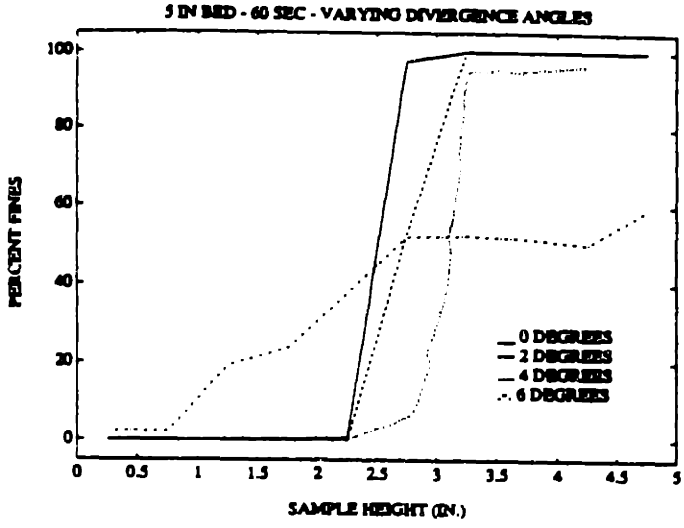

Figure 2-13: Segregation quality of diverging beds

Chapter 3

Problem Statement, Research Needs and Experimental Procedures

The experimental research work on particle breakage and material transport is divided into three parts, i.e., single particle tests, particle bed tests and fluidization tests. The following sections will deal with the respective research objectives and experimental procedures.

3.1 Single Particle Test

Most practical crushing machines crush a bed of particles. But study of the breakage behavior of a particle buried in a bed is difficult since the particle cannot be retained in experimental control. Single particle tests are therefore convenient and important, at least to gain a first order knowledge of a meaningful failure criterion of a particle undergoing comminution. A particle within a bed is acted upon not only by a major load which ultimately causes its fracture (meaning catastrophic failure) but also by numerous other forces which act through the various points of contact of the particle with neighboring particles or with the piston and crushing chamber wall surface. In these single particle tests 1" diameter clear soda lime glass spheres were used for reasons given earlier in chapter 2. The experiments subjected each sphere to opposed loads between parallel plates applied by an Instron 8501 machine, as shown in Figure 3-1. These loads represent the primary axial loads (which ultimately causes the failure of the sphere). Lateral loads were simultaneously applied along the equator of the specimen (i.e. at right angle to the major opposed loads) in a manner described in detail in the following paragraph. Though this simple lateral loading condition does not represent the typical conditions of a particle under confining loads within a particle bed,

it is nevertheless a simplest approximation of that condition and adequate for the present research purposes.

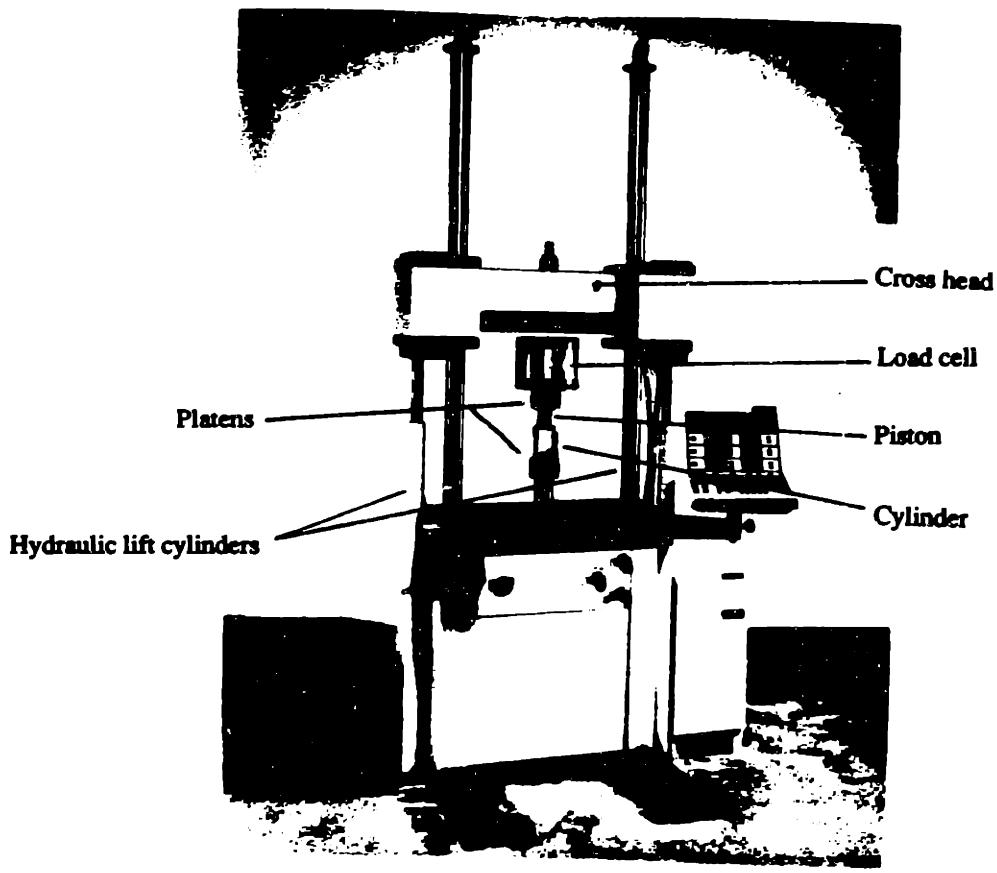

Figure 3-1: Experimental setup for single particle test

The main objective of this test was to determine if secondary or lateral loads in the equitorial plane of a brittle glass sphere, subjected to opposing primary or axial loads between flat plates, has any inhibiting effect on the fracture of the sphere. This was an extension of Kurfess's work to a situation where the lateral loads approached the primary loads in magnitude.

A steel cylinder with a removable base (working as a fixed piston) as shown in Figure 3-2 was mounted on the lower platen of the Instron machine. A sphere was placed in

the steel cylinder in the middle of the removable steel piston base, allowed to settle, and then the hydraulic cylinders (described later) of the lateral loading mechanism as shown in Figure 3-3 were activated to give just enough force to hold the sphere in position. The upper steel piston was then inserted from the top and the Instron machine activated to apply primary load on the upper piston. The removable base and the steel piston were in-laid with tungsten carbide inserts at the center of their contact surface with the sphere. The Instron 8501 machine transferred the primary load to the sphere inside the cylinder through pistons and the base. The upper platen of the Instron machine was kept fixed while the lower platen moved upward at a slow compression rate of about 0.001"/second. For some experiments compression rates were increased to 0.01"/second. The purpose of these experiments was to see the effect of compression rate on the failure load of a glass sphere. Four secondary loads, evenly spaced around the equator of the sphere, were applied by four Dayton hydraulic cylinder rams capable of producing 10,000 pound load (at 10,000 *psi*) with the pressure supplied from a hand pump. The supporting assembly for these rams was a heavy and strong steel frame made out of 1" thick steel plate. During experiment, the steel frame was supported on styrofoam pads placed on the table of the Instron machine. The side loads were transferred from these rams to the sphere by four 1/2" diameter 2" long hard steel dowel pins which passed through the holes in the cylinder wall.

Figure 3-3 shows the scheme for applying the four side loads. Force-displacement graphs were plotted using the computerized plotter of the Instron machine. In different experiments side loads of various magnitudes, all the way up to the primary load, were applied simultaneously, side loads always lagging slightly behind the rising primary load in magnitude.

Experiments with 1" acrylic plastic spheres were similarly conducted to study the effect of lateral loads on primary fracture of plastic materials.

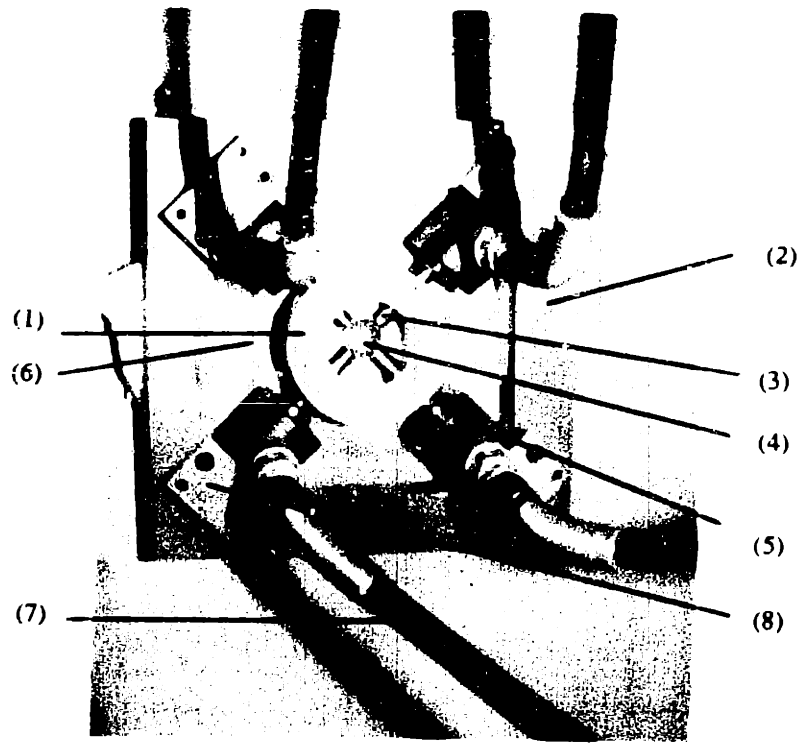

Figure 3-2: Piston-cylinder apparatus for 1" glass sphere fracture test

1. (1) 2" I.D., 3.5" O.D., 2.5" high, hollow mild steel cylinder with four holes, spaced 90° apart at a height of 1" from the bottom, through which 4 dowel pins can pass through with a snug fit. (2) 1" thick, 1.5" wide steel plate with 10.75" x 10.75" O.D. steel plate to which the four hydraulic rams are attached. (3) 0.5" diameter, 1.85" long hard dowel pins (4 in number) which transmits the side loads from the 4 hydraulic rams to the sphere at 4 points, spaced 90° apart in the equitorial plane of the sphere (when the sphere rests on the removable base). (4) 1" diameter soda lime glass sphere. (5) 5 ton maximum capacity Dayton hydraulic rams (4 in number) with 5/8" throw and 0.994 square inch effective piston area, operated by a hand pump, (not shown) connected to it by a 1/4", 10,000 *psi* rated flexible hydraulic hose. These rams are attached to steel brackets (which in turn, are welded to the steel holding frame) by screws. (6) Removable base with a 2" diameter solid steel piece, with a small tungston carbide insert in the center of its top flat surface (the point of contact with the 1" diameter glass sphere), and attached to a 5" square, thick steel base plate by screws (screw heads flushing with the steel base plate surface). This piece is identical to the top piston and can be interchangeably used as a piston. (7) 1/4" I.D., 10,000 *psi* rated flexible hydraulic hose pipes (4 in number) connecting the hand operated pump (not shown here, but shown in Fifgure 3-3) to the hydraulic rams. (8) 0.5" thick, 2" long, 1" high steel anchors or supports (4 in number) for the hydraulic rams, welded to the steel holding frame [item 2 above].

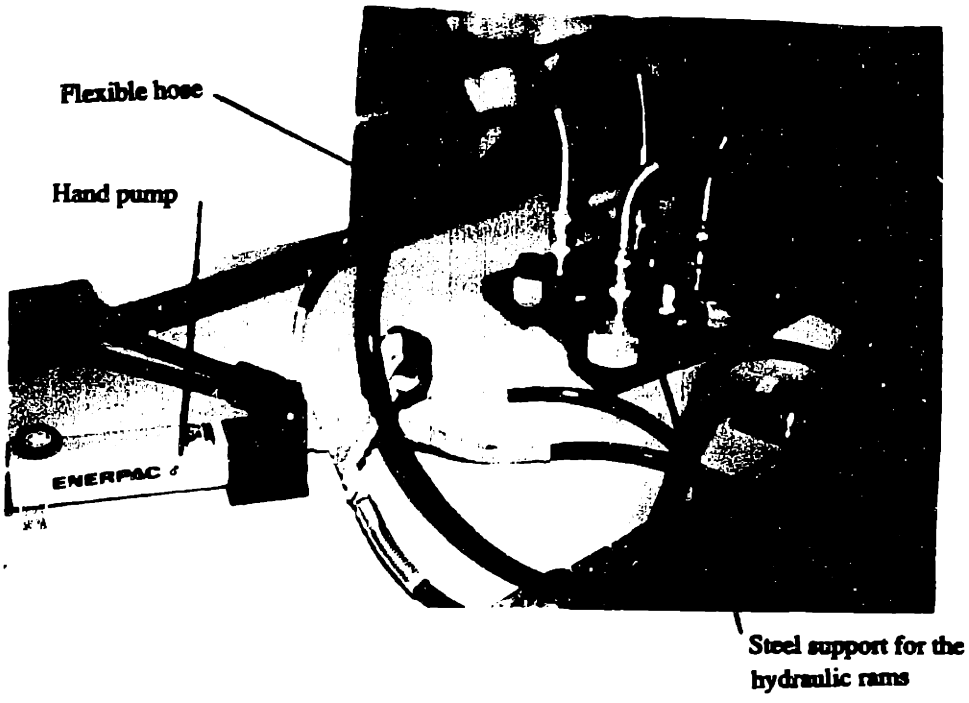

Figure 3-3: Hand operated hydraulic ram mechanism to apply four side loads to a 1" glass sphere

3.2 Particle Bed Tests

The main objective of these tests was to study the effects of bed height, rate, and amount of bed compression, size distribution within the original bed, combined compressive and shear loading, etc. (as discussed in chapter 1) on fracture efficiency, so as to identify the optimum bed and other compression parameters to enhance comminution efficiency.

Spherical glass beads, ranging in diameter from 1.7 mm to 2.0 mm (similar to those used by Laffey and Ghaddar) were confined within a cylinder piston apparatus (similar to the one used by Ghaddar) to form a particle bed. The mild steel pistons used by

Ghaddar were replaced by hard tool steel pistons, heat treated to a value of 65 or more on Rockwell hardness 'C' scale (which is much harder than glass beads with 45-48 Rockwell hardness value.) The reason for this was that in earlier experiments the mild steel pistons were getting indented while compressing the bed of glass beads. It was necessary to determine if the lost energy due to this deformation of the steel had a significant effect on the calculated fracture efficiency of the particle bed.

Figures 3-4 (a) and (b), and 3-5 show the experimental setup, and the piston-cylinder apparatus. Force-displacement data were recorded by the automatic data acquisition system of the Instron machine and a personal computer connected to the Instron machine.

Bed height for each experiment was directly measured using a vernier-calliper. Weighing of the sample was done by a precision weighing machine with an accuracy of $\pm$ 0.001 g. The average weight of a glass bead (sphere) was determined from the weight of a sample of 500 beads. Since the purchased glass beads were not of uniform size, they were presieved and only the fraction with a size range between 1.7 mm and 2.0 mm was used (Ghaddar and Annis also used particles of similar size).

Since crushing within the bed is treated entirely (at least as a start) as the primary fracture of full-sized particles, the number of glass beads broken in each experiment must be known so that the fracture efficiency can be calculated. This was done by determining the weight of the broken spheres. The crushed sample was unloaded carefully and then sieved using ASTM screens and a shaker, following ASTM sieving guidelines. The material passing through 1.7 mm screen was the broken material. The weight of the broken spheres divided by the average weight of an individual bead gives a reasonable estimate for the total number of broken spheres.

The bed work (i.e., the input energy to the bed) was determined by calculating the area under the force-displacement curve using trapezoidal rule. Lotus 1-2-3 software was

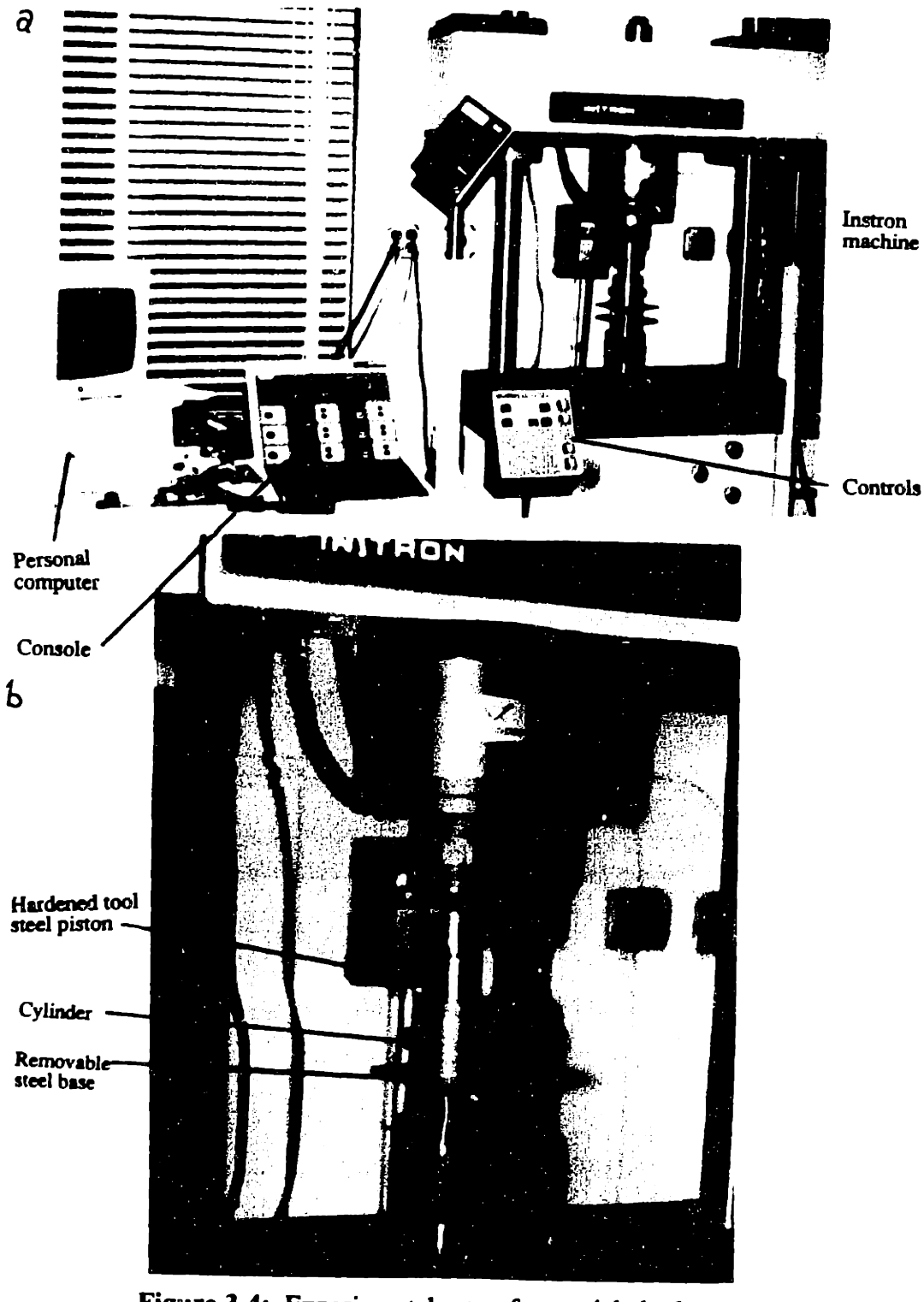

Figure 3-4: Experimental setup for particle bed test

(a) Instron machine with console and computerized data acquisition system, piston-cylinder apparatus shown by (p); (b) Close-up view of Instron machine showing piston-cylinder apparatus placed between the two platens.

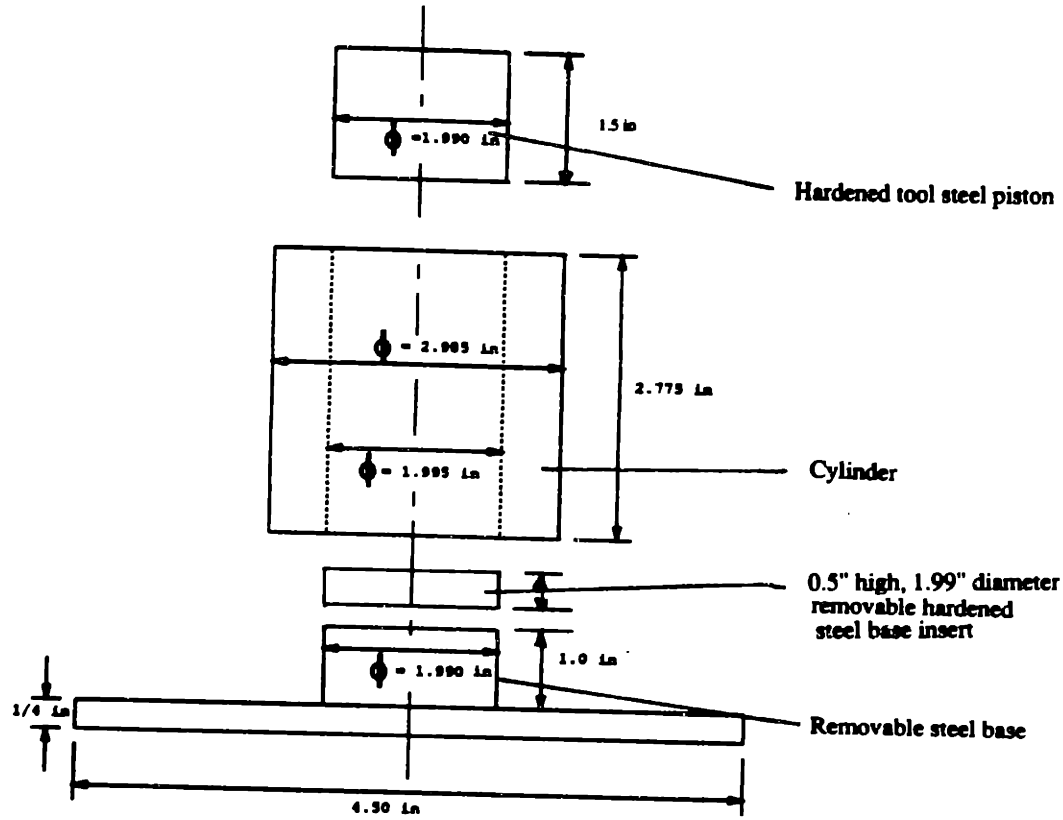

Figure 3-5: Dimensioned sketch of the Cylinder-piston apparatus for particle bed test [from Ghaddar 91]

used for these calculations. From this bed work the average work needed to crush one sphere within the particle bed can be reasonably determined by dividing the bed work by the number of particles broken.

Compliance of the Instron machine and piston-cylinder apparatus reflected or included in the deflection or compression data increases the calculated bed work, and therefore, unduely penalyzes the calculated bed fracture efficiency. To see the effects of this compliance, blank tests were performed.

Force-displacement data were recorded for these blank tests, performed with no particle bed within the cylinder. By writing a computer program the displacements or

compliance of the vertical column between the load cell on the fixed upper cross head and the lower compression head corresponding to a certain load was subtracted from the recorded displacement of the bed from the experiment at the same load magnitude. After correcting the displacement data for the machine compliance, the corrected bed work was determined using the method outlined in the earlier paragraph. It was noted that this correction was very minor, increasing the calculated bed efficiency by an insignificant amount (about one percentage point). Since these corrections were requiring much computer disk usage, computer time and effort with not much usefullness, it was decided not to incorporate these corrections in the bed work calculations.

Another required quantity for the calculation of the bed fracture efficiency is the ideal bed work, i.e., the ideal energy needed to fracture a single particle by compression between two platens in the absence of particle-to-particle or particle-to-wall friction. This was done by running several tests on monolayers of 50 particles separated from one another and placed away from the cylinder walls. Care was taken in calculating the monolayer bed work so that the energy input for primary crushing only was calculated. The force-displacement data and graph show fracture of one or more spheres at a time by the peaks and drops in the load. This is due to the fact that the spheres are not exactly uniform in size and not all of them touch the two platens at the same time because of this size difference. When all the 50 particles were crushed a sharp drop in load was noticed. The appropriate area under the force-deflection curve was calculated to determine the bed work. Average value of the bed work for several tests divided by 50 gives the average energy needed to crush a single sphere under this ideal condition.

To assure accurate recording of load and deflection data, the Instron machine was calibrated before each run. On several runs the deflections of the compression heads were also measured using a caliper and it was found to be very accurate.

In a practical comminution device the particle bed is not laterally confined by walls (like the cylinder walls), therefore, wall friction is absent. To simulate real machine situation in experiments the wall friction effect should be eliminated or minimized. To minimize the effect of wall friction the cylinder was lifted up from its normal rest position on the removable base of the apparatus, held in this position by hand and then the compression test standard. In a few seconds the cylinder became locked with the bed of the particles so that it was no longer necessary to hold the cylinder up. Thus as the compression proceeded the cylinder moved down along with the average displacement of the bed of particles. By doing so the relative motion between the cylinder and the particles was decreased and so the wall friction was minimized. Following this procedure a minor improvement in calculated breakage efficieny (about one percentage point) was obtained compared to that obtained by not following this procedure.

From previous experiments it was noticed that the inner cylinder wall caused some friction on the upper moving piston. To minimize that the inner cylinder wall and the outer surface of the pistons were polished before each experiment using sand paper to ensure snug fitting.

To ensure an identical packing conditions of the glass beads within the cylinder, as far as practicable, for all experiments, the top of the bed after pouring the glass beads in the cylinder was leveled up by tapping the cylinder while compressing the bed by hand between the steel piston and the removable steel base.

Several sets of experiments were conducted for monolayer of 50 separated particles and multilayer particle beds of following thicknesses: 0.112", 0.135", 0.200", 0.262", 0.500", 0.740", 1.000", 1.500" and 2.000". For each bed thickness several experiments were conducted each for a different amount of compression to determine the effect of bed compression on fracture efficiency.

To determine the effect of compression rate on fracture efficiency a limited number of experiments were conducted on identical beds with identical amounts of compression but using compression rate varying by more than an order of magnitude.

A few experiments were done to see the effect of wall friction on fracture efficiency in a qualitative way. A crude method was adopted. A 1/16" thick styrofoam liner was placed inside the cylider and the rest of the experimental procedure was as before. It was assumed that work done in deforming the liner will be very insignificant compared to the total bed work and the presence of the styrofoam will reduce the wall friction (i.e, the particle within the liner will not rub against the cylinder wall directly while the bed is being compressed).

Experiments were also done with particle beds of presieved granular sands, with a size range between 1.7 - 2.0 mm particle diameter (identical to the glass beads). These experiments were conducted to see the effect of bed compression and bed height on bed fracture efficiency for real particles and to see if a qualitative similarity in results of these experiments with the experiments using particle bed of uniformly sized glass beads exists.

The particle size distribution within the bed greatly affects the fracture of the particles. Laffey and Ghadder noticed a decrease in the length of the middle section of the force-displacement curve, in which most fracture occur, at the percentage of smaller particle increases (refer to chapter 2). To see the effect of fines in the initial composition of the bed on the fracture efficiency, particle beds composed of 50:50 mixtures of minus 2.0 mm (1.7 - 2.0 size range) and 0.4 mm (nominal size) by weight were tested. In some of these experiments 1/8" diameter steel balls were also included in the particle bed to see the effect of local load concentration on fracture efficiency of mixed size particle bed.

Many actual comminution processes utilize both compressive loading, as well as shear loading. To see the effect of shear loading on fracture efficiency of a particle bed

undergoing compression, an intuitive method was devised. The surfaces of the removable piston base and the upper piston between which the particle bed is compressed, were ground to give a slanted configuration with a 7.5 ° angle of slant as shown in Figure 3-6. With this set up the particles will slide while being compressed, and therefore, be subjected to shear loading in addition to compression loading.

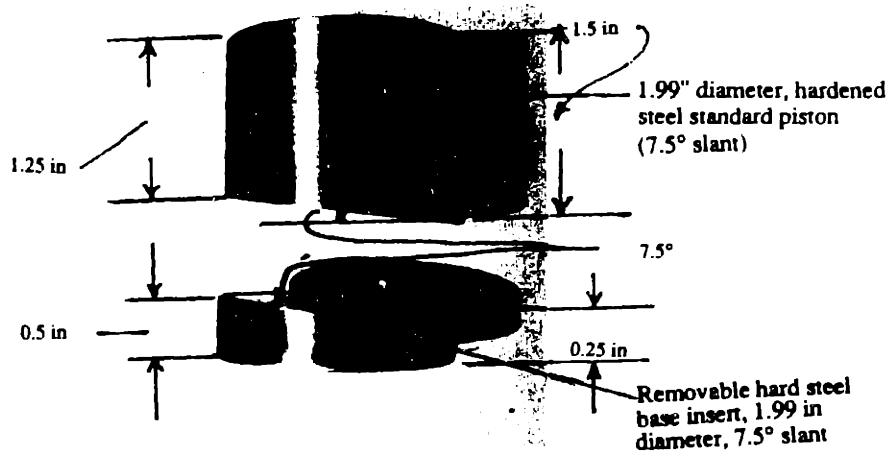

Figure 3-6: Slanted base and piston

Some experiments were conducted with the removable base and the upper piston made of mild steel and the calculated fracture efficiency values compared with those obtained by using heat treated tool steel components under similar conditions of compression and bed geometry. The objective of these experiments was to determine the effect of energy lost in excessive piston wear and denting on the fracture efficiency.

Sieving of the particle bed was done using ASTM screens after unloading the material from the piston cylinder apparatus onto the 1.7 mm screen very carefully so as to avoid or minimize loss of very fine particles. Seiving was done using an automatic shaker as described earlier and following ASTM screening guidelines for a period long enough to

ensure that the gain in the under-size amount passing any screen between 2 consecutive screenings was insignificant (less than 1%). The purpose of these screening or seiving tests was to gain a qualitative idea of the amount of fines produced at optimum compression of the bed due to primary fracture. Here the fines may be defined as the product of crushing which has undergone a specified size reduction (for example a size reduction of 6:1 will mean that the ratio of the mean diameter of the coarse particle to the mean diameter of the fine particle equals six).

The effect of the presence of water or lubricant (like gear lubricant) in the particle bed on fracture efficiency was also investigated to see if it has any beneficial effect. The ideas behind these tests were that water may have a reducing effect on the fracture stress of a particle and lubricant may reduce the inter-particle friction. Both these factors may therby decrease the bed work. Friction plays a very important role in particle breakage. High inter-particle friction helps the building up of a stronger load structure within the bed leading to failure of particles; but high friction causes more energy loss and reduces fracture efficiency.

3.3 Fluidization Tests

As discussed earlier, fluidized solid transport is envisaged as an efficient way to promptly remove the fines and segregate the coarse particles within the crushing zone in between crushing strokes for better utilization of the crushing energy. The focus of this research was to gain a solid theoretical knowledge of the fluidization process through literature review, particularly the elutriating and segregating behavior of particles in a fluidized bed so that objectives and experimental procedures for further fluidization research could be formulated. Based on this review, the conclusions regarding the feasibility of the fluidization process to achieve our desired objectives were presented and discussed in the regular weekly meetings of our comminution group

at MIT. Annis conducted the fluidization tests concurrently and her work is presented in her Masters thesis [5]. Limited experiments were also conducted by the author of this thesis. Chapter 5 of Annis's thesis describes the experimental apparatus and procedure. However, the following is a brief description of the procedure:

Binary mixture of spherical glass beads containing 50% fine material, (0.8 mm nominal size glass beads) and 50% coarse material, (2.0 mm nominal size glass beads) by weight were fluidized in a plexiglass column of 1" x 1" cross section. Most of these experiments were done using water as the working fluid. Limited experiments were also done using air as the working fluid and using a round plexiglass tube with 1" internal diameter. In some experiments the fluidized bed had a slightly diverging cross section while in others the bed was inclined from the vertical. In these experiments with water-fluidized beds the effects of various bed parameters, such as divergence of the cross section of the bed, the inclination from vertical, pulsation of the water flow and the height of the static bed on the quality of segregation were explored. Figure 3-7 (a) and (b) shows Annis's experimental set up.

Limited experiments were done by the author with a binary mixture of granular sand particles. The mixture consisted of 50% by weight of 2 mm (nominal size) and 50% by weight of 0.8 mm (nominal size) sand particles to observe their qualitative segregating behavior in a 1" round vertical glass tube using water as the fluidizing liquid.

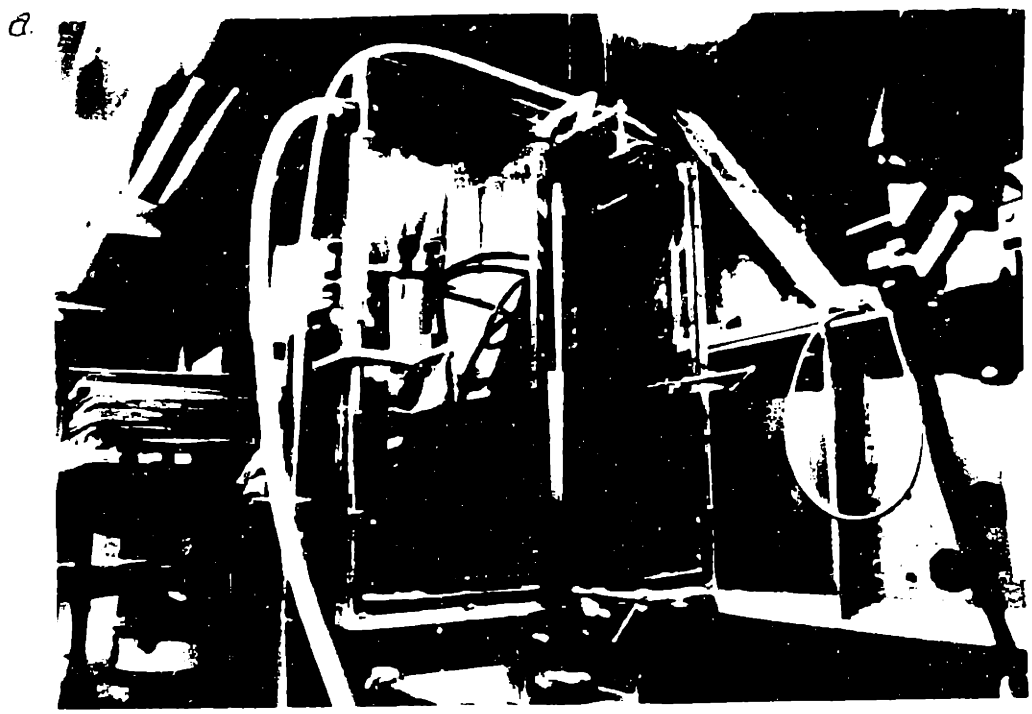

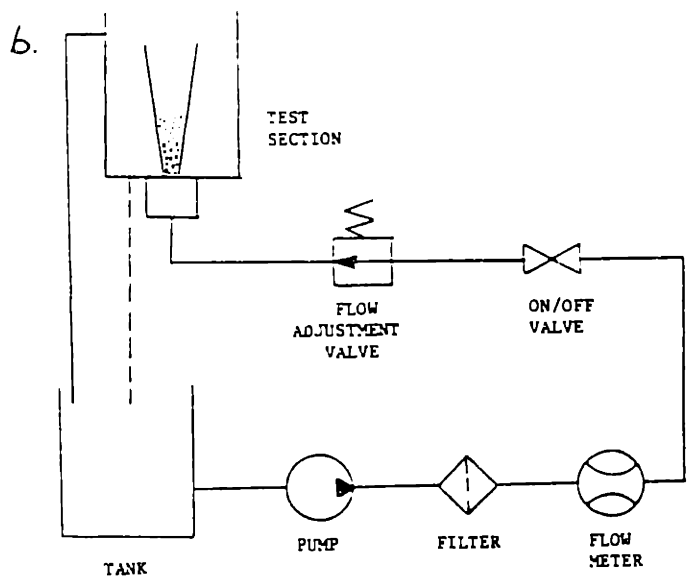

Figure 3-7: Set up for fluidization behavior test of binary size mixture of glass beads

(a) fluidized bed test section; and (b) schematic of flow loop [Annis 91]

Chapter 4

Experimental Results and Discussions

Fracture efficiency in compressive comminution of a particle bed is influenced by device specific variables (such as intensity, method and velocity of loading); size, shape and homogeneity of the particles; method of solids transport; and other bed conditions. This chapter deals with the experimental study of the dependence of fracture efficiency with many of these variables. Experimental results are presented in three sections under appropriate headings, followed by discussions. Experimental data are tabulated in the appendix. Purpose of the experiments are already discussed in chapter 3. Usefullness of the findings of these experiments will be discussed in chapter 5.

4.1 Single Particle Test

Nine tests were conducted by simply compressing the 1" diameter glass spheres to fracture between the platens of the Instron machine, with no side loads. This yielded an average fracture stress of 39.7 MPa (defined as fracture load over the sphere cross section, $F/\pi r^2$, where F = the load, and r = the sphere radius), with a standard deviation of 4.82 MPa. This compares well with what Kurfess obtained for fracture stress (41 MPa). As the experiments continued with simultaneous application of 4 side loads of increasing magnitude, about the equator of the sphere, along with primary load, hardly any effect was observed on the magnitude of the average fracture test, excepting that there was some scatter of data as in the case without the side load. This is shown in Figure 4-1. This indicates that failure of brittle spheres is unaffected by lateral loads, even when these loads approach the primary load in magnitude. Therefore, simple two-point failure criterion adequately describes the behavior of multiple-loaded brittle

spheres. The lateral loads, however, caused more production of fines due to particle degradation at the four contact points.

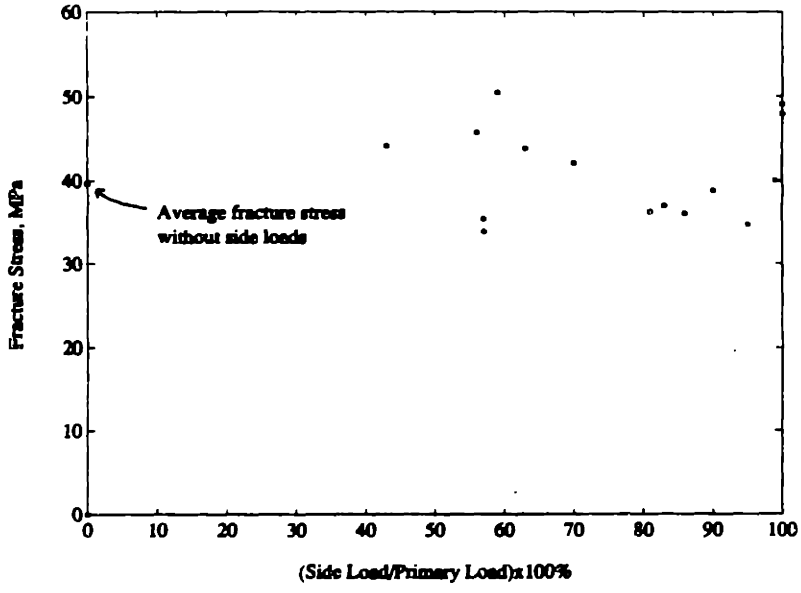

Figure 4-1: Effect of side loads on the fracture stress of 1" diameter glass spheres

Figure 4-2 shows typical force-deformation curves for varying side loads. The fracture stress in all these cases were caused by the normal primary load, whose magnitude was nearly the same. In these curves the *deflection* recorded was actually the motion of the machine crosshead plus its compliance, but error due to compliance (as discussed in chapter 3) was negligible. The slopes of the force-displacement curves are very similar, again indicating that lateral loads have no inhibiting effect on primary fracture of brittle spheres.

Within an actual crushing machine, the number of lateral loads on a granular particle will probably be more than four and their points of application need not be at right angles to the primary load. In the above experiments, the number and locations of the

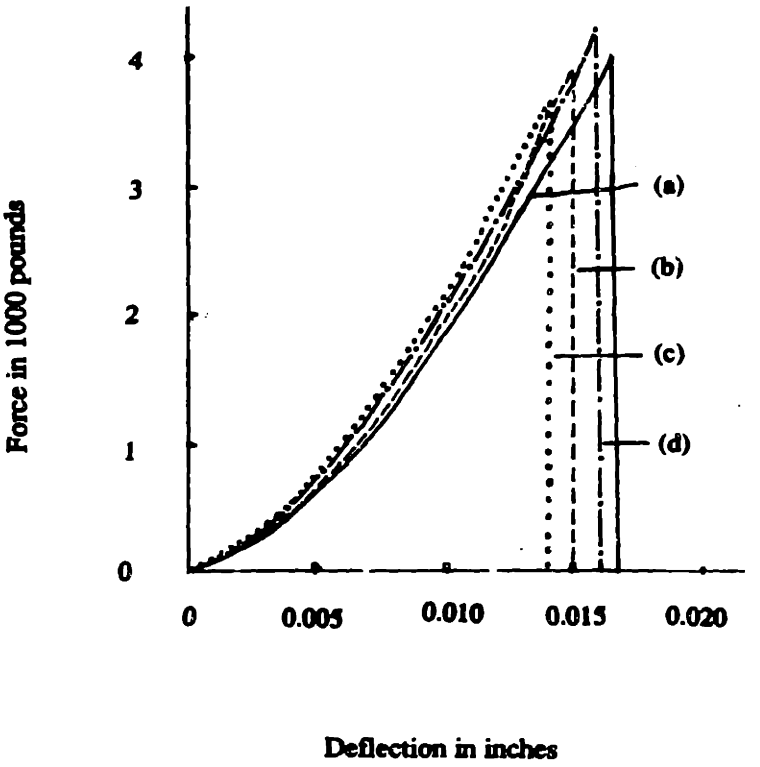

Figure 4-2: Force-deformation curves for fracture tests of 1" diameter glass spheres with varying side loads

(a) with no side load; (b) with side equal to 63% of primary load in magnitude; (c) with side load equal to 83% of primary load in magnitude; and (d) with side load equal to 99% of primary load in magnitude

side loads are chosen in such a manner that inhibiting effect from the side loads on crack propagation and subsequent primary fracture, if any, should show up in the test. Therefore, this configuration of side loads is, at least as an approximation, a simple but reasonable representation of actual confining loads. It appears that for elastic brittle spheres the state of stress beneath the primary load is practically independent of loads at other locations. Crack growth is initiated in an area beneath the primary load and it becomes unstable very near this area causing failure of the sphere. Underneath the area of force contact, cone shaped zone of stress concentration is observed in which particle

degradation is intense. More fines are produced from this zone and much coarser products from the rest of the sphere. The size distribution of the crushed product is primarily bimodal.

From the above discussion it is concluded that for brittle material maximum normal force or stress is a reasonable criterion. However, it is known that external loads on a coarse particle can be *blunted* or distributed over large numbers of contact points if excessive fine materials are present around the particle. Provided the crushing machine has sufficient capacity, it will have to produce greater external load to create the same maximum stress as required to crush the coarse particle individually. The importance of prompt removal of fines from the crushing zone is thus obvious. It is also obvious that, even if the fines are removed, the thickness of the particle bed should be such that the required maximum failure stress for the coarse particles is still developed within the particle bed from the application of the maximum safe load of the crushing machine.

Two tests were conducted on the glass spheres with 10 times faster rate of application of the primary load i.e., 0.01"/second to see the effect of compression rate on the fracture stress. It should be noted that the rate of application of force is important for visco-elastic materials, which are better comminuted by impact. The experimental data are presented in the appendix. It was observed that failure was unaffected by the rate of application of the primary load, indicating that faster compression stroke in a crushing machine would be advantageous from the standpoint of throughput.

Eight tests conducted on 1" diameter plastic sphere yielded an average fracture stress of 34.1 MPa, in the absence of side loads, with a standard deviation of 2.33 MPa. Failure of plastic spheres, however, was significantly inhibited by lateral loads. Typical force-deflection curves for varying side loading conditions are shown in Figure 4-3. Side loads of 50% of primary loads in magnitude showed more inhibiting effect than side loads of other magnitude. Failure of plastic spheres is very complicated compared to that of glass spheres and there is no simple failure criterion.

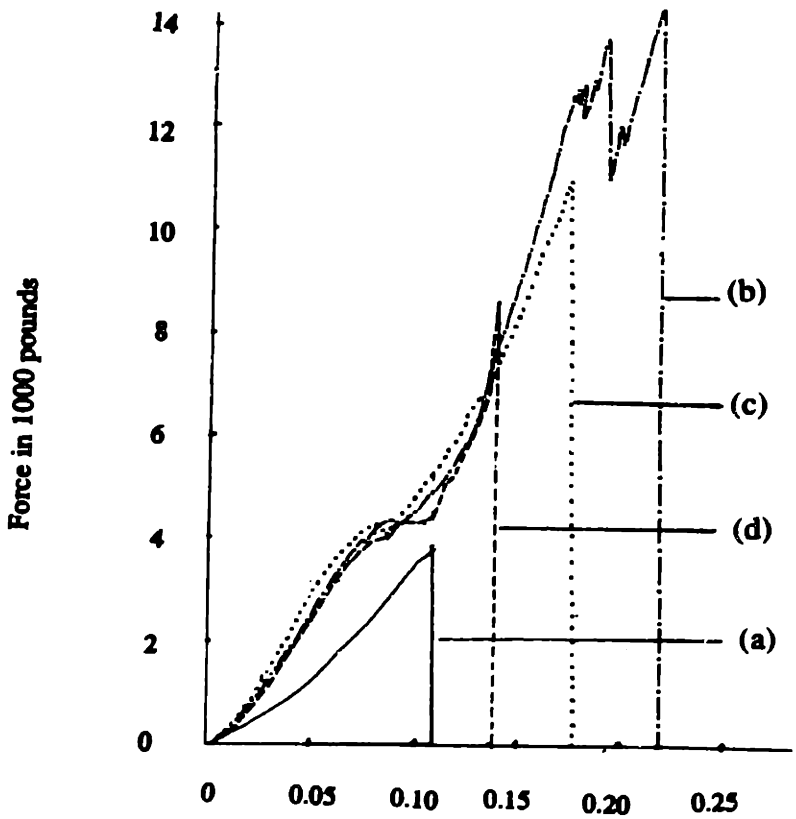

Figure 4-3: Force-deflection curves for fracture tests of 1" diameter plastic spheres with varying side loads

(a) with no side load; (b) with side load equal to 50% of primary load in magnitude; (c) with side load equal to 70% of primary load in magnitude; and (d) with side load equal to 100% of primary load in magnitude.

The effect of side loads on the failure load of a plastic sphere is shown in Figure 4-4. Failure of plastic sphere will be important for very fine crushing (in the range of 1-50 μ diameter product size depending on materials) of brittle materials since they behave

plastically when reduced to such fine size. Further discussions are beyond the scope of this thesis.

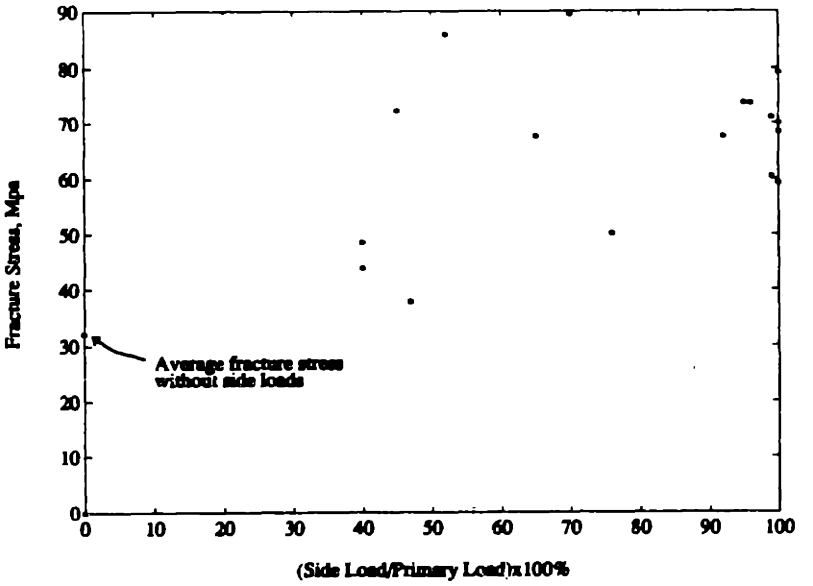

Figure 4-4: Effect of side loads on the fracture stress of 1" diameter plastic spheres

The experimental data are tabulated in appendix (Table I and II for glass sphere test and Table III and IV for plastic sphere test).

4.2 Particle Bed Test

4.2.1 Bed Efficiency as a Function of Bed Compression

The average weight of a glass sphere (for the size 1.7 mm - 2.0 mm) was determined. Table V shows the relevant experimental data. The average weight is 0.0128975 g for one sphere.

Seven tests on beds of monolayer of 50 separated particles were conducted, which gave

the average value of 0.235131 in-lb for the energy needed to fracture one glass sphere. Table VI shows the experimental data. The following points regarding these tests should be noted:

- spheres were not touching each other and were away from the cylinder wall,
- monolayer bed height = 0.067" to 0.079",
- clearance between piston and cylinder wall was 0.005", to avoid wall friction,
- correction for Instron machine compliance was negligible,
- the spheres were not of exactly uniform size, the size difference between the biggest and the smallest spheres being about 0.012". Because of this size difference, as compression progressed, the spheres broke either one or a few at a time, as all the unbroken spheres were not touching the moving piston at the same time. Thus, the piston displacement recorded does not reflect the compression needed to break an individual sphere, but it reflects the total piston displacement to break all the spheres,
- average energy needed to break 50 glass spheres = 11.757 in-lb and for one sphere = 0.235131 in-lb, and
- according to the definition in this study, particle breakage in monolayer is considered as 100% efficient (in the absence of wall friction and inter-particle friction.) The value 0.235131 in-lb has been used as the ideal work for the fracture of single glass bead (2 mm nominal diameter) in this report.

Separate tests with 10 and 100 separated particles in a monolayer bed also gave results comparable to 50 particle test (See appendix).

Force-deflection graph for the fracture test of a typical monolayer bed of glass spheres is shown in Figure 4-5.

Experimental procedures were performed on beds of glass spheres ranging in height from 0.112" to 2". Each experiment was for a particular bed compression. Fracture efficiency was investigated with compression strokes up to about 30% of the initial bed height. The data obtained and calculations of fracture efficiency η_b are tabulated in the appendix (Table VII and VIII). The results obtained were very similar to those obtained by Ghaddar. Fracture efficieny increases with the continuing compression, as can be seen from the data, up to a maximum value at about 18 - 22% compression and then it

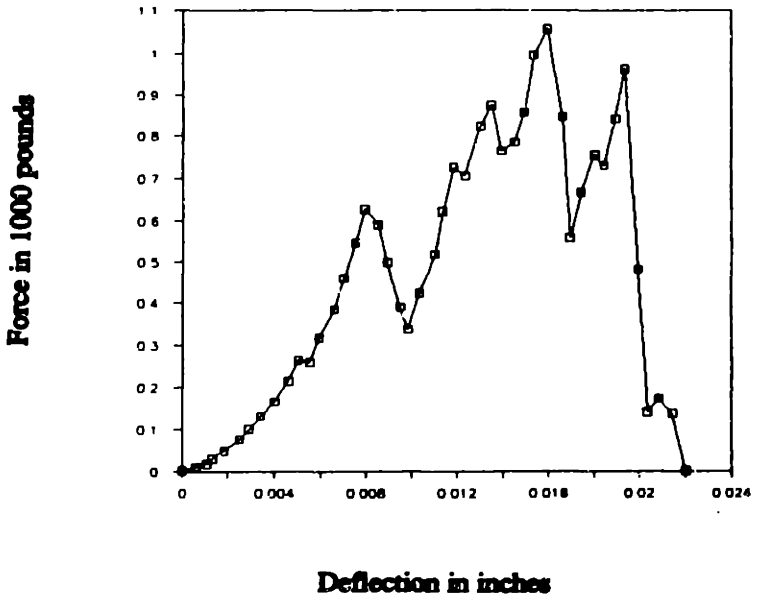

Figure 4-5: Force-deflection graph for the fracture test of a typical monolayer bed of 50 separated 2 mm diameter glass spheres

drops again. This behavior is consistent with beds of all heights examined (0.112", 0.135", 0.200", 0.262", 0.500", 0.740", 1.000", 1.500" and 2.000"), ranging from 1.5 to about 27 particles deep. More data were collected for the beds 1/2" thick and less, since Ghaddar's experiments did not cover thinner beds. Once the trend in variation of η_b with compression rate for various bed heights was established, number of experiments for thicker beds (3/4" to 2") was purposely limited. Laffey's experimental work on particle bed and Ghaddar's thesis explains the reason for the variation of η_b with % compression with the help of the force-deflection graphs. Typical force-defelection graphs for 1/8", 1/4", 1/2", 1" and 2" bed heights are shown in Figure 4-6.

Figure 4-7 shows the fracture efficiency vs compression curves for all the beds in the same frame.

In all these graphs there are three distinct zones as stated in chapter 2. In the first zone

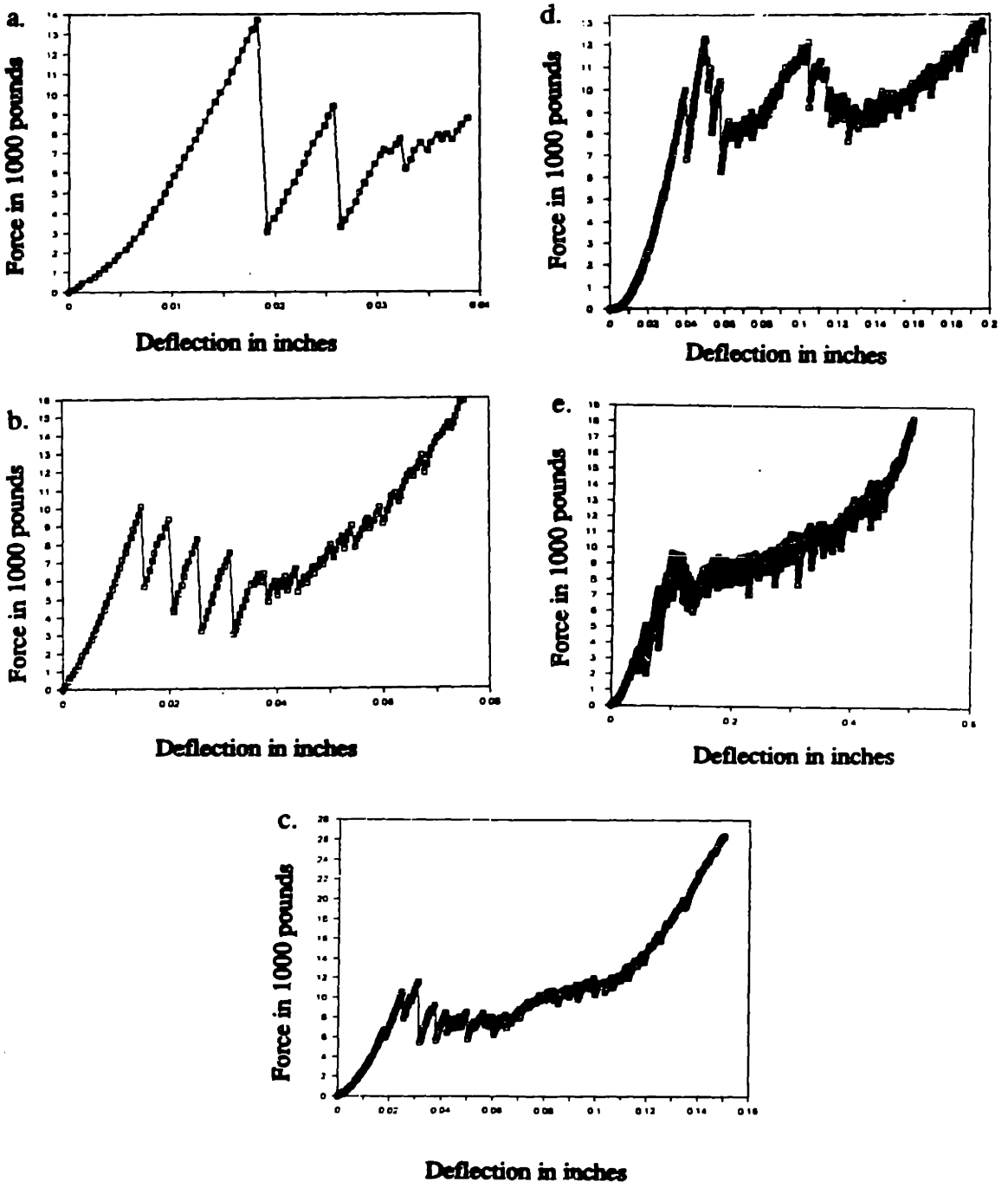

Figure 4-6: Force-deflection graphs for particle bed tests with various bed thicknesses

(a) 1/8" initial bed height undergoing 31.08% compression; (b) 1/4" initial bed height undergoing 28.74% compression; (c) 1/2" initial bed height undergoing 31.06% compression; (d) 1" initial bed height undergoing 20.27% compression; and (e) 2" initial bed height undergoing 25.05% compression

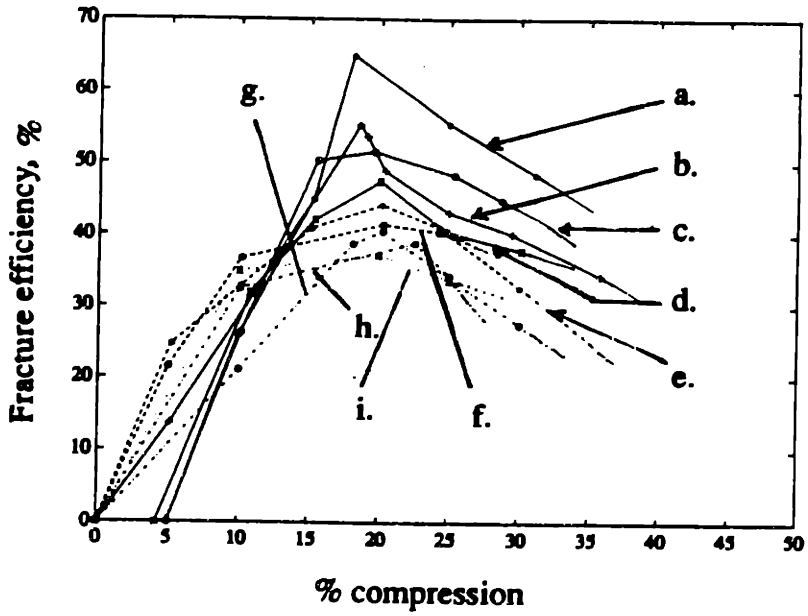

Figure 4-7: Fracture efficiency vs % compression for various bed thicknesses

(a) 0.112" bed height, (b) 0.135" bed height, (c) 0.2" bed height, (d) 0.262" bed height, (e) 0.5" bed height, (f) 0.744" bed height, (g) 1" bed height, (h) 1.5" bed height, and (i) 2" bed height

of the initial compression, η_b is very low for small compressions, but increases slowly as the bed is only rearranged, deformed, and compacted with little fracturing and storage of the input energy in elastic deformation of the particles in the bed. In the second zone (which is a long zone), η_b increases at a faster rate as more fracture occurs due to higher level of stress (which stays almost constant at a mean value). In this middle zone, where the bed behaves macroscopically, additional fracture occurs by the increase in displacement at relatively constant force level. The peaks noted in this region, as mentioned earlier in chapter 2, are due to build up and collapse of internal frictional load substructures, as fracture progresses. The progressive fracture during this stage at a more or less constant value of force (or stress) with a much slower rate of energy input causes the rise in η_b up to the end of this stage. In the third zone of the force-deflection graph η_b decreases at high compressions as the accumulation of fine

material in the void spaces around the larger spheres blunts the effects of the external loads, thus delaying fracturing till higher energy levels (and stress levels) are reached. The graphs show fewer smaller peaks in the force in this region, but the rate of rise of force level is steepest. This indicates solidification of the bed requiring more additional energy input for fracturing compared to middle zone and thus η_b drops sharply with progressive compression. At about 30% compression the force limit was close to the Instron machine's limit and so no further tests with any higher compression were done.

Chapter 5 discusses how this behavior may be important in the design of a crushing machine.

4.2.2 Bed Efficiency as a Function of Bed Height

Ghaddar's recent study of the variation of η_b with bed height gave results which were contrary to what was anticipated. His study did not include thinner beds (less than 3.5 particles deep) and thicker beds (more than 18 particles deep). This study extended his work to thinner beds down to a monolayer in thickness and thicker beds up to 27 particles deep to gain further insight into this behavior.

Experimental data for this study are tabulated in the appendix (Table VII and VIII). Maximum fracture efficiency for the bed of glass spheres (which typically occurred at a compression equal to about 18 to 22% of initial bed height) was observed to increase with decreasing bed height, climbing to 100% for a monolayer bed (by definition). This is because, particle-to-particle friction losses which are the major losses in a particle bed undergoing comminution, is absent in a monolayer bed. The decrease of maximum fracture efficiency with increase in bed height may be due to several factors:

- the increase of contact-number in the 3-D space makes comminution difficult, and the additional side constraints, which are used to keep the particle-packing in the bed from collapsing, cause further lowering of efficiency;

- friction energy loss due to the cylinder wall increases with bed thickness possibly in a non-linear but increasing manner;
- as the bed height decreases the proportion of the free void spaces between the particles and the confining walls increases with respect to the total bed voidage. This increase in void space makes the middle zone in the force-deflection curve longer with consequent increase in fracture efficiency;
- the sensitivity of the particles in a bed to external loads or to propagation of fracture stress increases as the bed gets thinner; and
- the effect of upper and lower surfaces, through which the external normal load is transmitted to the particles, influences the bed behavior as well. With decreasing bed height the proportion of particles in direct contact with these surface obviously increases causing improved propagation of fracture stress and more particle failure. Therefore, the possibility of particles being broken increases in thinner beds.

The efficiency drops from a maximum value of 100% for a monolayer bed of separated particles, not touching the cylinder walls (meaning friction is absent) to about 50% for a 2.6 particle deep bed. This drop is just because of energy losses due to friction. After that point η_b decreases at a slower rate with increasing bed thickness until the bed is about 10 particles deep. Beyond that point the rate of drop in efficiency, with further increase in bed thickness, is very small. The maximum bed thickness that could be studied was 2" (about 27 particles deep) due to the limitations of the apparatus and the Instron machine. In passing, it is worthwhile to mention that in practical crushing machine, the bed thickness is well within this value in terms of mean diameter of the feed particles.

Another important observation is that the maximum efficiency occurs at a slightly lower value of compression as the bed gets thinner. This is possibly due to the difference in bed packing condition, wall effect, and the fact that the possibility of breakage of particles in a thinner bed is more even for a smaller compression, compared to that in a thicker bed. Due to this the length of the second zone in the force-displacement graph (as mentioned earlier) becomes shorter as bed solidification starts earlier and subsequently the maximum efficiency occurs at a lower %

compression. It is noted that the point of maximum efficiency is marked by the end of the middle zone in the force-deflection curve.

The graph for maximum η_b versus bed thickness (in terms of particle diameter) is shown in Figure 4-8 which has been drawn with the help of data from the appendix (Table IX). The knowledge of this behavior is very important in the design of a crushing machine (further discussion in chapter 5).

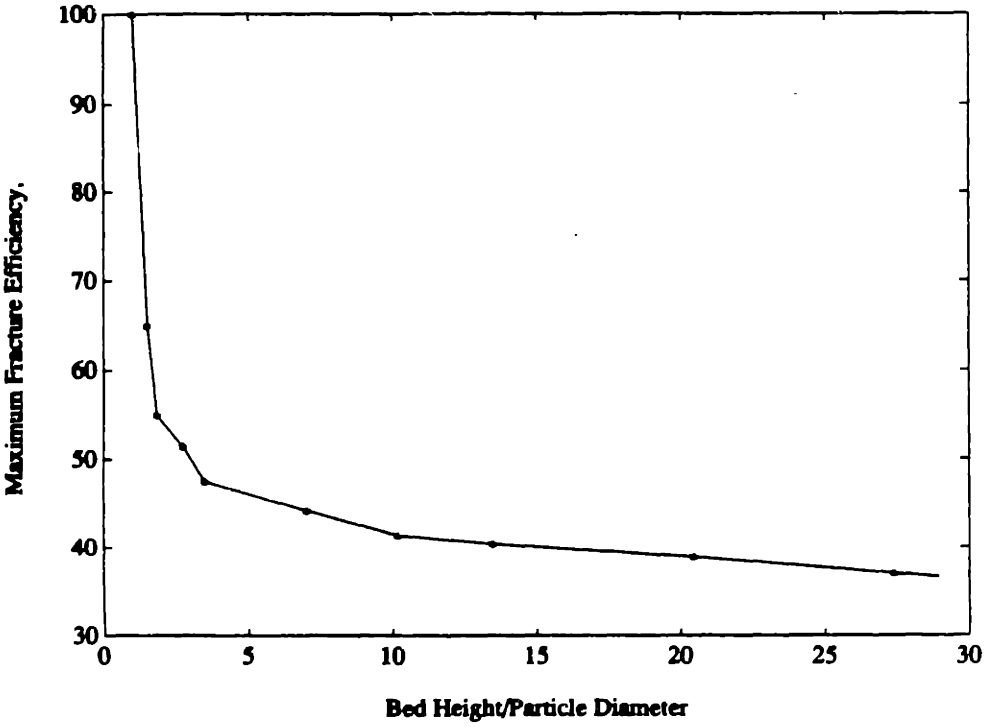

Figure 4-8: Maximum fracture efficiency vs. bed thickness

4.2.3 Variation of Fracture Efficiency with Rate of Compression

Only three experiments were performed, each with a 1/2" bed and for a 24% compression, with compression rates of 0.001"/second, 0.01"/second, and 0.025"/second. The experimental data are summarized in the appendix (Table X]. It was observed that fracture efficiency is practically unaffected by the rate of

compression, even when the latter changed by an order of magnitude. This is possibly due to the fact that the speed of fracture propagation (which is equal to the speed of sound) is several orders of magnitude faster than the compression speed. In practical crushing machine, of course, the compression rate is much faster than 0.025"/second, but it is still several orders of magnitude less than sound speed. Testing at this speed was not possible due to limitations of the data acquisition system to obtain meaningful data at that high speed. Nevertheless, from the insensitivity of η_b to the variations of compression rates in these experiments, it is postulated that η_b will also be practically unaffected by the compression rate of practical crushing machines. The amount of fines produced and bed work were, however, lesser for higher compression rates.

4.2.4 Effect of Wall Friction on Fracture Efficiency

As explained in chapter 3, this investigation utilized a crude method. The inner wall of the cylinder was lined with a 1/16" thick styrofoam liner which assumably would reduce wall friction. Three tests with 0.139", 0.560" and 0.736" beds at about 20 - 24% bed compression showed increase (4 - 8 percentage points) in fracture efficiency (increase being slightly more for thicker beds than for thinner beds) compared to tests carried out without styrofoam liners. The data for these experiments are tabulated in the appendix (Table XI). These experiments were not intended to be performed with much precision. All that was expected was a qualitative study. These experiments qualitatively confirmed that wall friction does affect the fracture efficiency. Its diminishing effect on efficiency increases with bed height. However, for the rest of the experiments for this thesis, the procedure outlined in chapter 3 (p 51) was used to eliminate or minimize the effect of wall friction, so that the fracture test data for varying bed thicknesses will be unaffected by wall friction, and thus be meaningful for comparison purposes.

4.2.5 Effect of Piston Hardness on Fracture Efficiency

As mentioned in chapter 3, compression tests on particle beds indented the mild steel pistons used by Ghaddar. Energy loss in the plastic deformation of piston material increases the bed work and, therefore, reduces the fracture efficiency. To alleviate this effect a heat treated (hardened) tool steel piston and the base (harder than glass spheres) were used in this research. However, just to see the effect of piston surface hardness on fracture efficiency parallel experiments were performed with identical bed thickness, compression amount and rate, but using mild steel pistons for some tests while hardened tool steel pistons for others. Results are tabulated in the appendix (Table XII) which show a small increase in the fracture efficiency when hard pistons were used (about 1 -2%). Pictures of the indented mild steel piston surface indented after a single test and after 10 tests are shown in Figure 4-9 (a) and (b) to give an idea of the energy lost or absorbed by piston material. Hard steel pistons were hardly indented by the glass beads. Hardness of the piston and crushing chamber walls should be kept in mind while designing a crusher. Metal wear not only reduces crusher efficiency, but it is an expensive item in the total comminution cost in the industry.

4.2.6 Effect of Presence of Fines in the Initial Composition of the Particle Bed on Fracture Efficiency

To see this effect two experiments were done, both with 3/16" bed height undergoing about 20% compression. In one experiment all the glass spheres were of 2 mm nominal size (1.7 - 2.0 mm size range), while in the other 30% of the bed weight was composed of 0.4 mm (nominal size) glass spheres. The bed weight in both cases were 15.924 g. To see if the inclusion of steel balls (bigger than the glass spheres) has any effect on η_b for a particle bed containing fines undergoing compressive loading (due to local load concentration and build up of stronger load bearing structure within the bed), the above

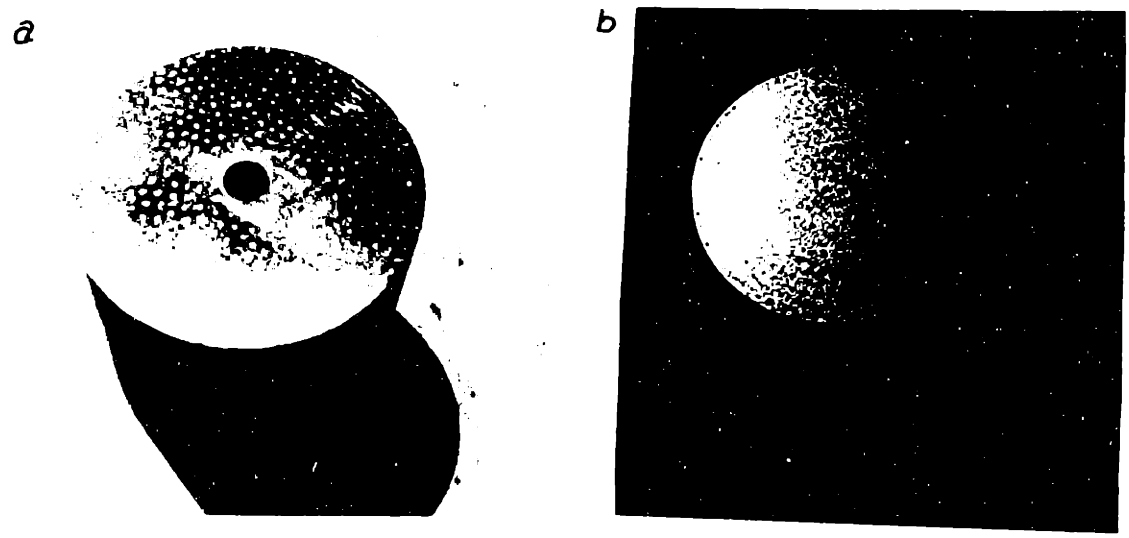

Figure 4-9: Pictures showing indentions on a mild steel piston by glass beads during bed compression tests

(a) After only one test; (b) after 10 compression tests

two experiments were repeated adding 25 pieces of 1/8" round hard steel balls ensuring that the effective compression of the glass spheres is still 20% (without the steel balls). The results showed no effect on η_b and so no conclusion can be drawn. The data are not presented. The fracture efficiency, as shown in tabular data in the appendix (Table XIII) was only 34.3 % for the bed with mixed glass spheres while it was 51.5% for the bed with uniform sized glass spheres. This again confirms that the presence of fine particles around large particles blunts the applied load, reduces the available bed voidage, increases intra-particle friction due to large numbers of contact points and thus reduces the fracture efficiency. The probability of larger particles being broken is reduced by the increased number of contact points per particle. The need for prompt removal of fine particles of output size from the crushing zone was already emphasized earlier.

4.2.7 Effect of Combined Compressive Loading and Shear Loading on Fracture Efficiency

Many crushing machines in the industry combine both compressive loading and shear loading for comminution of particle beds. However, compressive loading is the major mode of force application. Therefore, the study of the mechanics of fracture within particle beds influenced by shear loading in addition to compressive loading is very important. The effect of combined compressive and shear loading on fracture was studied, using piston and base, both slanted at 7 1/2° and compressing the bed of glass spheres between their parallel faces. This intuitive device caused sliding and rolling of glass spheres during compression, which in turn caused shear loading by non-radial forces. The fracture mechanism of a brittle material under combined shear and compression is not quite well understood. Two things may occur: (1) the spheres might fail under increasing proportion of shear (which has a radial and a tangential component of forces) due to increase in tensile stress at the force contact area; or (2) shear may cause secondary crushing and distribution of the fragments within the bed.

Only a few experiments were conducted to determine the effect of shear loading in a qualitative manner. The experiments were done on particle beds of varying thicknesses. Experimental results are tabulated in the appendix (Table XIV). It was observed that the effect of addition of shear loading to compressive loading on η_b is more pronounced for thinner beds. It reduces the fracture efficiency as the bed gets thinner than 10 particles deep (1/2" and less in thickness for a bed of 2 mm diameter glass beads). There was hardly any effect when the bed was 10 particles deep or thicker. Thus, for a practical crushing machine crushing a particle bed, which is usually 10 times or more thicker than the mean diameter of the feed particle, the effect of shear loading will be negligible.

4.2.8 Amount of Fine Products at Optimum Fracture Efficiency

Ghaddar observed that primary fractures are the dominating fractures of full-sized glass spheres which take place within the bed of glass spheres under compression, at least up to the optimum % compression. He also observed that the fines (broken spheres) are produced at a maximum rate per unit of energy input for crushing up to the point of optimum compression of the bed. This is very important to know as the main goal of comminution is for the generation of fines which in most cases is a narrow size distribution of the product.

Reduction ratio (r) for crushers in practice, (based on maximum sizes of feed and product), ranges, according to maker's ratings, from a minimum of 1.5:1 to maximum of about 5:1, (general average being 2.5 - 3:1; greater ratios being recommended for large crushers than for small). Size reduction, except in the smallest plants, involves two or more stages of crushing. Also, size reduction in cone crushers is slightly greater than in jaw crushers. In this study it was important to know the amount of fines or the % of fines produced, say with a size reduction ratio of 2.4:1. Feed size was +1.7 mm to -2.0 mm glass spheres, 100% of which pass through ASTM screen size S-10 but is retained on S-12. Fraction of material, after the crushing experiment, which passes the S-25 screen (-0.71 mm size) represents the product with a reduction ratio of approximately 2.4:1. Size distribution of the crushed material from 1/4", 1" and 2" bed tests for a compression of 24% was determined, which are tabulated in the appendix (Table XV). Though 24% compression for these beds does not exactly represent the optimum compression in terms of fracture efficiency (η_b), still η_b at this compression is within a few percentage point of the maximum η_b. As seen in the tabulated data, % of fines produced with a size reduction of 2.4:1 at this selected compression due to primary crushing is over 33%. This value of the amount of fines produced was found to be almost same for all the bed heights tested (including a monolayer bed and even in

the fracture test of 1" spheres) so that a name can be given to this factor, say size reduction factor at a reduction ratio of 2.4 or simply $C_{2.4}$ (which is about 1/3 in this case). This is caused by just one stroke of the piston, at a fracture efficiency of over 40%, which is very encouraging. With subsequent strokes much more fines will be produced. In a practical device this figure is expected to be even higher as granular particles will produce more fines by secondary fractures also, since angular particles are more prone to secondary fractures along with primary fractures. If a higher % compression value (say 28%) is selected, then the % of fines (with r = 2.4) produced will exceed 50%, of course, with a little sacrifice of the fracture efficiency.

4.2.9 Fracture Efficiency Within Particle Beds of Brittle Granular Material.

Comminution devices in practice seldom process spherical particles. But, as mentioned earlier, researchers always choose particle beds of spheres to avoid complexity due to shape. In this study, a few experiments were conducted on beds of granular (sand of 1.7 mm - 2.0 mm size) material to compare the bed behavior of granular materials undergoing compressive comminution with that of beds of spheres, at least qualitatively.

Five experiments were conducted with beds of sand with 1.7 mm - 2.0 mm size range, about 0.645" high and weighing 50 g undergoing 5%, 10%, 15%, 20% and 25% compression (approximately). At 25% compression the maximum force limit of the Instron machine was reached, so further compression could not be done. The experimental data are tabulated in Table XVI in the appendix. It was observed that three zones in the force-deflection curve, are still evident (as seen in the force-deflection curves for beds of glass spheres). Figure 4-10 shows the force-deflection curve.

There are, however, some differences. Peaks and fluctuations in the force level are

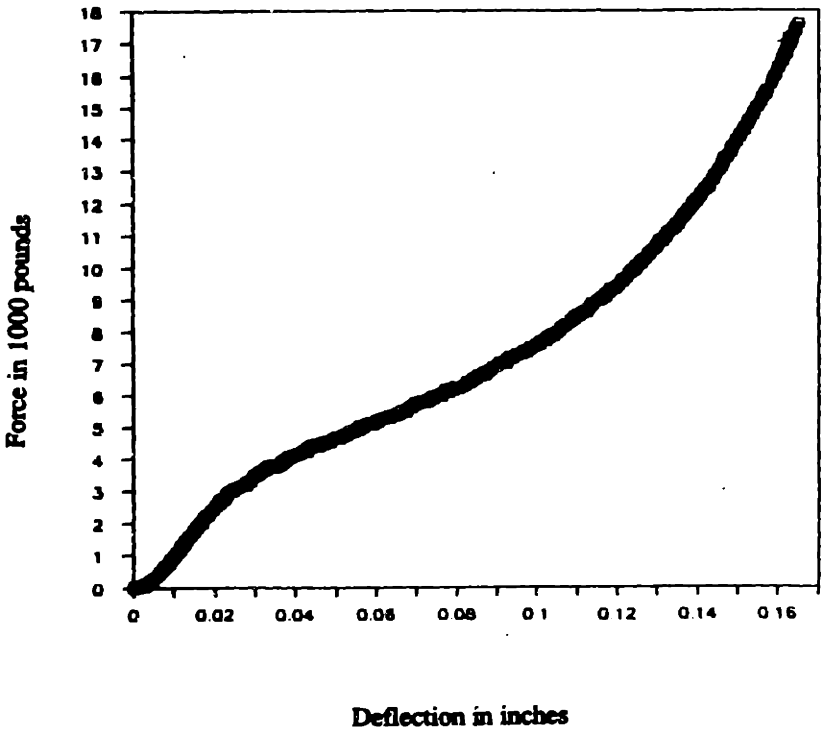

Figure 4-10: Force-deflection curve for a particle bed of granular material under compression loading (bed height - 0.645, at 25.6% compression)

almost non-existent and the force level in the middle zone is not held at a (more or less) constant value as in the case with a bed of glass spheres. These are owing to the facts that:

- granular particles do not exhibit sharp failures like spherical particles,
- bed packing is more tighter and voidage is less,
- secondary fractures almost always occur concurrently with primary fractures, and
- bed solidification starts earlier at a lower % compression compared to bed of spherical particles.

For the experiments with granular material actual η_b was not calculated, but instead, to keep things simple, amount of coarse material broken (g) per inch-pound of bed work was calculated for each experiment. This value differs from actual η_b only by a scaling

factor which is the ideal bed work (in-lb) to crush 1 g of granular material. This will be referred as η_b' or relative fracture efficiency. The graph of η_b' vs compression will give a qualitative idea of the variation of actual η_b vs % compression.

Variation of η_b' with % compression is shown in Figure 4-11.

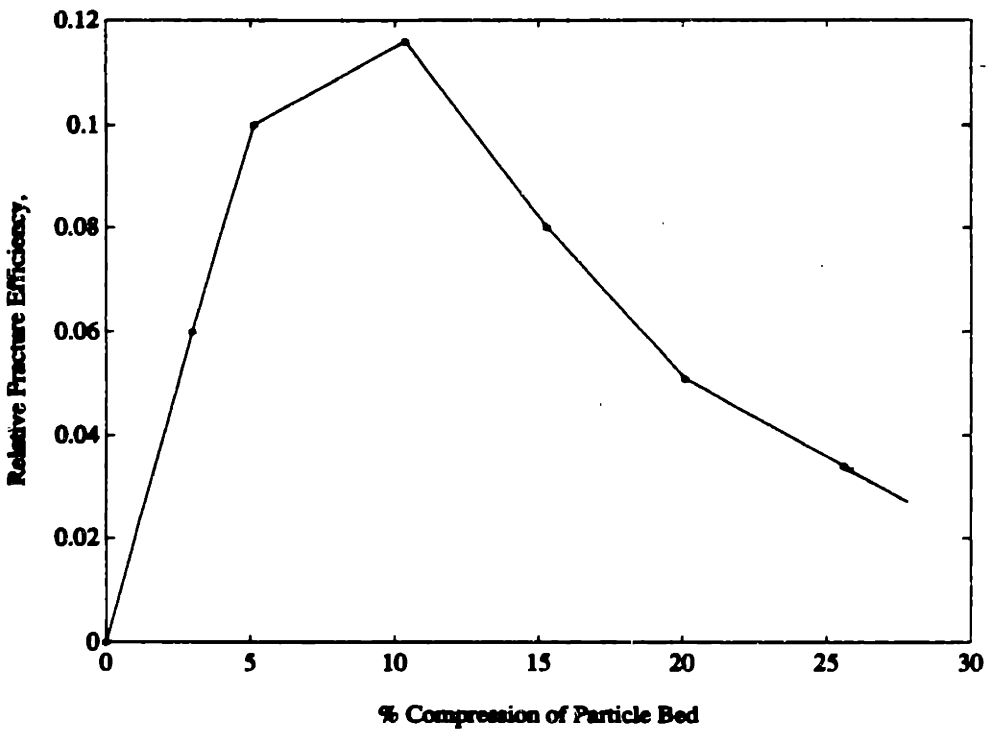

Figure 4-11: Variation of relative fracture efficiency with % compression for bed of granular material

Relative fracture efficiency was maximum at about 10% compression and was lower for both lesser and larger compression amounts. This means that to realize maximum utilization of crushing energy for brittle granular particles, the compression stroke has to be shorter than that required for a particle bed of spheres. The size distribution of the crushed material at optimum compression as estimated by eye, compared to that of the crushed material of a bed of glass spheres undergoing similar compression indicated larger % of fines produced which confirms earlier postulation. Figures 4-12 shows the pictures of the crushed products of beds of glass spheres and granular material of nearly identical bed height and undergoing identical % compression.

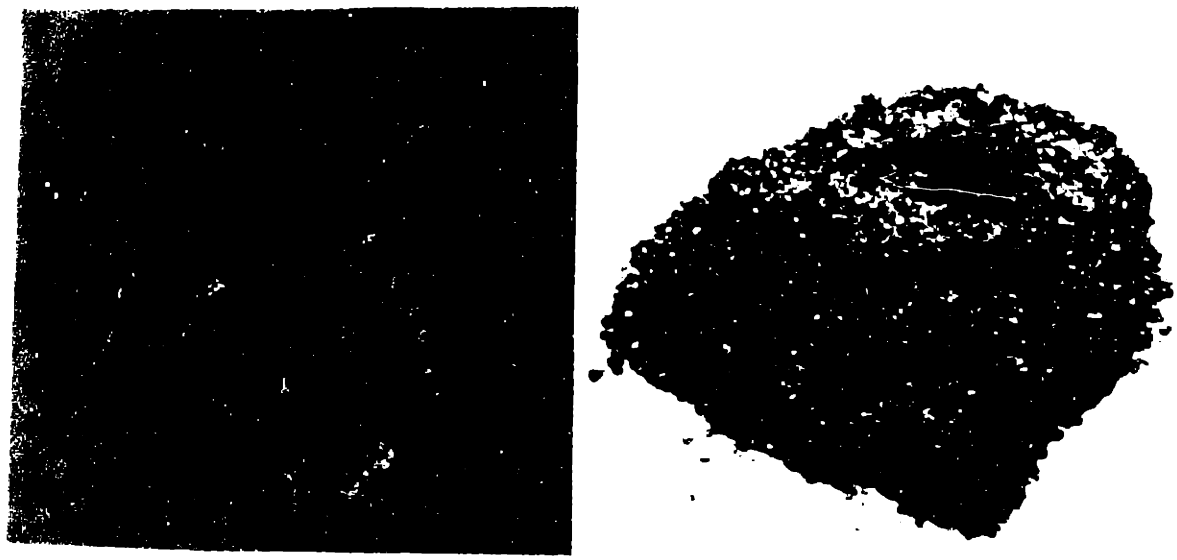

Figure 4-12: Picture showing crushed products of beds of glass spheres and granular material

The experiments with beds of granular materials were time consuming, primarily due to difficulty in sieving. Therefore, no experiments were conducted to see the effect of bed height on η_b. However, it is postulated that the behavior will be qualitatively similar to that exhibited by beds of glass spheres, excepting that the rate of drop in η_b with bed height will be steeper than that observed in beds of spheres due to more energy loss in inter-particle friction within the bed. Because, with increasing bed height primary and secondary crushing together will be producing more fines resulting in more contact points to blunt the crushing forces.

One experiment conducted with slant piston and base on a 0.645" high bed of granular material indicated no significant effect of shear loading on η_b.

4.2.10 Effect of Presence of Water and/or Oil in the Particle Bed Undergoing Compression on η_b

In many cases, in practice, wet crushing is often adopted (such as in water-flush cone crusher), since for downstream processing or end use of the fine products, slurried form is desirable. Water is generally used for wet crushing. Again in some cases the fine

products of crushing are treated in a flotation cell (for separation of minerals from gangue material) which uses water and oil (often pine oil). In this research one of the objectives, as mentioned in chapter 3, was to see if water and/or oil has any beneficial effect on η_b. Only four experiments were conducted with 1/2" beds of glass spheres, two of which used wet glass spheres, while the other two experiments used glass spheres lubricated with machine oil. The results are shown in Table XVII in the appendix. Results were similar to that obtained by Laffey, indicating practically no effect of the presence of water or oil on η_b. It is believed that at very high stress encountered within the crushing zone, the particle-to-particle friction behavior is not influenced by the presence of any fluid.

4.2.11 Effect of Instron Machine Compliance on η_b Calculation

As mentioned in chapter 3, η_b will be slightly underreported (by about 1% or so) if the compliance of the Instron machine is ignored in the calculation of actual bed work. Force-deflection curve was generated from the data obtained with a blank test, with no particle bed inside the cylinder (Figure 4-13).

The force-deflection curve shows that the force in 6,000 lb to 18,000 lb interval (between points B & C in Figure 4-13) varies linearly with deflection where the deflection in inches x due to machine compliance (in fact the compliance of the vertical column of the Instron machine between the load cell on the fixed upper cross head and the lower compression head) is found by calculation to be equal to:

$$x = 0.01331+8.13333\text{x}10^{-7}\text{x}(\text{F-}6{,}000) \ldots (1)$$

where F is the magnitude of the force.

For the portion of the curve AB (Figure 4-13), six equally spaced data sets for force and deflection were selected and curve fitting technique using exponential regression analysis was used to determine the force vs deflection relation. The result showed that:

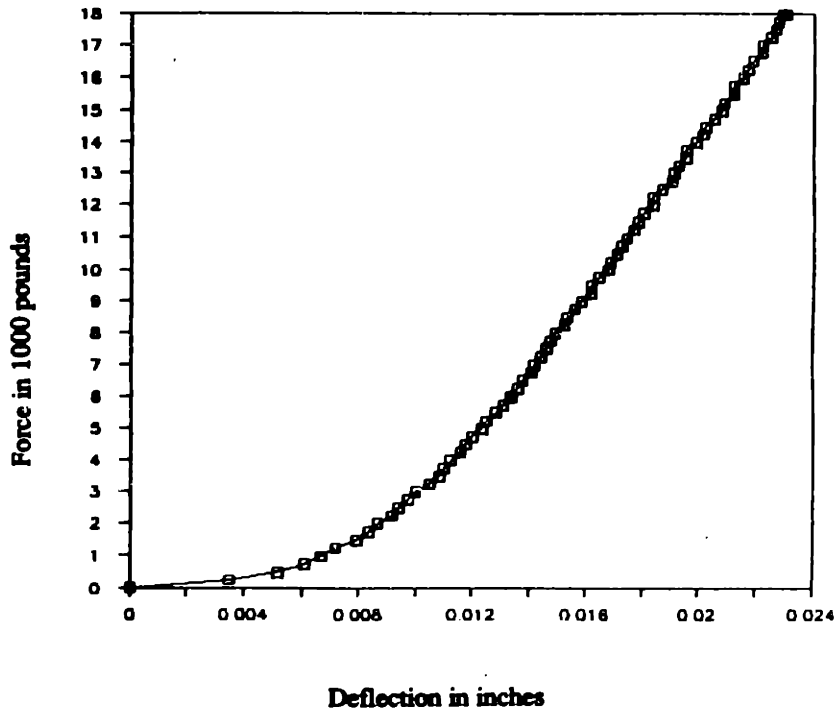

Figure 4-13: Force-deflection curve for Instron machine compliance test

$x = 4.919212 \times 10^{-4} \times F^{0.378122}$ . . . (2)

In the calculation of the bed work, the deflection corresponding to a certain force was corrected by subtracting the machine compliance, x, calculated by using the appropriate formula (1) or (2). Lotus 1-2-3 software was very useful for these calculations. These calculations involved much computer disk usage and time, and therefore, were done only for tests with 1/8", 1/2", and 2" bed thicknesses. Table XVIII shows that the calculated values of η_b, corrected for machine compliance, is only about 1% more than the corresponding uncorrected values. For this reason it was not condsidered worthwhile to correct the rest of the η_b values in this thesis. However, it is worthwhile to note that a machine itself consumes some amount of energy due to its compliance, which reduces the overall efficiency of the crushing process.

4.3 Study of Fluidization Behavior of Binary Mixture of Glass Spheres

The importance of material transport in enhancing comminution efficiency was emphasized in chapter 2. It was recognized that by intermittent fluidization between crushing strokes fine particles of product size can be effectively elutriated by size-dependent relative motion and coarse particles can be segregated according to size within the crushing zone. These are important from the energy utilization or efficiency point of view, as discussed earlier, as presence of fines reduces the crushing efficiency.

The major thrust of this research relative to material transport was on the survey and review of past and current work on fluidization of binary mixture of glass spheres. The results and discussions relating to this study have been summarized in chapter 2, and therefore, not repeated here. The findings of this theoretical study were verified and reinforced by experiments conducted by Annis, the results of which are reported in her thesis and summarized in chapter 2. However, the following discussions are presented below.

Gas-solid fluidization within very limited range of low fluid velocity, and in the laminar, smooth, and low Reynold's number flow regime only, where the $Fr>1$ (refer to chapter 2), may lead to segregation in a fluidized bed of a binary mixture of particles. The ratio of the minimum fluidization velocities for the two sizes of particles must be at least two. The bed expansion is more in gas-solid fluidized bed compared to liquid-solid fluidized bed, which will require a taller working space. All these constraints, plus the difficulty in effectively controlling the low gas velocity, do not make gas (meaning generally air) an attractive fluidization medium. Therefore, gas-fluidized transport process of fine products may only be considered for integration with a dry crushing process. Even then, a very effective removal of fines and segregation of coarse materials within the crushing zone may not be achievable. But it is expected that comminution efficiency will still be enhanced even with partial segregation.

Liquid (meaning generally water) can serve as a better fluidization medium to achieve better segregation and elutriation. Velocity control is also easier in liquid-fluidized beds. It is believed that an efficient material transport system, into, through, and out of the crusher is feasible realizing appreciable gain in crushing efficiency, using water as the working fluid.

Segregation in a liquid-fluidized bed is a time cosuming process, which requires several seconds to complete even in a 10" high experimental bed of a binary mixture of glass spheres (2 mm & 0.8 mm sizes). Since segregation has to occur during the time interval between two crushing strokes (say within a jaw crusher) the overall fluidization process including elutriation of fines will be like a *batch* process. Furthermore, crushing should not commence until the segregated coarse material has time to settle, otherwise, the excessive void space in the expanded fluidized bed will make clamping of coarse particles between the crushing elements and subsequent crushing difficult and ineffective.

Settling of the coarse particles after segregation is thus very important from the particle breakage efficiency point of view. Proper segregation followed by settling will place the coarse particles at right locations, with right bed packing condition and minimum points of contact for optimum utilization of the crushing energy. This requires *on and off* or periodic fluid flow. Time needed for segregation and subsequent settlement of the coarse particles will be a constraint on the frequency of the crushing strokes, and therefore, on the production capacity of the crushing device, since in a practical crushing machine the number of crushing strokes are a few hundreds per minute. However, it is expected that overall improvement in the combined crushing/transport process can still be achievable by proper design and integration of the crushing and fluidization subprocesses and using optimization techniques.

Control of bed expansion will be necessary to minimize the space within the crushing

chamber. Inclination from vertical and divergence of the crushing chamber walls have to be limited to ensure effective segregation. This may be accompanied by proper design of the crushing chamber.

Actual crushing machines process granular material. Therefore, fluidization experiments were conducted by the author using a 1" diameter round vertical glass tube and a binary mixture of granular sand (equal proportion of 2 mm and 0.8 mm glass spheres by weight). After a short period of fluidization, a sharp separation of the two sizes were accomplished. Fluidization behavior was similar to that observed with binary mixture of glass spheres. This demonstrates the feasibility of the fluidizatio process with mixtures of granular particles.

Chapter 5

Application of Research Findings

The findings of any research are more meaningful when they can find direct applications in the real world, for example in making processes productive and efficient. This research was focussed on two very important subprocesses which occur within a crushing machine (well known for its inefficiency), i.e., particle breakage and material transport. These two subprocesses jointly govern the efficiency of the crushing machine and thus must be optimized together. This chapter will discuss how the research findings can be rendered useful in the formulation of a mathematical model of the integrated crushing material transport process and in making selection of preliminary design criteria of a high-efficiency comminution device. The applications of the research findings are discussed below.

5.1 Single Particle Breakage Test

The fact that side loads, even up to the magnitude of the primary normal crushing load, do not inhibit fracture of brittle particles implies that the simple failure criterion of a particle under two-point compressive loading adequately describes the behavior of multiple-loaded brittle spheres. This criterion can be effectively utilized in particle bed simulation. This also has a direct application in the design of a crushing machine because the crushing elements must create the necessary failure stress level for fracture to occur. And since the crushing load is blunted by the number of points of contacts (between particles themselves or between the particles and wall or particles and the crushing element), even higher force must be developed by the machine than is required to crush the particles under two-point loading. Or, in other words, a more

robust machine will be needed to crush a particle bed if excessive fines are present. The thickness of the particle bed (sometimes expressed in terms of the number of particle diameter) must, therefore, be such that the crushing machine can safely develop the required failure stress for as many particles as possible. Another fact that brittle material in the micron size level behave plastically and its failure is inhibited by lateral confining loads will be important in the design of crushing devices for very fine crushing.

5.2 Particle Bed Fracture Test

The fracture efficiency, as defined by Ghaddar, is a meaningful concept used to good advantage in comparison of energy test data. This is a measure of the efficiency of utilization of the available crushing energy for compressive comminution of a particle bed. Factually speaking, fracture efficiency should also have another dimension which relates to the fineness of the products (or size-distribution). This simple definition, however, is based on the number of full-sized particles broken, regardless of the size to which they are broken and so it does not take size-distribution of product into account. However, as evident from the size-distribution results, two things became apparent:

- the size-distribution due to primary crushing is always bimodal, and
- the proportion of fines, say at a reduction ratio of 2.4 (a very practical ratio for primary crushers), is also approximately constant. Therefore, for all practical purposes we can, for the time being, ignore the size-distribution aspect.

The importance of prompt removal of fines from the crushing chamber was clearly evident from the force-deflection curve of a particle bed undergoing compression. As the inter-particle voids get filled up by the products of crushing the fracture efficiency begins to drop. There is an optimum % compression which depends on material

properties (such as size, shape, hardness, brittleness, etc.) and bed conditions (such as bed thickness, presence of confining walls, presence of fines in the initial composition of the bed, etc.). For particle beds of round glass spheres (2 mm in size) this % compression was about 18 - 22 %, while for beds of granular sand particles it was about 10%. These compression figures can however, be increased by about 5% with a small sacrifice in η_b.

This behavior of η_b vs compression is therefore, very important in optimizing the length of stroke of the crushing element. Again it should be noted that if the fines can be promptly removed then a longer stroke could be utilized for crushing a thicker bed at the highest efficiency.

Fracture efficiency within particle beds under compressive comminution increases with decrease in bed height. This implies that processing of thinest possible beds with the fastest possible rate and frequency of compression, which can still meet the production throughput requirement, is more desirable. This will improve the crushing efficiency and at the same time the crushing element will not be required to develop a higher force level (which is beneficial from the point of view of machine wear and safety).

It has been recognized earlier that crushing efficiency is better utilized when the particles within a bed undergoing compressive comminution are of uniform size, meaning that number of force contact points are minimum. Much energy is wasted when larger particles are comminuted within a bed of fines due to excessive number of force contact points. Within a crushing machine the larger particles usually go through a progressive size reduction until the designed output size is obtained. This means that there is a size-distribution of materials present within the crushing chamber. Therefore, one of the major objectives of the material transport system design through the crusher will be to place the material at the right locations, segregating them vertically. In this situation the crushing elements will be acting like a number of crushers vertically

arranged, each crushing a bed of particles of one size at any one vertical location. As mentioned earlier a fluidized transport system has the potential to obtain this object efficiently.

The presence of fines within a particle bed just before the crushing stroke inhibits the fracture efficiency. Therefore, it will be advantageous to remove the fines, if present in an excessive amount, in the feed material by presieving the feed or by an efficient material handling scheme within the crushing chamber which can intermittently remove the fines in between two consecutive crushing strokes (such as fluidized transport system).

The facts that crushing energy utilization is more efficient in primary crushing of the particles (up to the compression amount at which the initial bed voidage is just filled with fines) and a significant amount of of the feed particles can be broken (more than 1/3rd) by primary crushing just by one stroke of the crushing element, again point out the importance of prompt removal of fines and segregating the coarse material before crushing, so that every stroke of the machine will act like a primary crushing stroke. This is much more important in the case of granular material (almost all the material crushed in the crushers in practice are granular and brittle material), because the bed voidage is lower and optimum % compression is also lower compared to particle beds of spherical materials. From the above findings it is clear that the main reason for low efficiency of the crushing machines in practice is repeating the crushing strokes on the feed material over and over again in order to break the larger particles buried in a bed of fines, using force of larger magnitude than necessary, and wasting energy. Thus, an improved crusher must optimize those bed conditions and compression parameters which lead to maximum particle breakage within the bed for every crushing stroke.

Crushing elements and the surface against which the particle bed is crushed should be made of material of proper hardness so that the energy lost in wear and plastic

deformation of these materials will be minimized. The design of the crushing cavity should be such that wall friction during crushing is minimum.

Fracture efficiency in compressive comminution is hardly influenced by the rate of loading. This indicates that faster crushing strokes, if otherwise permitted, will be more advantageous and meaningful from the production point of view, without any sacrifice in crushing efficiency.

It has been recognized and also experimentally verified that compressive loading is the primary mode of comminution for a crushing machine. The amount of particle breakage due to shear loading is limited to a minor amount due to secondary breakage abrasion, etc. Therefore, the crusher design should focus on the mechanism of normal compressive loading only and the best utilization of the same.

5.3 Material Transport

This study focussed on material transport subprocess using the concept of a fluidized bed which, when integrated into the overall crushing proces, is believed to improve the fracture efficiency of the particle breakage subprocess by attaining the objectives of prompt fines removal and segregation. The customary method of material transport through a crusher, which utilizes force of gravity to make the material flow through the machine, does not meet these objectives and is often responsible for choking problem at the exit area of product. Use of a classifier to remove the fines is also not a very effective option since it is an addition of equipment to the crushing circuit and, also, it cannot remove the fines between consecutive crushing strokes as that will necessitate unloading of the material after each stroke into the classifier for separation of fine particles, which is not productive.

In the design of the dry crushing process, air may be utilized as the fluidizing medium.

The rate to be selected will be determined from experiments or theoretical calculations making sure that segregation is enhanced by maintaining the fluidization in the particulate phase where no bubbling (therefore, no mixing) is present. Fluidized transport with air may not attain the objectives perfectly, but this process can easily be integrated with the crushing subprocess, and will not necessitate drying of the output material downstream.

Liquid-solid fluidization is more stable and well behaved, and elutriation of fines and segregation of coarser particles are more easily attainable and controllable than in the case of gas-solid fluidization. Fluidizing velocity and water flow rate for design purpose can be calculated for a mixture of particles to be fluidized in a manner, which working intermittently or periodically between two crushing strokes, will selectively remove the fines of product size and segregate the coarse particles within the crushing chamber. Batch process will work well since sufficient time should be allowed for elutriation of fines and segregation of coarser particles, as well as settling of the bed after fluidization just before the commencement of crushing stroke. More experimental study is necesssary to determine the feasibility of fluidized material transport systems for crushing for a continuously operating system. However, from the encouraging fact that just one crushing stroke produces a significant amount of fines by primary breakage at a sufficiently high fracture efficiency (40% or more), it is anticipated that the batch system is still a viable choice.

It was observed that segregation time varies linearly with bed height. For a conceptual fluid-flushed upward flow crushing machine of a practical size, it is anticipated that the segregation and settlement time, by proper design, will be of the order of several seconds only (probably less than 30 seconds). This compares favorably with tumbling machine operations where the residence time is of the order of several minutes.

In the design of the crushing chamber, which will also be the fluidizing space, attempts

should be made to keep the walls as close to vertical, and as little divergent as possible so as to eliminate or limit recirculating motion of the fluid and solid particles which inhibits segregation. Elutriation of the fines of product size can be maximized by fixing the superficial fluid velocity at a value which will just exceed the terminal velocities of the fine particles, but will still keep the entire bed of the mixture of particles minimally fluidized. Again, from the point of view of bed expansion, this velocity should be so chosen as to limit the bed expansion to the minimum, to minimize the size of the fluidization chamber. Another important aspect is the height of the static bed (just after the crushing stroke and before fluidization). This must be optimized so that the total time required to segregate the coarse material, elutriate the fine product and settle the bed again after segregation (which is a linear function of bed height), is acceptable from the production throughput point of view. Minimizing the amount of fines in the feed by presieving, as stated earlier, will also be helpful in this regard. Proper location of the outflow point of the fines in the machine will maximize the concentration of the particles of the desired output size range in the outflow stream.

The primary goal of this research was to find ways to optimize the fracture efficiency in compressive comminution, and to minimize the magnitude of force to be developed by the crusher, as well as the crushing energy, all these at a cost acceptable to the industry. From the above discussions it is evident that the knowledge gained from this research will be extremely useful in the selection of preliminary design parameters of a next generation high-efficiency comminution device. This research pinpoints the various aspects and parameters of the integrated particle breakage/material transport process and their effect on the fracture efficiency and thus provides a necessary foundation for subsequent detailed design. This research is unique in the sense that it does not treat the particle breakage and material transport on a piecemeal basis, but attempts to maximize the synergy of both these important subprocesses for efficient utilization of the available crushing energy within the crushing machine.

In passing, it is worthwhile to mention that with the advent of modern control systems engineering, all the design objectives mentioned in this chapter can be further augmented by incorporating various control systems in the crushing machine. For example, the control system can check the magnitude of compressive force, % compression (or strain), size-distribution or composition of feed and product, fluid flow rate and velocity, elutriation rate, etc. and then control the various subprocesses to further maximize the fracture efficiency and the production throughput.

5.4 A Simple Mathematical Model of the Combined Crushing/Material Transport System of a Conceptual High-efficiency Crushing Machine

In an attempt to maximize the synergy of the particle breakage and material transport systems a new conceptual fluid-flushed upward flow crushing machine has been envisaged at MIT. It is anticipated that this concept will combine both the crushing and fines removal processes in an efficient and compact way. Figure 5-1 shows a schematic representation of one possible expression of this concept. Details such as fluid distributor, piston drive assembly, support structure, fluid flow stabilizing section, etc. are purposely omitted in this sketch. In this machine periodic fluidization occurs between two consecutive crushing strokes of the piston, by which the progressively finer material are lifted up towards the top of the crushing zone and the fines of output size are elutriated. The feed is introduced at the beginning of fluidization process along with the fluid in a hydraulic transport mode. Inside the chamber, which is rectangular in cross section the velocity is reduced to a value which is required to elutriate the fine particles (produced by previous crushing strokes, as well as the fines present in the feed) but just sufficient to minimally fluidize the coarse particles so as to let the fines pass through them.

Elements of a typical cycle for crushing of a batch of coarse feed will be:

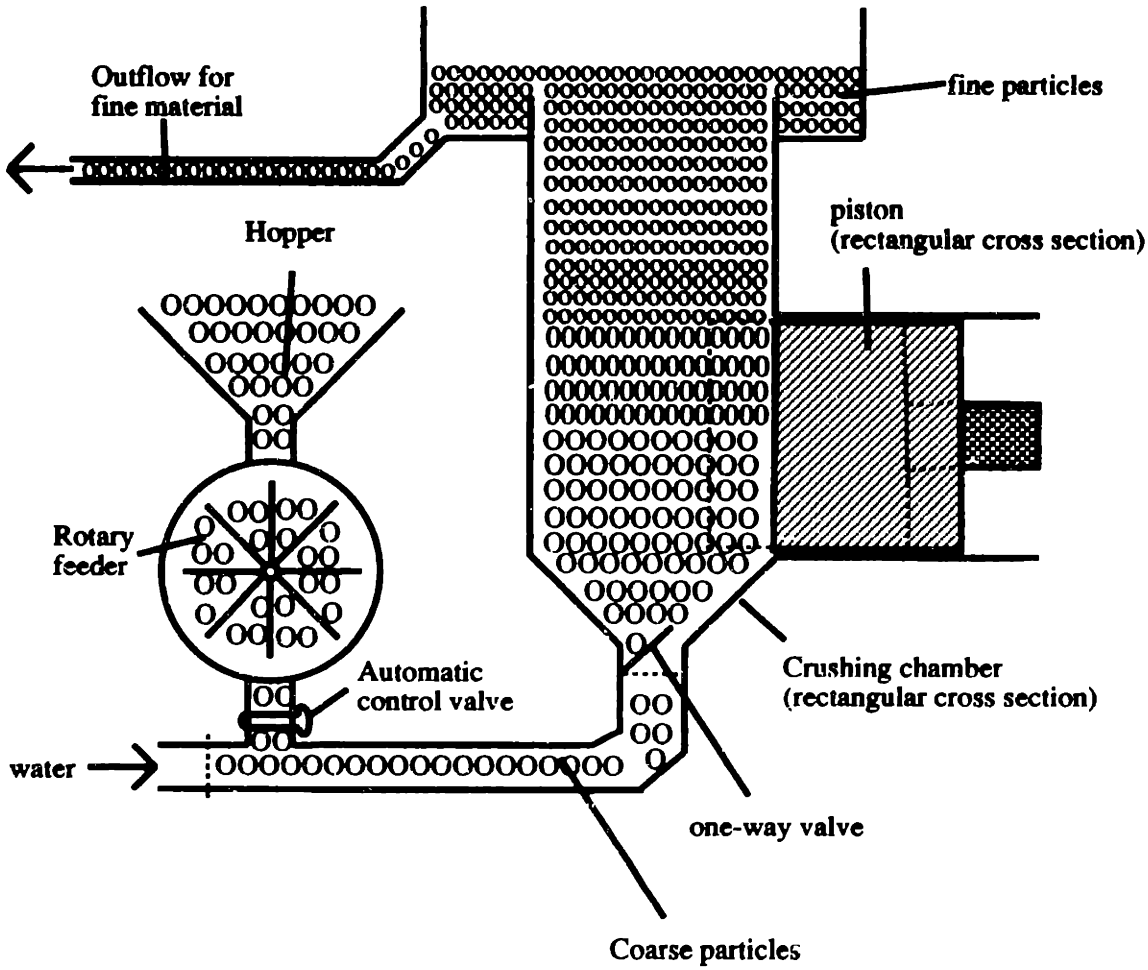

Figure 5-1: Schematic representation of one possible manifestation of the conceptual high-efficiency crushing machine

1. introduction of feed,
2. fluidization to segregate the particles and then a step increase in the fluid velocity to expand the bed high enough for the fine particles of output size to flow out through the exit,
3. stopping fluid flow to let uncrushed or partly crushed coarse material to settle, and
4. crushing the coarse material to optimum % compression.

Modelling this particular process will be simple since it is a batch process and the crushing and fluidization subprocesses are distinctly separate.

Certain assumptions are made as follows:

- there are only two sizes of particles to consider, one, the coarse size, and the other, the fines of desired output size;
- the ratio of of the diameters of the coarse to fine particles, is at least 2.2 to assure segregation (as discussed in chapter 2);
- ratio of the smallest chamber dimension to biggest particle diameter is at least 10.0 to eliminate wall effects (discusses in chapter 2);
- fluidizing velocity is so selected that it is at least equal to the minimum fluidization velocity for the bed containing binary size mixture of particles (which can be empirically determined) but greater than u_t of the fine particles, and Froude number for the flow regime is >1 (reasons are discussed in chapter 2);
- the flow is in the low Reynolds number laminar regime and the fluidization is in the particulate phase; and
- the % of fines produced at optimum compression due to primary breakage, or the breakage factor is constant (in fact nearly so) and secondary breakage is ignored (for the time being). With these assumptions the mathematical model can be expressed by a simple size-mass balance relationship.

The steps of the medelling process are given below:

Size-mass balance equation:

$$n(xW_F + CW_B) = W_P \text{ - - - (1)}$$

Where n = fines separation efficiency ; x = % of fines in the initial feed (if any); W_F = weight of feed per batch; W_B = weight of material in the bed (this will be nearly constant after about 5-10 batches when the amount of feed will equal to the amount of fine product elutriated; this is equal to the weight of the new feed plus weight of uncrushed or partly crushed coarse material remaining in the bed from previous batch or batches; c = breakage factor of the coarse material for one stroke of the piston (found from fracture tests of particle beds) and W_P = weight of product per one cycle of the process (i.e. pumping in feed, fluidization, elutriation of fines, settling of the coarse material and crushing of the coarse material).

$$W_F = W_P \text{ - - - (2)}$$

when the combined process is running at full capacity. Thus in this simple case, the amount of fine product is equal to amount of feed material per cycle of the batch process and the product is of the desired output size.

Bed expansion:

Bed expansion can be found by the serial model relation and Richardson and Zuki equation as discussed in chapter 2:

$$u/u_t = \varepsilon^n \text{ - - - (1)}$$

$$H = H_1 + H_2 \text{ - - - (2)}$$

$$H(1-\varepsilon) = H_1(1-\varepsilon_1) + H_2(1-\varepsilon_2) \text{ - - - (3)}$$

where subscript 1 and 2 represent the fine products and coarse products respectively; the rest of the items are described in p. 35.

The height of the expanded bed should be optimized keeping in mind the size and cost of the fluidization chamber (most of which is the crushing chamber itself) and the rate of elutriation of the fine products, which depends on the expanded height of the bed, fluidizing velocity, and the location of the outflow pipe.

The design fluidization velocity can be determined from the equations given in p. 36.

This simple model is too simple to represent a conceptual and integrated crushing/material transport process which will probably be a continuous and quasi-steady process with the crushing strokes occuring rapidly while the bed is in a continuously fluidized condition. In this model solids and fluids will be treated as coupled continua, describing comminution and solids transport in a form useful to design. Continua equation can be developed for both the fluid and solids transport, relating (empirically as a start) fluids and solids velocity to size-distribution of solids, and bed expansion, and elutriation rate, and crushing to breakage factor, particle shape, compression % and other parameters. This will require additional study (using a continuous fluidization process) of the elutriation rate, expansion of bed with a

distribution of sizes, etc. In these fluidized experiments the generation of the fines can be imitated by the addition of fines to the fluidized bed at a rate equal to the breakage rate due to crushing, and by the removal of coarse particles at the same time at an equal rate so that the bed weight remains constant and the process can be operated at a steady state. This will serve the purpose of modelling a combined crushing/solids transport process without going through a complicated design of an apparatus with actual crushing strokes.

The crushing strokes interrupt the fluidization process; but in actual machine these strokes will be fast and at a high frequency. Their effect on the fluidization process will be like a series of quick pulses added to a more or less steady constant fluidization velocity. Therefore, quick pulsing will be needed in the continuously fluidized bed experiments. The modelling of this process will not be too complicated but is outside the scope of this thesis.

Chapter 6

Conclusions and Recommendations

This research has looked at compressive comminution both from the particle breakage and material transport point of view in order to maximize their synergy to enhance crushing efficiency.

6.1 Conclusions

The most important conclusions of particle breakage study in this research are the following:

- the breakage efficiency in compressive comminution attains a maximum value at a % compression where the initial inter-particle voids are just filled with the fine products of comminution;
- the primary fractures of the coarse particles are the dominant fractures upto this optimum % compression;
- more than 1/3rd of the coarse particles are crushed to fine sizes at a reduction ratio equal to that of practical crushers;
- rate of compression and addition of shear loading to compressive loading have hardly any effect on breakage efficiency;
- maximum breakage efficiency decreases with the increase in thickness of the particle bed;
- increase in breakage efficiency is possible by prompt removal of fines from the crushing chamber in between consecutive crushing strokes; and
- behavior of particle beds of brittle granular material under compressive loading was qualitatively similar to that observed with beds of glass spheres; but the optimum crushing stroke was at a lower % compression.

The most important conclusions from the fluidization study are the following:

- fluidized separation of fine products from the crushing chamber is feasible, and it can also segregate the coarse materials remaining in the fluidized bed (meaning the crushing chamber of an integrated crushing/fluidizing machine) for better utilization of the crushing energy, due to lesser number of force contact points;

- liquid-solid fluidization is superior to gas-solid fluidization in terms of elutriation, segregation, and ease of control of fluid velocity;
- divergence of fluidized bed and inclination of the fluidized bed from the vertical cause recirculation and degrade segregation quality; however, divergence of the side walls of the bed upto about 4° from the vertical may be tolerable and beneficial in controlling excess bed expansion;
- segregation time is linearly dependent on the bed height;
- pulsation of fluid flow is harmful in terms of quality of segregation for taller beds than that for shorter beds;
- miniumum fluidizing velocity for binary mixture of particles, height of the expanded bed, and elutriation rate can be predicted using various correlations available in published research materials;
- fluidization behavior of beds of granular material is qualitatively similar to that of beds consisting of spherical particles; and
- segregation time for granular particles in a fluidized bed is slightly less compared to spherical particles of similar characterisitc dimension due to shape effect.

Final conclusion from this in-depth study of the overall compressive comminution process is that substantial improvement in crushing efficiency within a particle bed is possible with appropriate design of the crushing machine which optimizes the various parameters relating to particle bed, crushing load, compression, and material transport.

6.2 Recommendations

Compressive comminution or crushing is recognized as the most efficient mode of comminution of materials and it performs the major comminution task in the industry in terms of tonnage handled. Because of these reasons, comminution industry is now thinking in terms of progressive replacement of the tumbling machines (whose efficiency is very low, only about 0.1 to 1.0%) by crushing machines for fine crushing of solids. This makes compressive comminution more attractive and important. The current research has looked into various ways of enhancing the crushing efficiency. But more research will be needed in the near future to realize the full benefits of crushing. The following is a list of suggested topics for future research:

- study of fracture efficiency within particle beds undergoing compressive comminution, at various compression rates and for different bed heights, without interrupting the test for sieving, using advanced techniques, such as acoustic means to distinguish between primary and secondary fractures;
- study the effect of cyclic loading on fracture efficiecny during bed compression. This knowledge will be valuable since in practical machines particles are progressively crushed to finer sizes by repeatation of crushing strokes which occur at a specified frequency;
- fracture tests of beds of granular materials to gain quantitative knowledge of the effect of bed height and other compressive parameters on fracture efficiency;
- fracture tests with unconfined beds, i.e., having insignificant edge or wall effect;
- extend the definition of fracture efficiency to include other dimensions of the crushing process, i.e., fineness of products by determining size-distribution;
- study the effects of additional external influences on fracture efficieny in particle bed comminution (such as shock wave; vibration, chemical additive, heat, different shapes of converging wall and piston surface configurations, etc.;
- in-depth study of fluidization behavior of ternary mixture of particles or even a mixture of particles with a wide size-distribution in a fluidized bed;
- fluidization study with multiphase flow such as air, water and mixtures of solid particles of different sizes and shapes;
- fluidization tests in continuous operations as suggested in chapter 5;
- in-depth study of the unsteady and transient behavior of the bed during fluidization, especially the time vs. expanded bed height relation;
- fluidization study with moving boundary walls and creation of fine particles (in a manner suggested in chapter);
- study the effect of rapid pulsing on elutriation and segregation in a fluidized bed;
- study fluidization behavior with properly treated (generally with oil or other flotation reagents) air or fluid, which may enhance elutriation and segregation by flotation effect;
- tests in vibrofluidized bed;
- fluidization tests with granular particles of wide size-distribution and of varying depth;
- evaluate various methods to minimize bed expansion and segregation time and improve segregation and elutriation;

- study of elutriation rate and concentration of solids and different sizes inside the bed and in the outfloiw product during fluidization;
- study of settling behavior of the coarse particles after segregation; this is important for maximizing the utilization of the crushing energy;
- mathematical modelling of the integrated crushing/material transport process involving particle bed with a wide size-distribution, as well as beds of granular material to predict rate and size-distribution of output, and resident time of particles in the bed;
- computer simulation of the integrated crushing/material transport process (3-D model);
- exploring the feasibility of other conceptual designs of a crushing machine which will maximize the breakage efficiency and throughput (such as a machine where crushing occurs between the crushing chamber wall and the crushing element by the nutation of the crushing element about an eccentric drive, which creates a rotating zone of convergence). A fluid flushed upward flow crushing machine, crushing solids in a manner similar to that of a cone or gyratory crusher, is a possible choice for further study. Fluid mechanics and solid mechanics aspects of this conceptual machine must be studied in-depth to determine the effect of the bed voidage due to continuous operation, as well as the lateral motion of the particles, due to the nutation of the crushing element, on particle gripping and breaking capability and crushing efficiency. Crushing energy utilization is the primary focus here; and
- finally study should be made to see how the various techniques of modern control systems engineering can be applied to compressive comminution process to optimize the overall operation. For example, the control system can monitor the various parameters of the partiucle breakage and material transport subprocesses and then control the various activities using a feedback system to optimize the crushing energy utilization and throughput, to minimize energy consumption, and matal wear , etc.

It is hoped that someday in the future the science of size reduction will be developed to such an extent that the basic equations will be available whereby a secure calculation regarding the rate of production of fines, its size-distribution, energy requirement for crushing, etc. can be predicted without any prior empirical test. The research, like this one, will hopefully be preparing the way to gain such a knowledge.

Appendix

Table I: Force-displacement data for the fracture of 1" diameter glass spheres subjected to two-point primary compressive load

Expt. #	Sphere Dia., [in]	Fracture Load, F [lbs]	Fracture Stress, Mpa*	Displacement [in]
1	0.950	3950	38.4	0.012
2**	0.945	3300	32.4	0.015
3	0.956	3750	36.0	0.013
4	0.960	5100	48.6	0.012
5	0.957	4300	41.2	0.014
6	0.940	4370	43.4	0.016
7	0.962	4500	42.7	0.013
8**	0.960	3800	36.2	0.012
9	0.955	4000	38.5	0.016

* $F/(\pi D^2/4)x(6.895x10^{-3}MPa/psi)$ Average fracture stress = 39.7 MPa; Standard deviation = 4.82 MPa

** Compression rate = 0.01"/second; for the rest of the experiments compression rate = 0.001"/second

Table II: Force-displacement data for the fracture of 1" diameter glass spheres subjected to primary and four side loads

Expt. #	Sphere Dia. [in]	Primary Load, F [lbs]	Fracture Stress [Mpa]	Side Load, S [lbs]	(S/F)x100 [%]	Displace ment [in]
1	0.937	3900	38.9	3500	90	0.0165
2	0.942	5100	50.5	3000	59	0.0199
3	0.935	4200	42.1	3950	99	0.0157
4	0.930	3500	35.5	2000	57	0.0155
5	0.921	3500	36.2	3000	86	0.0161
6	0.967	5100	47.9	5100	100	0.0190
7	0.964	3680	34.8	3500	95	0.0127
8	0.968	4700	44.1	2000	43	0.0191
9	0.952	3500	33.9	2000	57	0.0154
10	0.895	3800	41.6	2500	63	0.0164
11	0.930	4500	45.7	2500	56	0.0179
12	0.945	3700	36.4	3000	81	0.0154
13	0.923	3700	38.1	3000	83	0.0156
14	0.955	5100	49.1	5100	100	0.0194
15	0.948	4300	42.1	3000	70	0.0187

Table III: Force-displacement for the fracture of 1" diameter plastic spheres subjected to two-point primary compressive load

Expt. #	Sphere Dia., [in]	Fracture Load, F [lbs]	Fracture Stress, Mpa	Displace ment [in]
1	1.00	3590	31.5	0.095
2	0.98	3500	32.0	0.106
3	0.05	3700	29.5	0.120
4	1.00	4100	36.0	0.137
5	1.06	3800	29.7	0.122
6	1.00	3700	32.5	0.118
7	1.00	3900	34.2	0.113

Average fracture stress = 32.2 MPa; standard deviation = 2.33 MPa

Table IV: Force-displacement data for the fracture of 1" diameter plastic spheres subjected to primary and four side loads

Expt. #	Sphere Dia. [in]	Primary Load, F [lbs]	Fracture Stress [Mpa]	Side Load, S [lbs]	(S/F)x100 [%]	Displace ment [in]
1	1.00	4300	37.8	2000	47	0.104
2	1.00	5000	43.9	2000	40	0.150
3	0.95	5000	48.6	2000	40	0.243
4	1.04	8900	72.3	4000	45	0.250
5	0.99	9600	86.0	5000	52	0.250
6	1.00	7700	67.6	5000	65	0.250
7	1.00	7700	67.6	7100	92	0.155
8	1.00	8400	73.8	8000	95	0.155
9	1.00	6900	60.6	6800	99	0.168
10	1.05	8800	70.1	8800	100	0.161
11	1.00	6770	59.4	6770	100	0.170
12	1.00	7800	68.5	7800	100	0.155
13	0.99	11000	98.6	7000	70	0.170
14	0.97	9850	50.2	7500	76	0.182
15	1.00	8400	73.7	8100	96	0.163
16	1.00	8100	71.1	8000	99	0.150
17	0.95	12000	116.8	5000	42	0.210
18	1.00	12000	105.4	6000	50	0.208
19	1.05	12000	95.6	6000	50	0.250
20	0.97	13000	121.3	7000	54	0.242
21	1.00	13500	118.5	7000	52	0.250
22	0.97	8500	79.3	8500	100	0.140
23	1.02	14500	122.4	7000	50	0.220

Table V: Test to determine the average weight of a glass bead of 2 mm nominal diameter

Expt. #	# Beads	Net Wt. [g]	Wt. per Bead [g]
1	500	6.365	0.012730
2	500	6.480	0.012960
3	500	6.427	0.012854
4	500	6.523	0.013046

Average bead weight = 0.0128975 g

Table VI: Experimental data for particle breakage test with monolayer of 50, 10 and 100 separated glass spheres under compressive loading

Expt. #	Piston Dis placement [in]	# beads broken	Bed work [in-lb]
1	0.0249	50	11.532
2	0.0293	50	12.494
3	0.0404	50	11.750
4	0.0278	50	11.588
5	0.0283	50	12.108
6	0.0260	50	11.367
7	0.0285	50	11.457
8	0.0148	10	2.451
9	0.0256	100	22.793

Average energy needed to fracture a single glass sphere (2 mm nominal diameter) = 0.235131 in-lb

Table VII: Experimental data for fracture test of particle beds under varying % compression for bed heights 0.112" - 0.262"

Expt. #	Appr. Bed Ht. [in]	Compr. %	Wt. Broken [g]	# Spheres Broken	I.B.W. [in-lb]	A.B.W. [in-lb]	η_b [%]
1	0.112	5.00	0.000	0	0.00	12.80	0.00
2	0.112	10.00	0.365	28	6.66	25.60	26.00
3	0.112	15.34	0.988	77	18.01	40.00	45.02
4	0.112	18.07	2.721	211	49.61	76.33	64.99
5	0.112	25.00	2.786	216	50.78	92.00	55.20
6	0.112	31.11	3.106	241	56.63	116.87	48.45
7	0.135	5.13	0.067	5	1.22	8.94	13.64
8	0.135	11.18	0.893	69	16.28	50.87	32.00
9	0.135	18.56	3.637	282	66.30	120.46	55.04
10	0.135	19.08	4.093	317	74.62	139.73	53.40
11	0.135	20.38	4.075	316	74.29	151.96	48.89
12	0.135	25.00	4.792	372	87.37	202.66	43.11
13	0.135	29.52	4.945	383	90.14	225.08	40.05
14	0.135	35.82	5.894	457	107.44	313.61	34.26
15	0.200	5.00	0.000	0	0.00	10.08	0.00
16	0.200	10.17	0.992	77	18.08	68.61	26.35
17	0.200	15.57	3.741	290	68.21	135.57	50.31
18	0.200	19.57	4.529	351	82.58	160.34	51.50
19	0.200	25.34	9.094	705	165.79	342.97	48.34
20	0.200	28.72	9.048	702	164.96	367.72	44.86
21	0.262	4.17	0.000	0	0.00	11.98	0.00
22	0.262	10.85	2.385	185	43.48	136.40	31.88
23	0.262	15.43	4.481	375	88.25	209.71	42.08
24	0.257	20.06	8.021	622	146.23	307.85	47.50
25	0.262	24.85	8.526	661	155.44	384.76	40.40
26	0.262	30.19	12.400	961	226.07	598.86	37.75

Expt. 1-6: Bed weight = 8.0 g; expt. 7-14: Bed weight = 11.282 g; expt. 15-20: bed weight = 16.924 g; expt. 21-26: bed weight = 22.565 g.

I.B.W. = Ideal Bed Work (see explanation in the next page); A.B.W. = Actual Bed Work, as calculated from the force-deflection curve.

Table VIII: Experimental data for fracture test of particle beds under varying % compression for bed heights 0.500" - 2.0"

Expt. #	Appr. Bed Ht. [in]	Compr. [%]	Wt. Broken [g]	# Spheres Broken	I.B.W. [in-lb]	A.B.W. [in-lb]	η_b [%]
1	0.500	5.19	1.635	127	29.81	120.70	24.70
2	0.500	10.17	4.560	354	83.12	252.89	32.87
3	0.500	15.17	11.220	870	204.54	500.59	40.86
4	0.514	20.19	19.420	1506	354.10	801.90	44.20
5	0.518	24.38	25.382	1968	462.67	1130.12	40.94
6	0.500	30.06	29.135	2259	531.16	1626.33	32.66
7	0.740	5.00	1.661	129	30.28	140.85	21.50
8	0.740	10.20	9.395	728	171.28	466.69	36.70
9	0.744	20.26	26.296	2039	479.40	1157.96	41.40
10	0.740	24.30	38.014	2947	693.02	1716.25	40.38
11	1.000	10.00	16.200	1256	295.34	1401.02	21.08
12	1.000	18.13	30.905	2396	563.43	1455.13	38.72
13	0.985	20.22	38.349	2973	699.13	1728.37	40.45
14	1.000	30.00	64.026	4964	1167.25	4241.45	27.52
15	1.500	10.08	15.755	1222	287.23	884.88	32.46
16	1.495	22.57	60.574	4697	1104.31	2842.51	38.85
17	1.500	25.05	70.642	5477	1287.86	3759.08	34.26
18	2.000	10.05	25.240	1957	460.15	1319.99	34.86
19	2.000	20.02	72.414	5615	1320.17	3562.24	37.06
20	2.000	25.05	85.765	6650	1563.56	4643.80	33.67

Expt. 1-6: Bed weight = 45.13 g; expt. 7-10: Bed weight = 67.695 g; expt. 11-14: bed weight = 90.26 g; expt. 15-17: bed weight = 135.39 g; expt. 18-20: bed weight = 185.085 g.

I.B.W. = Ideal Bed Work; meaning ideal energy required to fracture a monolayer bed of the same number of glass spheres, as were broken in the actual bed test, under two-point compressive loading configuration in the absence of particle-to-particle and particle-to-wall friction (see chapter 3, p. 50); I.B.W. = 0.235131 x No. of broken spheres (in-lb). A.B.W. = Actual Bed Work.

Table IX: Variation of maximum fracture efficiency with bed height for particle bed compression test

Bed Ht. [in]	Compr. % at Max. η_b	Calculated Max. η_b [%]	Bed Ht./ Particle Dia.
0.073	10.00	100.0	1.00
0.112	18.07	65.0	1.53
0.135	18.56	55.0	1.85
0.200	19.57	51.5	2.74
0.257	20.06	47.5	3.52
٦.514	20.19	44.2	7.04
0.744	20.26	41.4	10.19
0.985	20.22	40.4	13.49
1.495	22.57	38.9	20.48
2.000	20.02	37.0	27.40

Table X: Particle bed fracture test with varying compression rate

Expt. #	Compr. Rate [in-sec]	Compr. [%]	# Full-Size Broken	I.B.W. [in-lb]	A.B.W. [in-ib]	η_b [%]
1 *	0.001	25.380	1968	462.75	1130.1	40.9
2	0.010	22.930	1778	418.1	981.7	42.6
3	0.025	20.800	1613	379.3	960.8	39.5

Bed weight = 45.13 g; Bed height = 0.51''; Strain or % compression = 24% for all the experiments.

* average value from six experiments.

I.B.W. = Ideal Bed Work; A.B.W. = Actual Bed Work.

Table XI: Experimental data to see the effects of wall friction on η_b

Expt. #	Bed Ht. [in]	Compr. [%]	Wt. Broken [g]	No. Full-Size Broken	I.B.W [in-lb]	A.B.W. [in-lb]	η_b [%]
1	0.139	20.00	7.48	580	136.3	256.7	53.1
2	0.135	20.38	4.08	316	74.3	152.0	49.0
3	0.530	24.95	37.80	2930	689.0	1497.9	46.0
4	0.518	24.38	25.38	1968	462.7	1130.1	40.9
5	0.736	20.00	43.51	3374	793.3	1615.6	49.1
6	0.744	20.26	26.30	2039	479.4	1158.0	41.4

Test numbers 1,3, and 5 were conducted with a 1/16" styrofoam liner inside the cylinder; test numbers 2,4, and 6 were conducted without any liner in the usual way. Bed weights for various bed heights are identical to those in Table VII and VIII.

I.B.W. = Ideal Bed Work; A.B.W. = Actual Bed Work

Table XII: Experimental data to see the effects of piston hardness on η_b

Expt. #	Bed Ht. [in]	Compr. %	Wt. Broken [g]	No. Full-Size Broken	I.B.W. [in-lb]	A.B.W. [in-lb]	η_b [%]
1	0.262	20.56	7.98	619	145.5	319.0	45.6
2	0.257	20.06	8.02	621	146.2	307.8	47.5
3	0.490	20.28	18.49	1434	337.1	757.6	44.5
4	0.514	20.19	19.42	1506	334.1	801.9	44.2
5	0.744	20.36	26.66	2067	486.1	1194.4	40.7
6	0.744	20.26	26.30	2039	479.4	1158.0	41.4
7	0.971	20.27	36.30	2815	661.8	1697.0	39.0
8	0.985	20.22	38.35	2973	699.1	1728.4	40.4

Expts. 1, 3, 5, and 7 were done with soft steel piston and base and expts. 2, 4, 6, and 8 were done with hardened tool steel piston and base. Bed weights for various bed heights are identical to those in Table VII and VIII.

I.B.W. = Ideal Bed Work; A.B.W. = Actual Bed Work.

Table XIII: Experimental data for fracture test of 3/16" beds of uniform-sized and mixed-sized glass spheres

Expt. #	Bed Ht. [in]	Bed Wt. [g]	Compr. [%]	Wt. Broken [g]	# Broken	I.B.W. [in-lb]	A.B.W. [in-lb]	η_b [%]
1	0.182	15.795	20.84	5.395	418	98.4	286.8	34.3
2	0.189	16.924	19.57	4.529	351	82.58	160.3	51.5

Expt. 1 was conducted with a bed of a mixture of glass spheres consisting of 70% by weight of 2 mm (nominal size) spheres and 30% by weight of 0.4 mm (nominal size) spheres. Expt. 2 was conducted with a bed of 2 mm size spheres without fines.

I.B.W. = Ideal Bed Work; A.B.W. = Actual Bed Work

Table XIV: Effect of addition of shear loading on fracture efficiency in compressive comminution

Expt. #	Bed Ht. [in]	Compr. [%]	Wt. Broken [g]	# Full-Size Broken	I.B.W. [in-lb]	A.B.W. [in-lb]	η_b [%]
1	0.135	20.02	0.78	61	14.2	47.4	30.0
2	0.135	20.38	4.08	316	74.3	152.0	48.9
3	0.262	20.94	5.28	409	96.2	268.7	35.8
4	0.257	20.06	8.02	622	146.2	307.8	47.5
5	0.500	20.22	10.57	819	192.6	520.6	37.0
6	0.514	20.19	19.44	1507	354.4	801.9	44.2
7	0.750	20.41	22.84	1771	416.4	1028.1	40.5
8	0.744	20.26	26.30	2039	479.4	1158.0	41.4
9	1.000	20.25	31.57	2448	575.5	1431.7	40.2
10	0.985	20.22	38.35	2973	699.1	1728.4	40.4

Experiments numbered 1, 3, 5, 7, & 9 were done with slanted piston and base, and 2, 4, 6, 8, & 10 with flat piston and base. Bed weights for various bed heights are identical to those in Table VII and VIII.

I.B.W = Ideal Bed Work; A.B.W. = Actual Bed Work.

Table XV: Size-distribution data for compression tests on particle beds

Bed Ht. [in]	Compr. [%]	Total Wt. [g]	Broken Wt. Passing S-25	Broken Wt. Passing S-50	% Broken [r = 2.4]	% Broken [r = 5.7]
0.257	22.75	22.565	7.672	4.739	34.0	21.0
0.741	24.30	67.695	23.693	12.534	35.0	18.5
0.985	24.00	90.260	30.390	17.201	33.7	19.1
2.000	25.05	185.085	62.559	38.128	33.8	20.6

Total weight = initial weight of particle bed of glass spheres before crushing (size range 1.7mm - 2.0 mm)

Broken weight passing S-25 = weight of material with size smaller than 0.71 mm after crushing, i.e., with reduction ratio (r) = $\frac{1.70}{0.71}$=2.4

Broken weight passing S-50 = weight of material with size smaller 0.3 mm after crushing, i.e., with reduction ration (r) = $\frac{1.70}{0.3}$=5.7

S-25 and S-50 are ASTM screen sizes with 0.71 mm and 0.3 mm screen opening respectively.

Table XVI: Experimental data for particle bed of granular material undergoing compression

Expt. #	Bed Ht. [in]	Bed Wt. [g]	Compr. [%]	Wt. Broken [g]	Bed Work [in-lb]	Relative η_b'
1	0.645	50	3.00	1.302	21.7	0.060
2	0.642	50	5.12	5.252	52.5	0.100
3	0.650	50	10.38	19.735	170.7	0.116
4	0.645	50	15.30	28.235	351.4	0.080
5	0.645	50	20.11	34.655	677.2	0.051
6	0.645	50	25.60	40.345	1189.6	0.034
7 *	0.645	50	24.36	22.25	580.6	0.030

* Experiment done with slant piston and base to see the effect of shear loading

Table XVII: Experimental results of fracture test of a bed of particles lubricated with water and oil

Expt. #	Bed Ht. [in]	Compr. [%]	Wt. Broken [g]	# Full-Size Broken	I.B.W. [in-lb]	A.B.W. [in-lb]	η_b [%]
1	0.514	20.19	19.420	1506	354.10	801.90	44.20
2	0.508	20.00	19.606	1520	357.43	789.20	45.29
3	0.510	20.20	18.466	1432	336.65	780.72	43.12
4	0.500	30.06	29.135	2259	531.16	1626.33	32.66
5	0.500	30.08	29.780	2309	542.99	1597.03	34.00
6	0.502	30.13	29.808	2311	543.43	1610.15	33.75

Note: Bed weight = 45.13 g; expts. 1 and 4 were done with dry particle bed; expts. 2 and 5 with glass spheres wetted with water and expts. 3 and 6 with glass spheres lubricated with oil.

I.B.W. = Ideal Bed work; A.B.W. = Actual Bed Work.

Table XVIII: Effects of machine compliance on the calculations of fracture efficiency

Bed Ht. [in]	Compr. [%]	Wt. Broken [g]	# Broken	I.B.W. [in-lb]	U.B.W. [in-lb]	η_b [%]	C.B.W. [in-lb]	η_b' [%]
0.135	20.38	4.075	316	74.29	151.96	48.89	150.02	49.52
0.514	20.19	19.420	1506	354.10	801.90	44.20	772.47	45.84
2.000	25.05	85.765	6650	1563.60	4643.80	33.67	4499.70	34.75

Note: Bed weight can be found from Tables VII and VIII; η_b = fracture efficiency, uncorrected; and η_b' = corrected fracture efficiency.

I.B.W. = Ideal Bed Work; C.B.W. = Corrected Bed Work (for machine compliance); U.B.W. = Uncorrected Bed Work

References

[1] Committee on Comminution and Energy Consumption, National Advisory Board, National Academy of Sciences.
"Comminution and Energy Consumption".
Reprint No. NMAB-364, May, 1981

[2] Kurfess, Adriana D.
"Fracture Criterion for Brittle and Plastic Spheres".
Master's thesis, Massachusetts Institute of Technology, May, 1989.

[3] Ghaddar, Chahid Kamel.
"Fracture Efficiency within Particle Beds".
Master's thesis, Massachusetts Institute of Technology, January, 1989.

[4] Peterson, C. R.
"Energetics of Comminution" and "Comminution of Energy Materials".
Massachusetts Institute of Technology, Unpublished Drafts, 1990 ; 1991.

[5] Annis, Karen.
"Segregation Control of Binary Size Particles in a Comminution Device".
Master's thesis, Massachusetts Institute of Technology, August, 1991.

[6] Bilby, B. A.
"Putting Fracture to Work".
Proc. 4th Tewksbury Symp., Fracture, 1:1 - 1:44 , 1979.

[7] Rittenger, von P. R.
Lehrbuch der Aufbereitungskunde.
Berlin, 1867.

[8] Kick, Frederich.
Das gesetz der Proportionalen Widerstande und Seine Anwendungen.
Leipzig, 1885.

[9] Hukki, R. T.
"An Experimental Study of the Principles of Comminution".
D.Sc. Thesis. Massachusetts Institute of Technology, 1944.

[10] Bond, Fred C.
"The Third Theory of Comminution".
Min. Eng. Trans. AIME, 193, 484-494 , May, 1952.

[11] Holmes, J. A.
"A Contribution to the Study of Comminution: a Modified Form of Kick's Law".
Trans. Inst. Chem. Eng., 35, 125-156 , 1957.

[12] Charles, R. J.
"Energy-Size Reduction Relationships in Comminution".
Trans. AIME, 208, 80-88 , 1952.

[13] Marshall, V. C.
"Crushing and Grinding: Critique of Existing Laws".
Chemical and Process Engineering , April, 1966.

[14] Schonert, K.
"Aspects of the Physics of Breakage Relevant to Comminution".
Proc. Fourth Tewksbury Symp., Fracture, Melbourne , 1979.

[15] Weiss, M. A., Klumpar, I. V., Peterson, C. R., and Ring, T. A.
"Shale Oil Recovery Systems Incorporating Ore Beneficiation".
DOE Report No. MIT-EL 82-041 , 1982.

[16] Prasher, C. L.
Crushing and Grinding Process Handbook.
John Wiley & Sons Ltd., 1987.

[17] Larson, Arnold.
"The Effect of Size and Contact Geometry in Single Particle Crushing".
Master's thesis, Massachusetts Institute of Technology, August, 1986.

[18] Laffey, Kathleen M.
"Fracture within Particle Beds Under Compressive Loading".
Master's thesis, Massachusetts Institute of Technology, June, 1987.

[19] Austin, L. G.
"A Commentary on Kick, Bond and Rittenger Laws of Grinding".
Powder Technology, 7, 315-317 , 1973a.

[20] Austin, L. G.
"Note on Rittinger's Law of Grinding".
Trans. SME/AIME, 254, 310-311 , 1973b.

[21] Austin, L. G. and Luckie, P. T.
"Grinding Equations and the Bond Work Index".
Trans. SME/AIME, 252, 259-266 , 1972c.

[22] Schonert, K.
"Method of Fine and Very Fine Comminution of Materials having Brittle Behavior".
U.S. Patent 4,357,287, November, 1982.

[23] Schonert, K.
"About the Particie Breakage and the Possibilities and Limits for Improving Size-Reduction Processes".
In Powder Technology, 331-345, Hemisphere Publications, 1984.

[24] Schonert, K.
"Advances in the Physical Fundamentals of Comminution".
In Advances in Mineral Processing, Somasundaran, P., ed., SME, Littleton, CO, 19-32, 1986.

[25] Karra, V. K., and Magerowski, A. J.
"Method and Apparatus for Energy Efficient Comminution".
U.S. Patent 4,671,464, June, 1987.

[26] Karra, V. K., and Magerowski, A. J.
"Apparatus for Energy Efficient Comminution".
U.S. Patent 4,750,679, June, 1988.

[27] Obert, L., Windes, S. L., and Duvall, W. I.
"Standardized Tests for Determining the Physical Properties of Mine Ores".
Technical Report, US Bureau of Mines Report of Investigations, 3891, 1946.

[28] Hiramatsu, Y., and Oka, Y.
"Determination of the Tensile Strength of Rock by a Compression Test of an Irregular Test-piece".
Intl. J. Rock Mech. Miner. Sci., 3, 89-99 , 1966.

[29] Snow, R. H., and Paulding, B. W.
"Prediction of Fragment Size Distribution from Calculations of Stress in Spheres and Discs".
H. Heywood Memor. Symp., 17-18. Loughborough University of Technology, September, 1973.

[30] Easter, James R.
"A Finite Element Crack Growth with a Tip Position Parameter".
Master's thesis, Massachusetts Institute of Technology, May, 1989.

[31] Drlik, G. J.
"Simulation of the Crushing of a Two-Dimensional Particle Bed Due to Compressive Loading".
Master's thesis, Massachusetts Institute of Technology, May, 1987.

[32] Pflueger, J.
"The Behavior of Particle Beds in Simulation".
Master's thesis, Massachusetts Institute of Technology, January, 1988.

[33] Kendall, K.
"The Impossibility of Comminuting Small Particles".
Nature, 272, 710-711 , 1978.

[34] Arbiter, N., Harris, C. C., and Stambolitzis, G. A.
"Single Fracture of Brittle Spheres".
Trans. SME/AIME, 244, 188-133 , 1969.

[35] Kunii, Daizo., and Levenspiel, Octave.
Fluidization Engineering.
Robert E. Krieger Pub. Co. Ltd., Inc., 1969.

[36] Wilhelm, R. H. and Kwauk, M.
"Fluidization of Solid Particles".
Chem. Eng. Progr., 44, 201 , 1948.

[37] Katz, H. M.
"Argone National Laboratory Report No. 5725 M".
Technical Report, Argone National Laboratory., 1957.

[38] Rowe, P. N., Nienow, A. W., and Agbim, A. J.
"The Mechanisms by which Particles Segregate in Gas Fluidised Beds-Binary Systems of Near Spherical Particles".
Trans. Instn. Chem. Engrs., 50, 310-323 , 1972.

[39] Kondukov, N. B. and Sosna, M. H.
"Khim. Prom., 6, 402".
1965.

[40] Chen, J. L.-P., and Keairns, D. L.
"Particle Segregation in a Fluidized Bed".
The Canadian Journal of Chemical Engineering, 53, 395-402 , August, 1975.

[41] Kennedy, S. C., and Bretton, R. H.
"Axial Dispersion of Spheres Fluidized with Liquids".
1966

[42] Dutta, B. K., Bhattacharya, Suman., Chaudhury, S. K. and Barman, B.
"Mixing and Segregation in a Liquid Fluidized Bed of Particles with Different Size and Density".
The Canadian Journal of Chemical Engineering., 66, 676-702. , 1988.

[43] Fan, Liang-Tseng, Schmitz, James A., and Miller, Eugene, N.
"Dynamics of Liquid-Solid Fluidized Bed Expansion".
American Institute of Chemical Engineering Journal, 9:2, 149-153 , 1962.

[44] Richardson, J. F., and Zaki, W. N.
"Sedimentation and Fluidization: Part 1".
Trans, Instn. Chem. Engrs., 32, 35-52. , 1954.

[45] Couderc, J. P.
"Incipient Fluidization and Particulate Systems" - Chapter 1 in Fluidization; 2nd Ed.".
Academic Press, 1985.

[46] Noda, K., Uchida, S., Makino, T., and Kamo, H.
"Minimum Fluidization Velocity of Binary Mixture of Particles with Large Size Ratio".
Powder Technology, 46, 149-154 , 1986.

[47] Huarui, Yu., and Yanfu, Shi.
"Characteristics of Fluidization of Binary Particle Mixtures".
Fluidization'85 Science and Technology Conference; 2nd China-Japan Symposium , 1985.

[48] Lewis, W. K.
Chem. Eng. Progr., 48, 603.
1952.

[49] Jean Rong-her and Fan, Liang-shih.
"On the Criteria of Solids Layer Inversion in a Liquid-Solid Fluidized Bed Containing a Binary Mixture of Particles".
Chemical Engineering Science, 41:11, 2811-2821 , 1986.

[50] Gibilaro, L. G., Waldram, S. P., and Foscolo, P. U.
"A Simple Mechanistic Description of the Unsteady State of Expansion of Liquid-Fluidized Beds".
Chemical Engineering Science, 39:3, 607-610 , 1984.

[51] Poncelet, Denis., Navean, Henry., and Nyns, Edmund-Jacques.
"Transient Response of a Solid-Liquid Model Biological Fluidized Bed to a Step Change in Fluid Superficial Velocity".
J. Chem. Tech. Biotechnol., 48, 439-452 , 1989.

[52] Patwardhan, V. S., and Tien, C.
"Sedimentation and Liquid Fluidization of Solid Particles of Different Sizes and Densities".
Chemical Engineering Science, 40 , 1985.

[53] Masliyah, J. H., Nasr-el-din, H., and Nanadakumar, K.
"Continuous Separation of Bidisperse Suspensions in Inclined Channels".
Int. J. Multiphase Flow, 15:5, 815-829 , 1989.

[54] Shi, Yan-Fu., Yu, Y. S., and Fan, L. T.
"Incipient Fluidization Condition for a Tapered Fluidized Bed".
Ind. Chem. Fundam., 23:4, 484-489 , 1984.

[55] Ganguly, U. P.
"Elutriation Characteristics of Solids from Liquid Fluidized Bed Systems: Part 1 - Onset of Elutriation; Part 2 - Prediction of Equilibrium Bed Concentration".
The Canadian Journal of Chemical Engineering, 60, 466-469 and 470-473 , August, 1982.